



**CFMR**  
COMITÉ FRANÇAIS  
DE MÉCANIQUE  
DES ROCHES

## Jean Mandel Lecture 2020:

Towards a conceptual model of rock mass post-failure behavior

4<sup>th</sup> December 2020

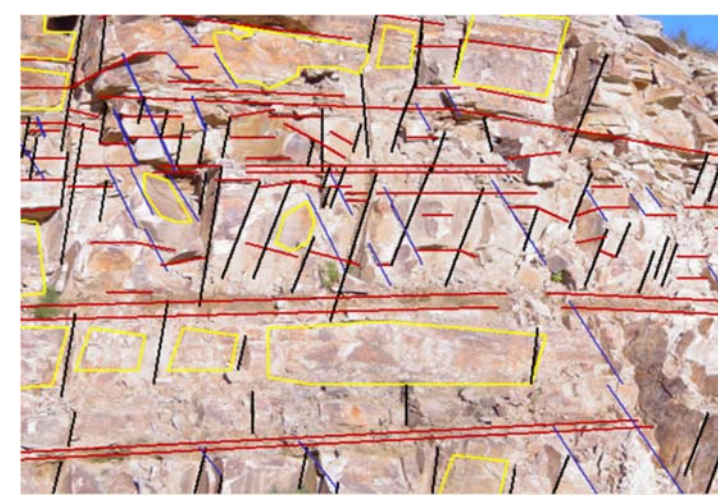
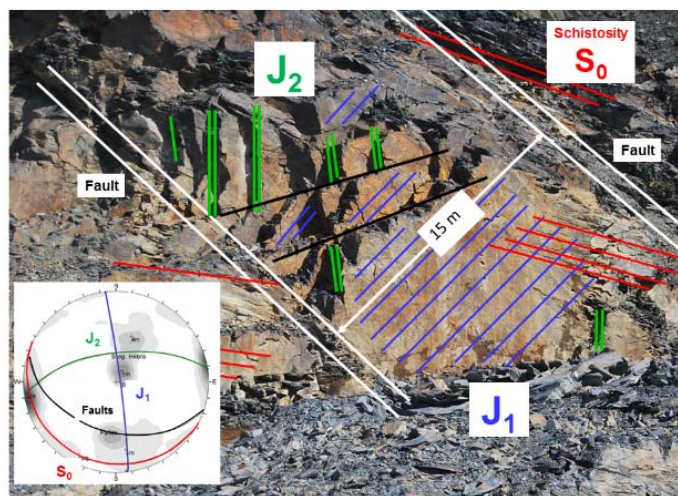
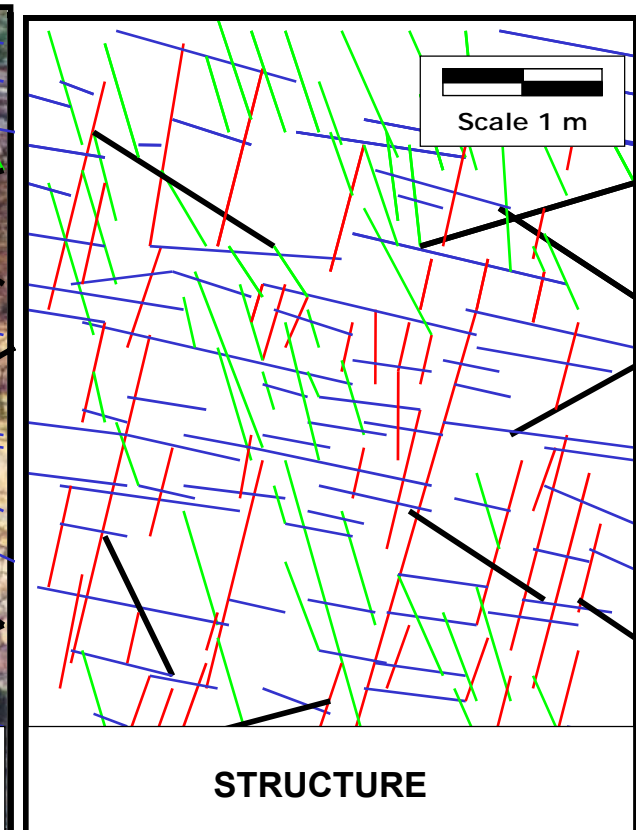
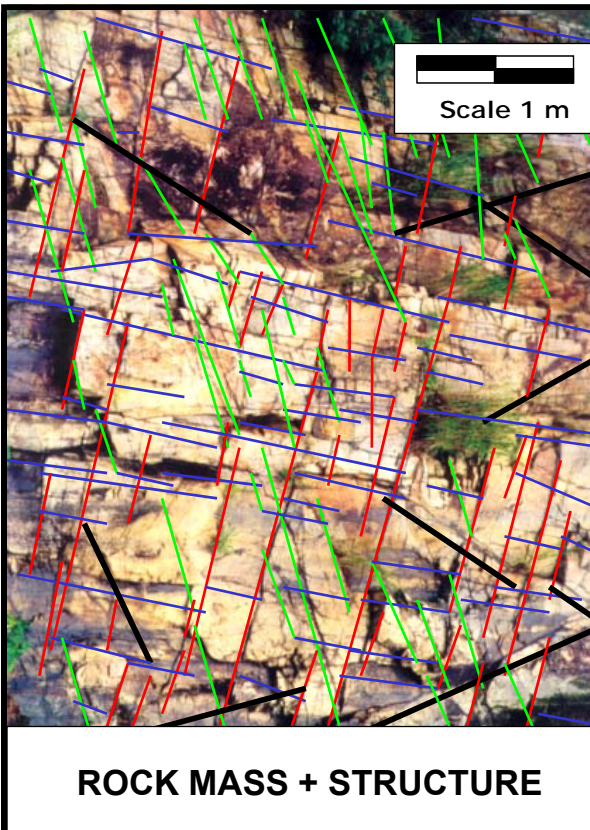
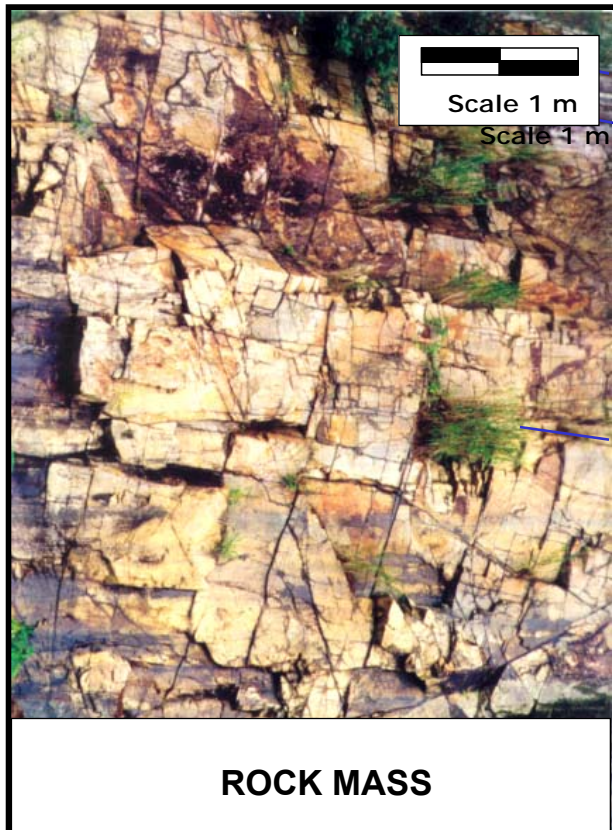


Google Earth

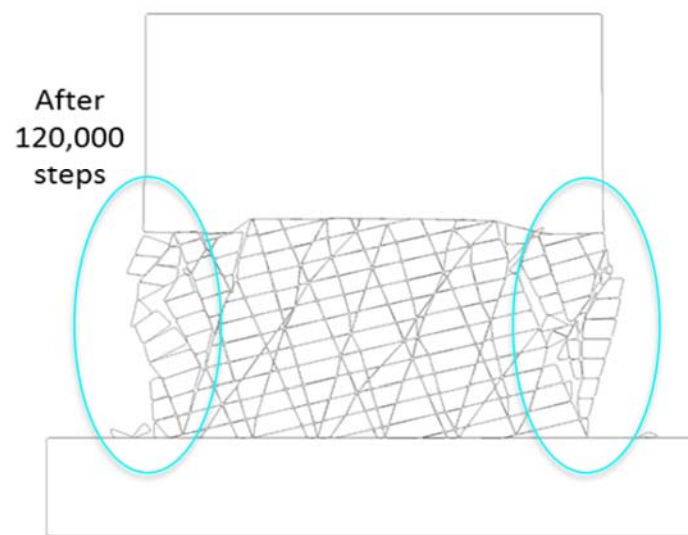


Leandro R. Alejano,  
Prof. of Rock Mechanics, University of Vigo, Spain  
ISRM VP for Europe

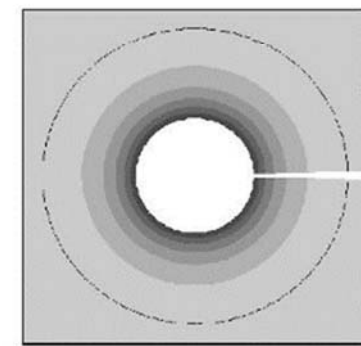
**eME**  
UniversidadeVigo



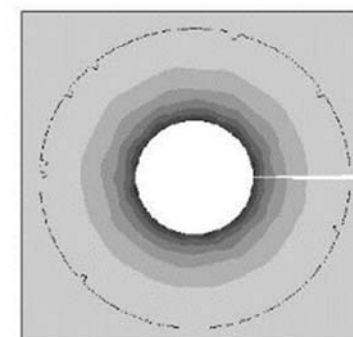
# Mine pillars



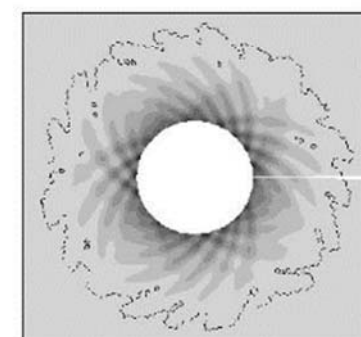
# Mine drifts



a) Grid size in tunnel wall= $a/20$



b) Grid size in tunnel wall= $a/35$



c) Grid size in tunnel wall= $a/50$

### 1. The first years 1995-2005:

Motivation & first studies on dilatancy

### 2. The following decade 2005-2015:

Understanding dilatancy, firs studies in lab & dilatancy models

### 3. Hoek & Brown's inspiration

### 4. 2015-2020: Recent developments:

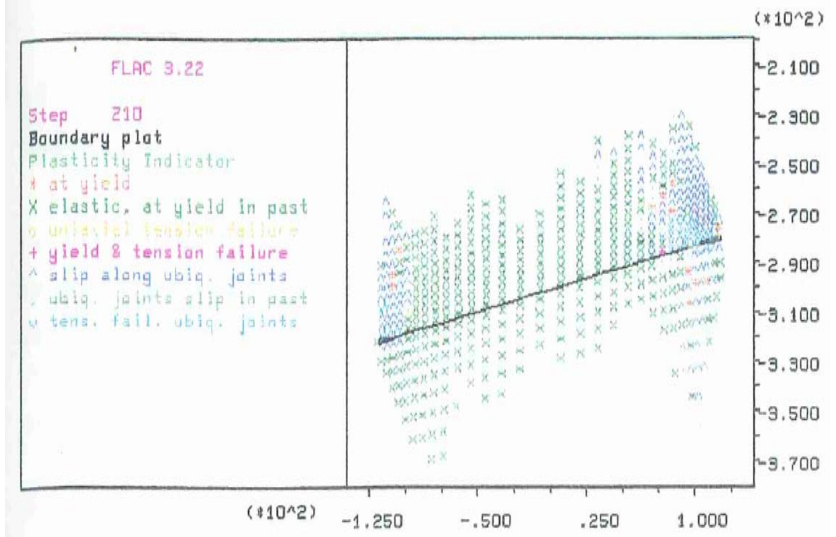
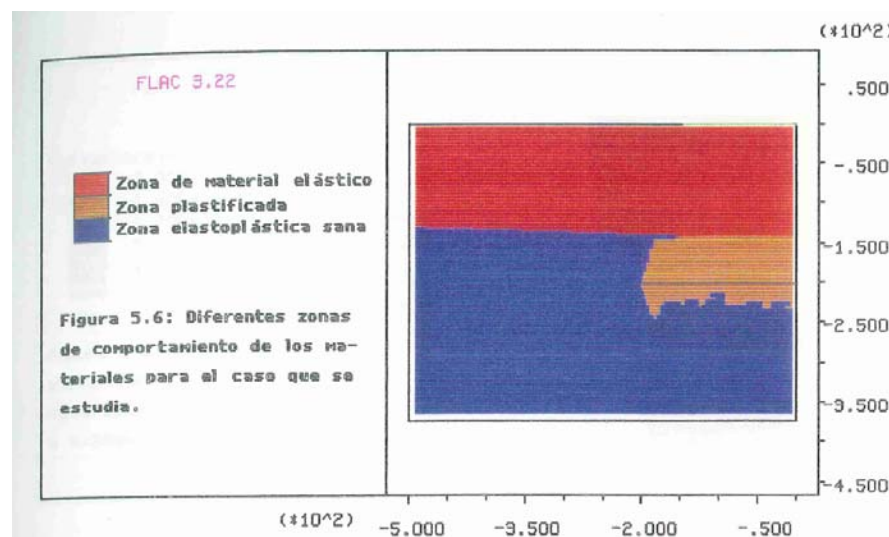
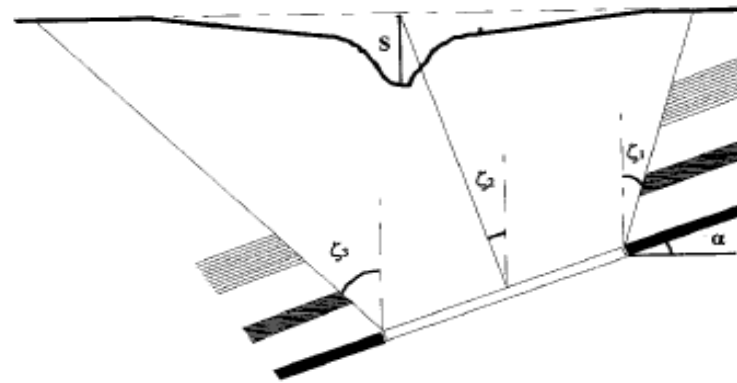
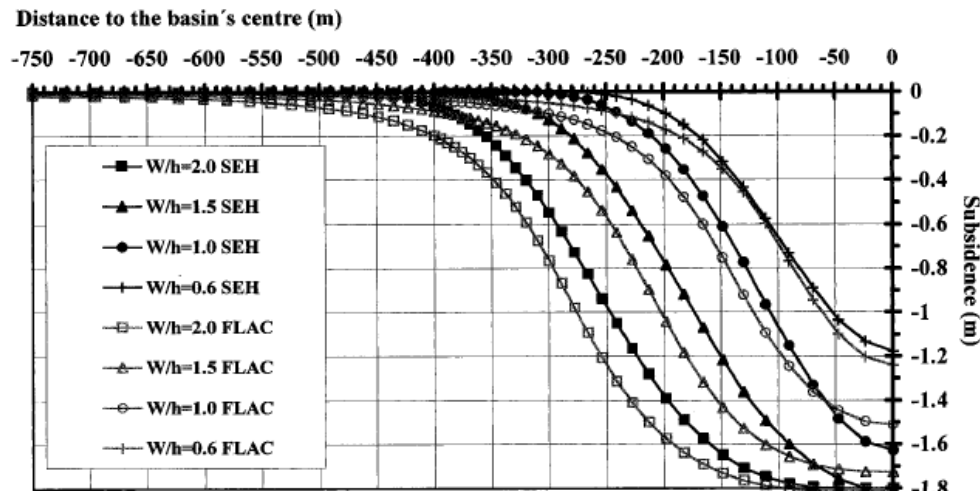
Jointed sample approach, tests on jointed samples, strength and post-failure

### 5. A conceptual model of rock mass behavior.

### 6. Numerical modelling

### 7. Conclusions

Ph.D. Thesis on subsidence over inclined coal seams (1996).



Alejano, L.R., Ramírez-Oyanguren, P., Taboada, J. FDM predictive methodology for subsidence due to flat and inclined coal seam mining (1999) International Journal of Rock Mechanics and Mining Sciences, 36 (4), pp. 475-491.

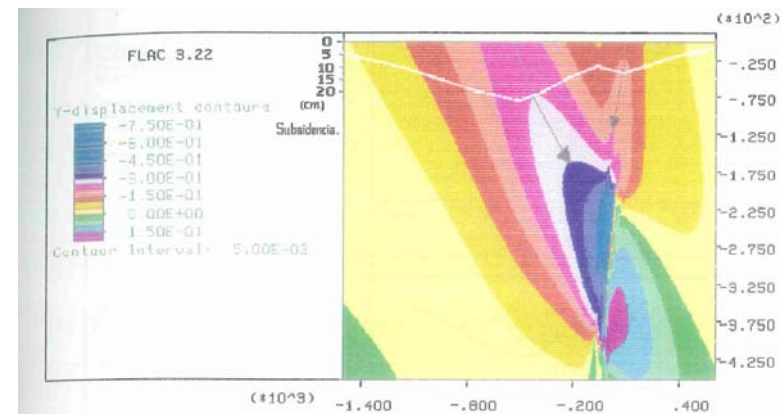
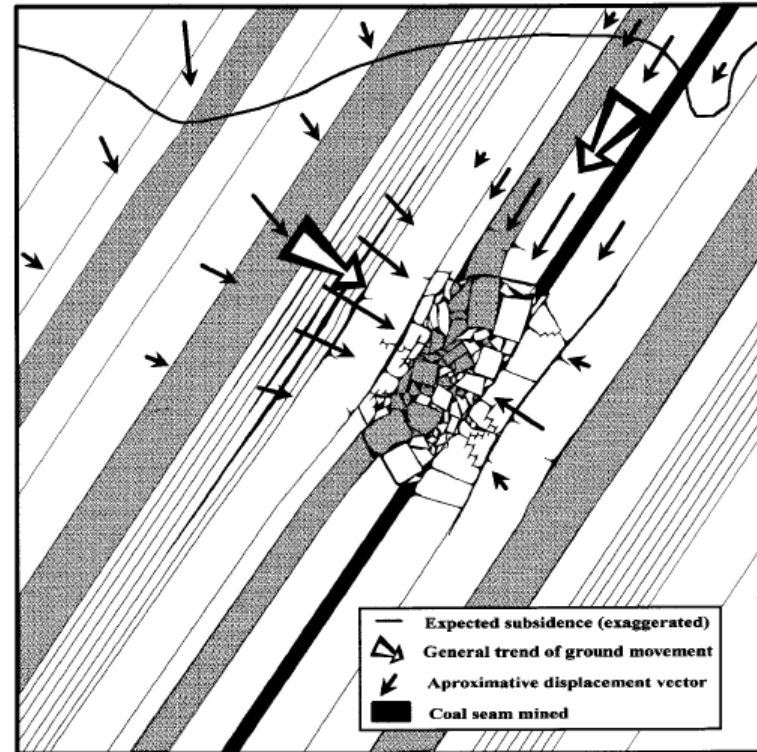
Main conclusions:

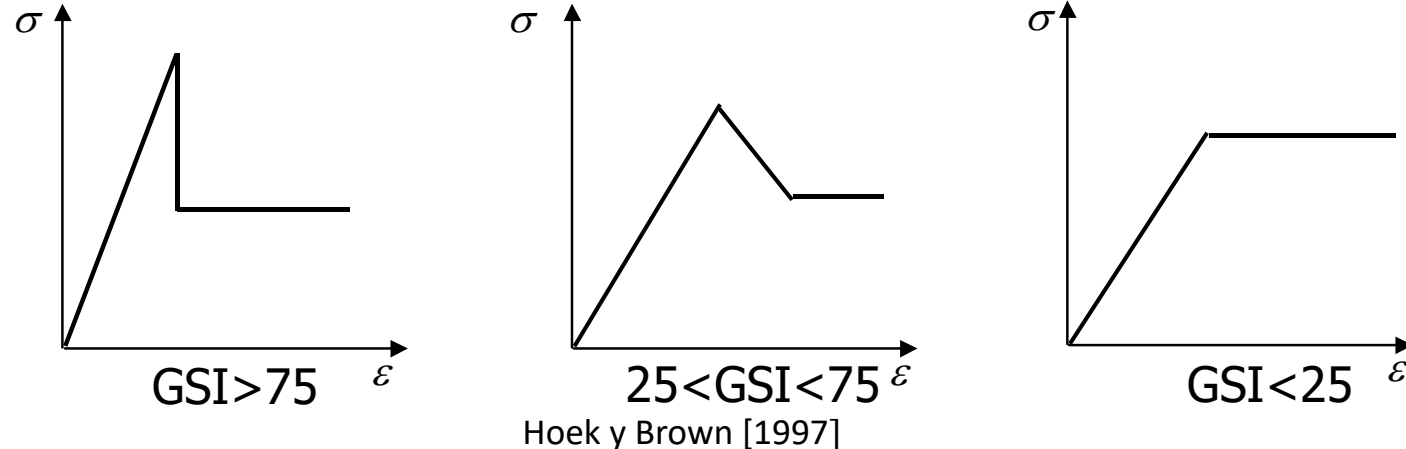
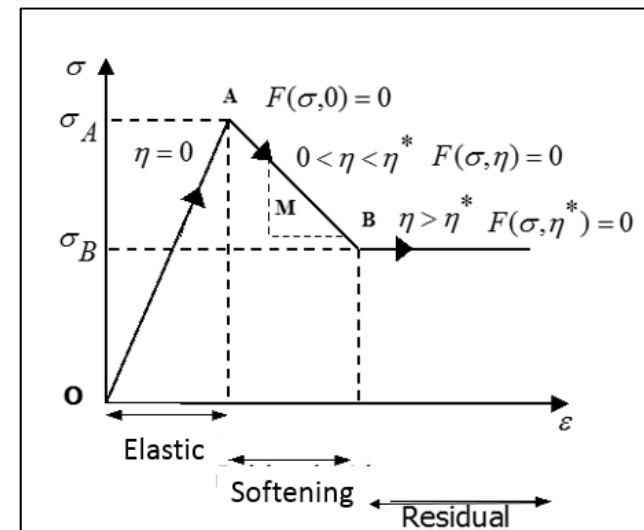
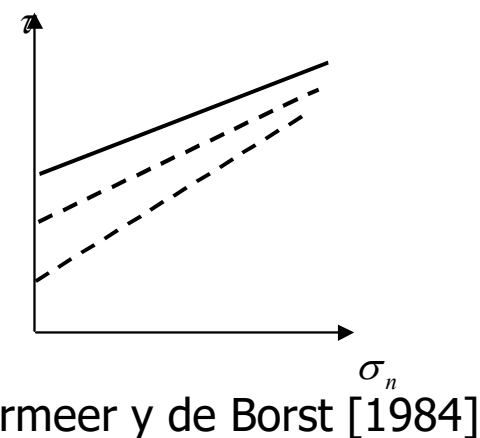
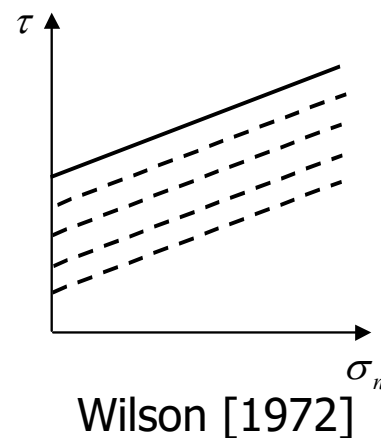
1. Elasto-plastic models need the following parameters:  $E$ ,  $\nu$ ,  $c$ ,  $\phi$ ,  $\sigma_t$  &  $\psi$ .

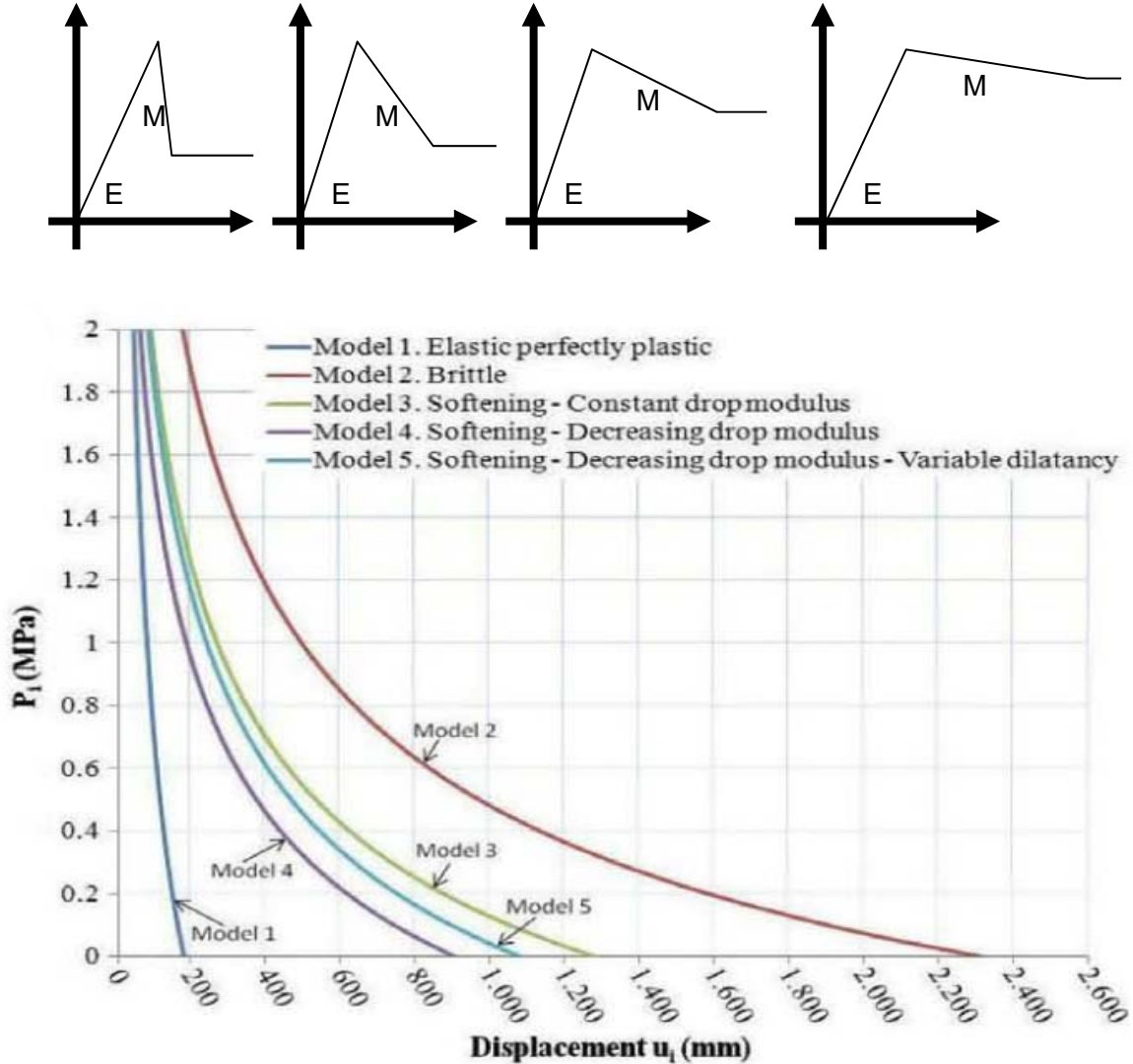
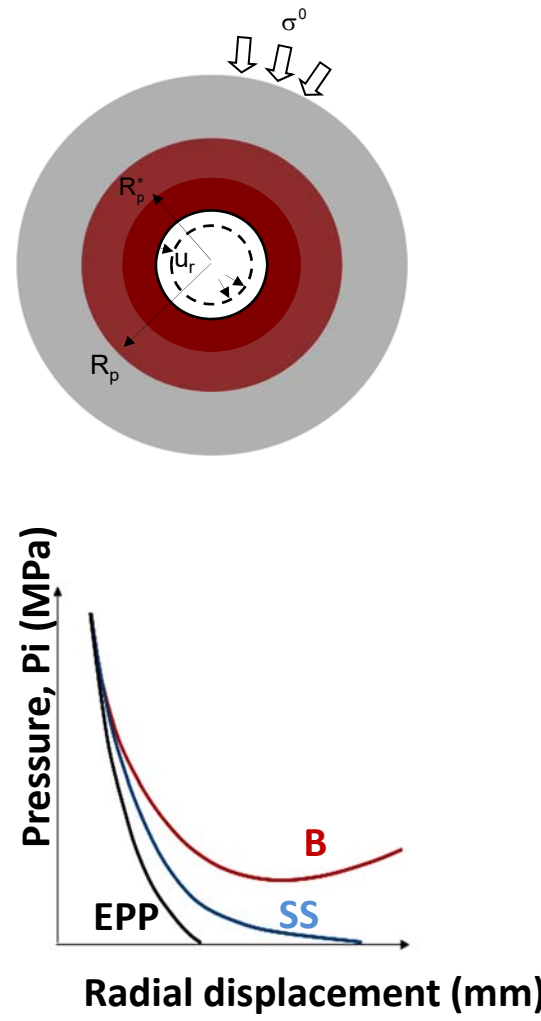
What is  $\psi$ ?

2. Elasto-plastic models cannot simulate the actual behavior of rock masses.

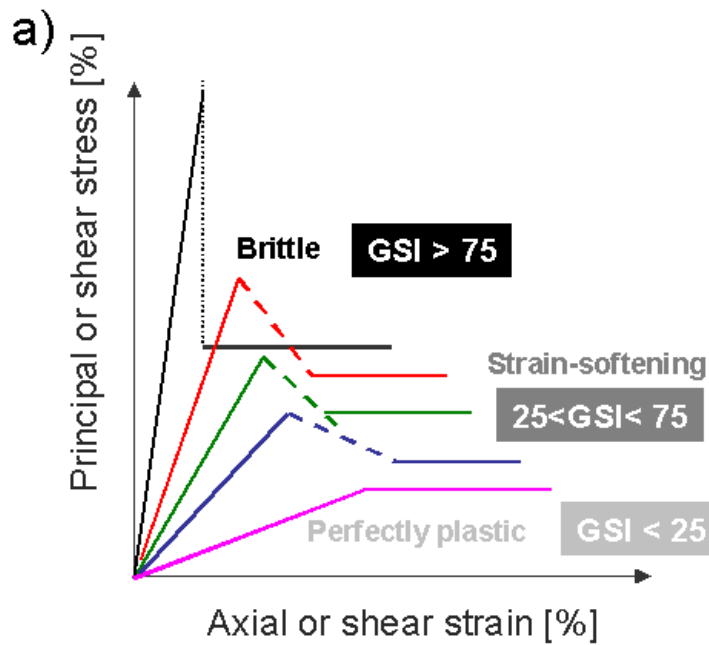
Let us try with strain-softening models...



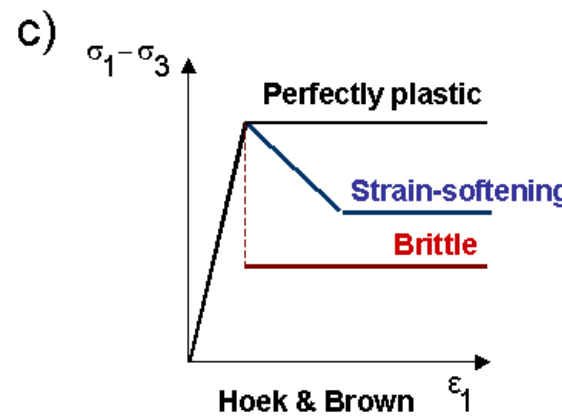
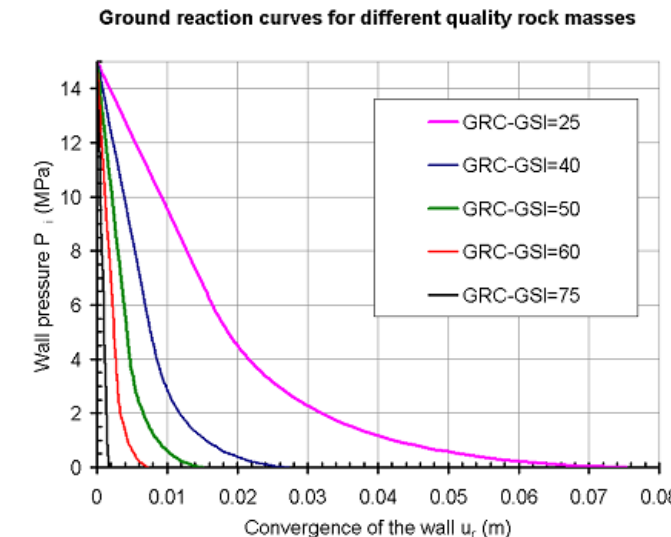
**Hoek & Brown proposal:**

**Various approaches to implement strain-softening behavior.**




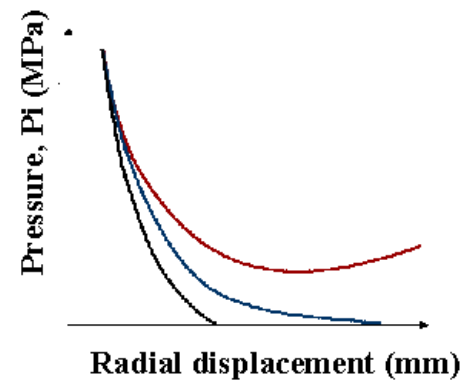
Alejano LR et al. 2009. Ground reaction curves for tunnels excavated in different quality rock masses showing several types of post-failure behavior. Tun. & Undergr. Sp. Tech. 24. 689–705



b)



d)

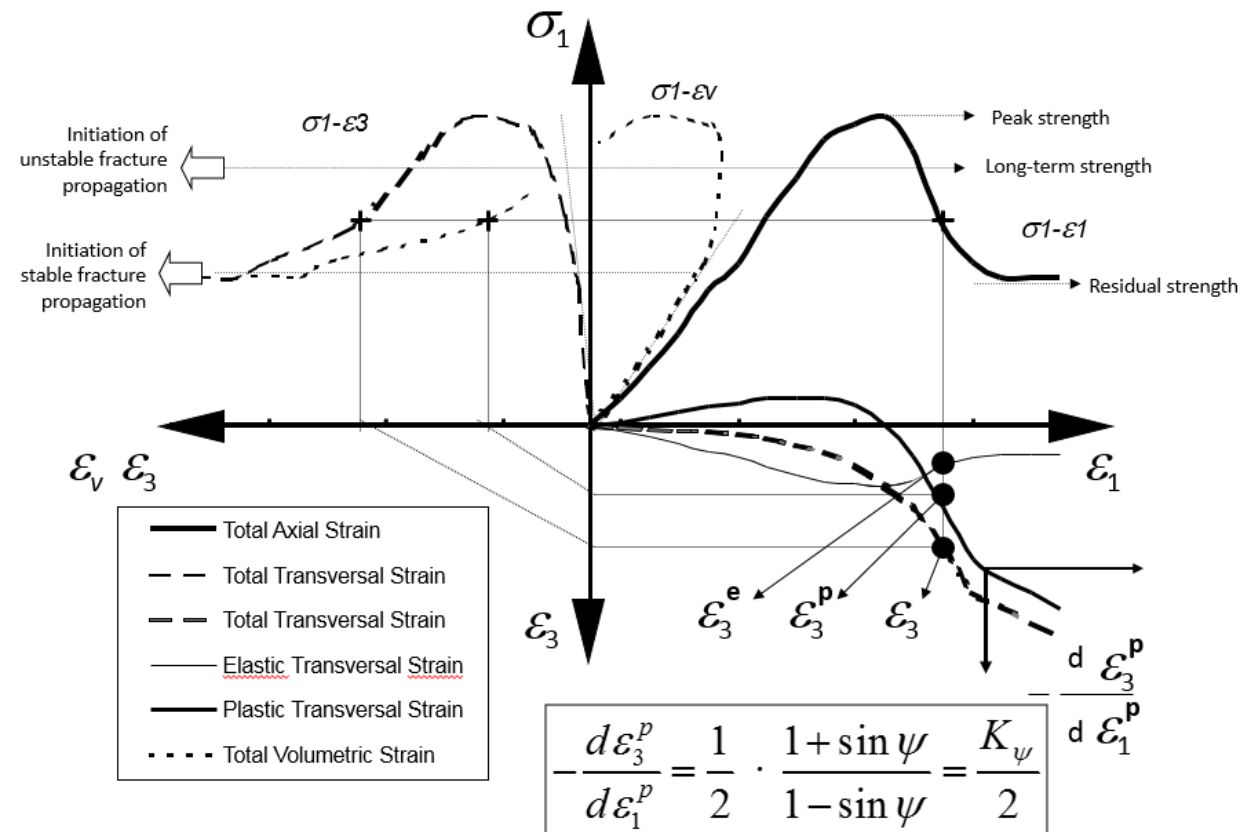


- I look for providing a consistent approach to estimate the dilatancy angle ' $\psi$ ' for rock masses, to use in numerical modeling or analytical studies. To improve the simplistic approach of associated flow rule ' $\phi=\psi$ ' or null dilatancy ' $\psi=0^\circ$ '. To test the empirical Hoek & Brown (1997) proposal of  $\psi=\phi/4$ ,  $\psi=\phi/8$  and  $\psi=0$  for good, average and bad quality rock masses. Considering the shear plastic strain and confining stress dependent nature of  $\psi$ .

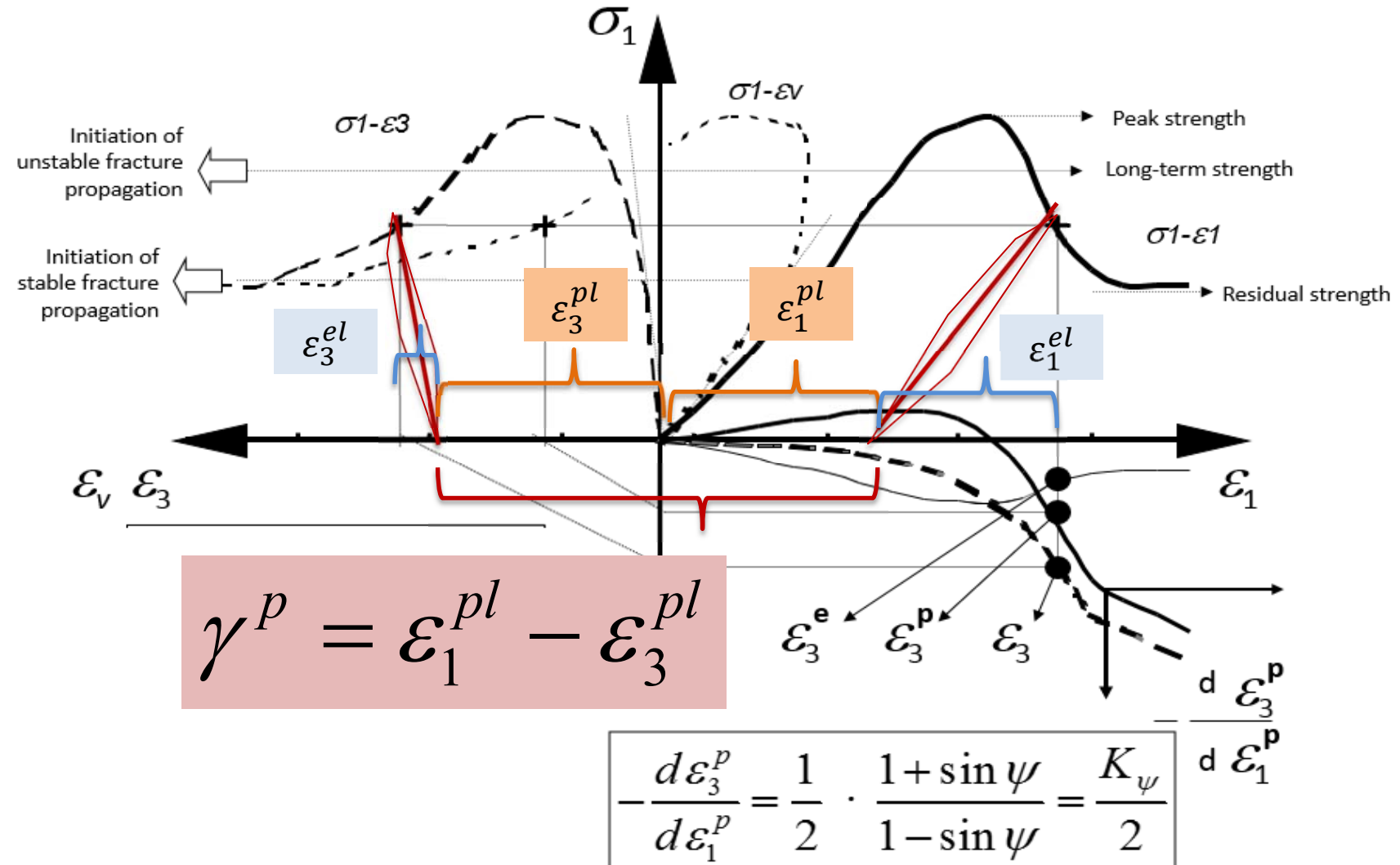
**Complete stress-strain curve for a test:**

Vermeer & de Borst, 1984:

$$\psi = \arcsin \frac{\dot{\varepsilon}_v^p}{-2 \cdot \dot{\varepsilon}_1^p + \dot{\varepsilon}_v^p}$$



## Plastic parameter as plastic shear strain:



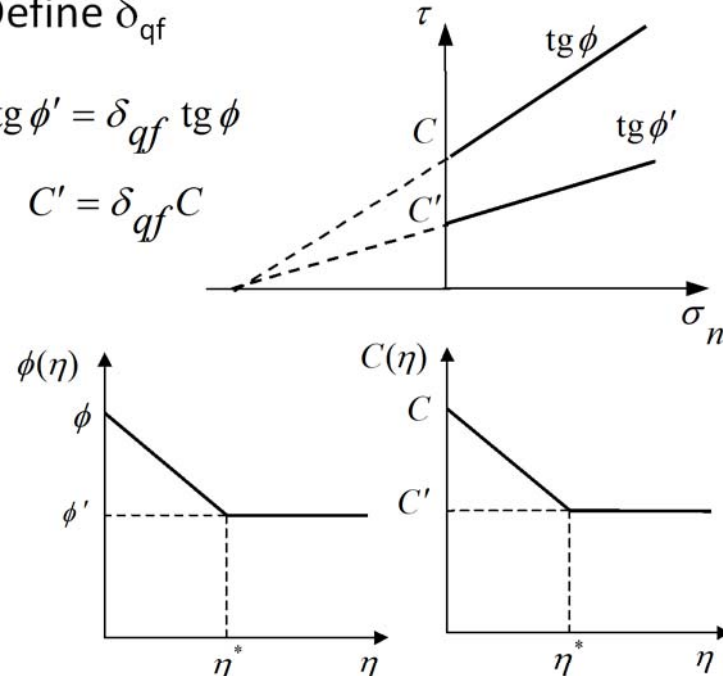
Vermeer PA, De Borst R (1984) Non-associated plasticity for soils, concrete and rock. HERON 29:1–64

A possibility to implement strain-softening in an easy manner.

Define  $\delta_{qf}$

$$\operatorname{tg} \phi' = \delta_{qf} \operatorname{tg} \phi$$

$$C' = \delta_{qf} C$$



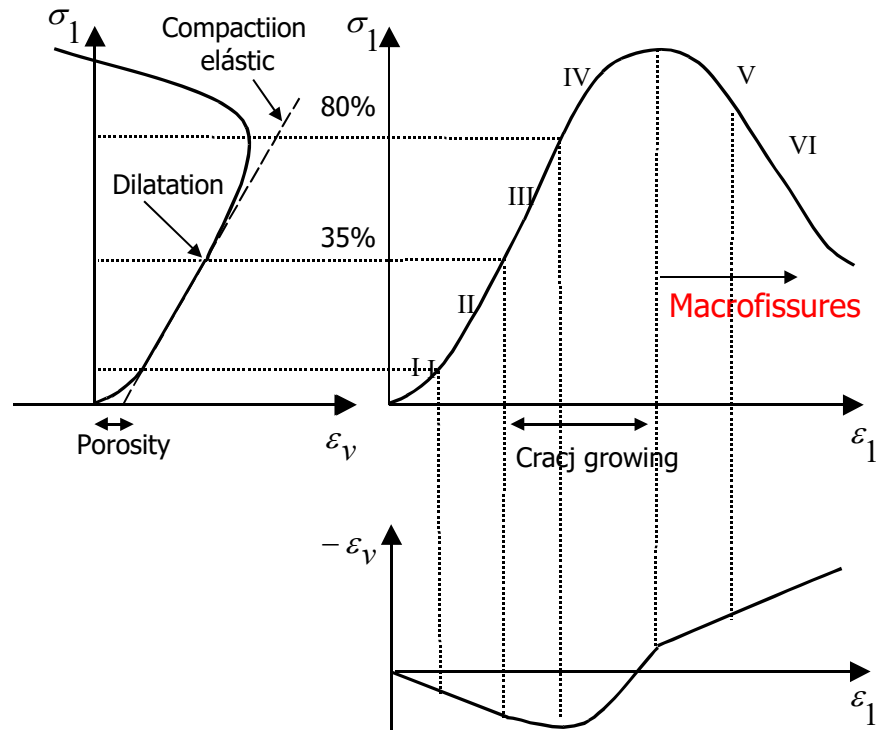
Brown et al. [1989]

Connecting test results and numerical models:

$$\eta_{FLAC} = \frac{\sqrt{3}}{3} \sqrt{1 + K_\psi + K_\psi^2} \frac{\gamma^p}{1 + K_\psi}$$

Ideas to understand dilatancy

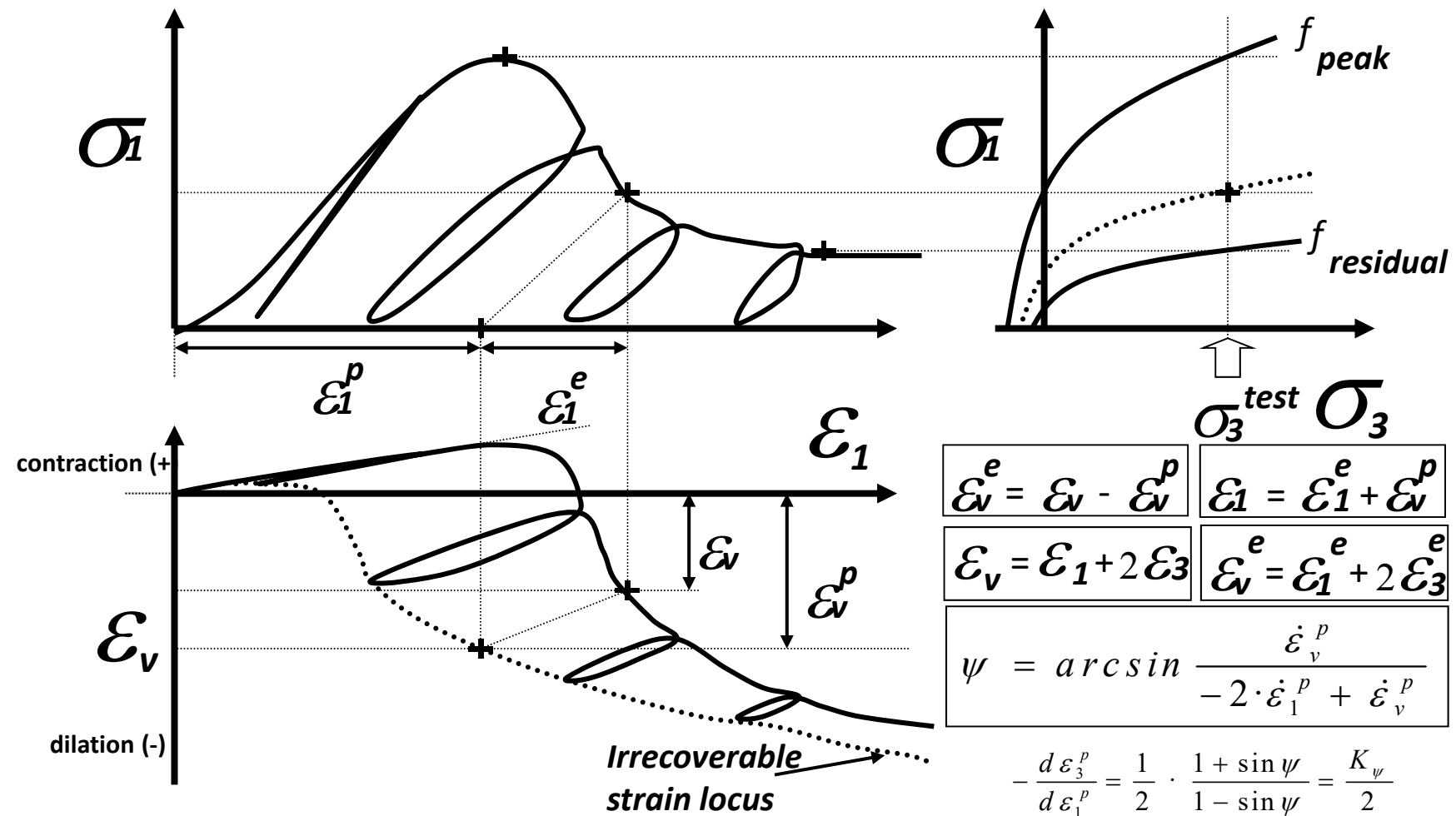
Plastic potential:  $G = \sigma_\theta - K\sigma_r$   $K_\psi = \frac{1 + \operatorname{sen} \psi}{1 - \operatorname{sen} \psi}$



$$\operatorname{sen} \psi = \frac{\dot{\varepsilon}_v^p}{-2\dot{\varepsilon}_1^p + \dot{\varepsilon}_v^p} \quad \text{Vermeer y de Borst [1984]}$$

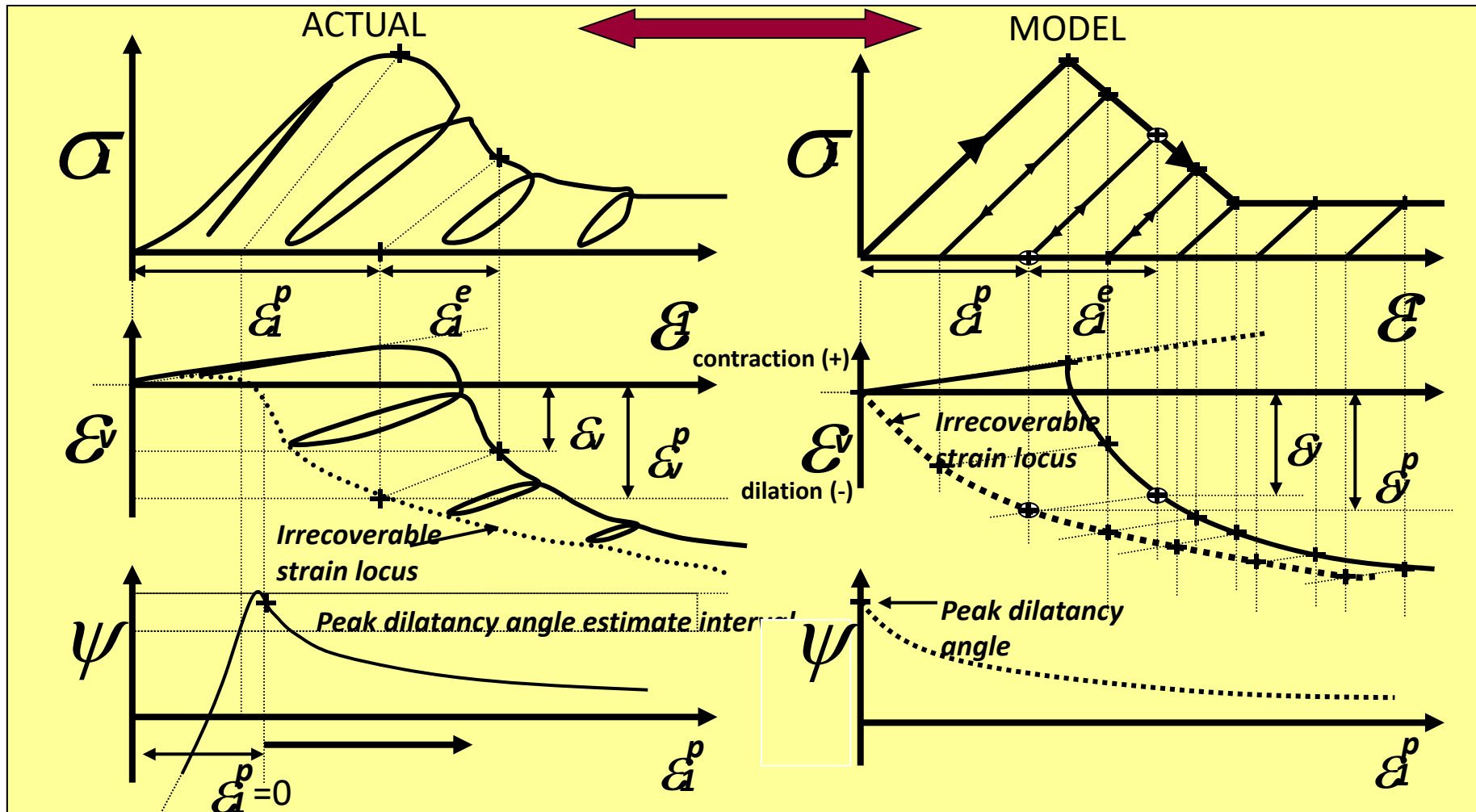
Alonso E, Alejano LR, Varas F, Fdez-Manin G, Carranza-Torres C. 2003. Ground reaction curves for rock masses exhibiting strain-softening behaviour. Int J Numer Anal Methods Geomech 2003;27:1153–85.

Dilatancy is defined as a change in volume resulting from the shear distortion of an element in a material.



$\psi$  is a suitable parameter for describing dilatant behaviour, for it represents the ratio of plastic volume change to plastic shear strain.

Actual stress-strain relationships for a compressive test with unloading-loading cycles and ideal stress-strain relations as proposed in our model



Alejano LR, Alonso E. 2005. Considerations of the dilatancy angle in rocks and rock masses. Int J Rock Mech Min Sci;42(4):481–507.

## Reinterpretation of Medhurst's results

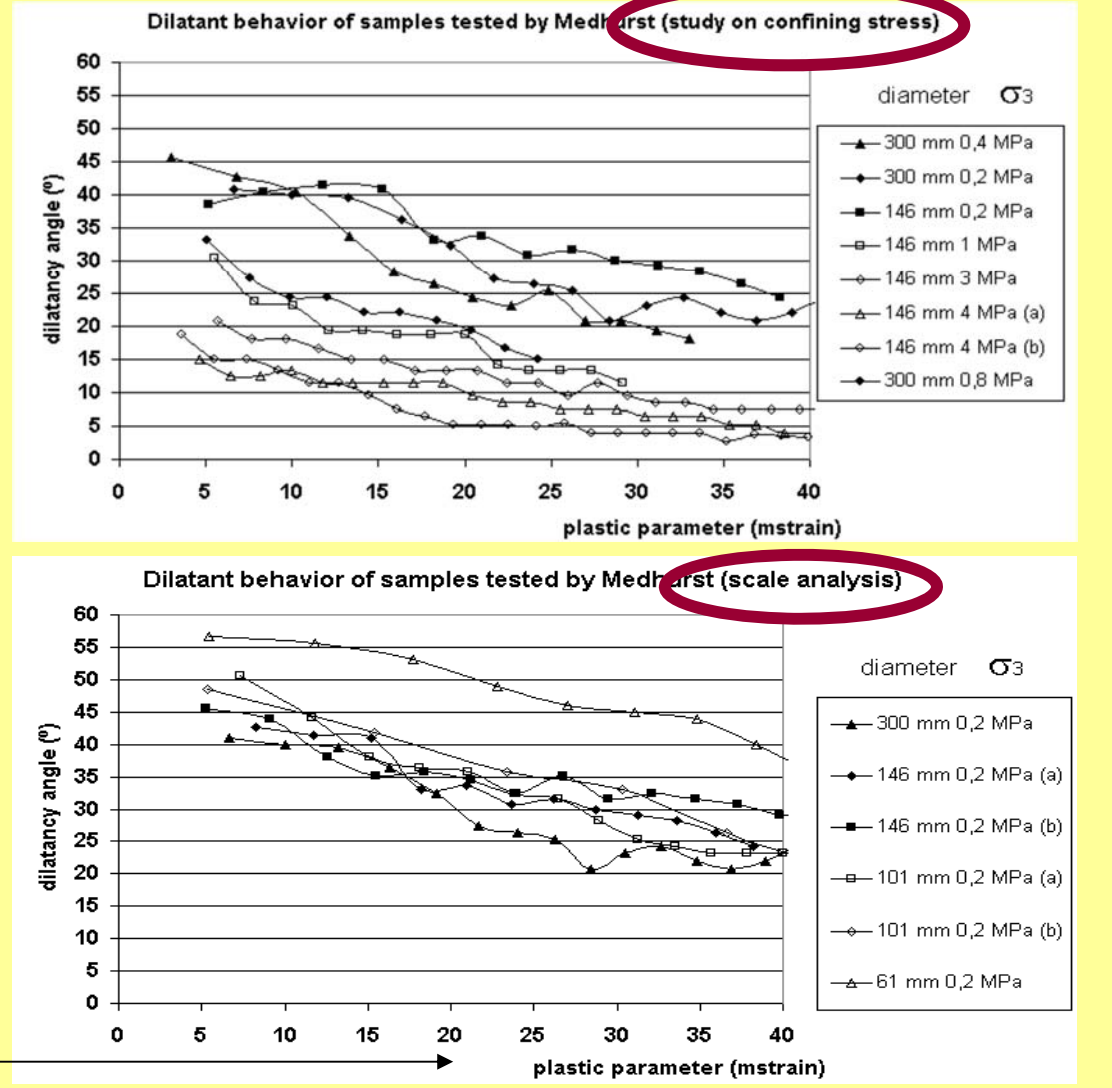
Medhurst (1996) performed an exhaustive and highly reliable series of triaxial compression tests on 61, 101, 146 and 300 mm coal samples using a servo-controlled press.

For some samples loading-unloading cycles were included as part of the testing procedure and recoverability curves were created.

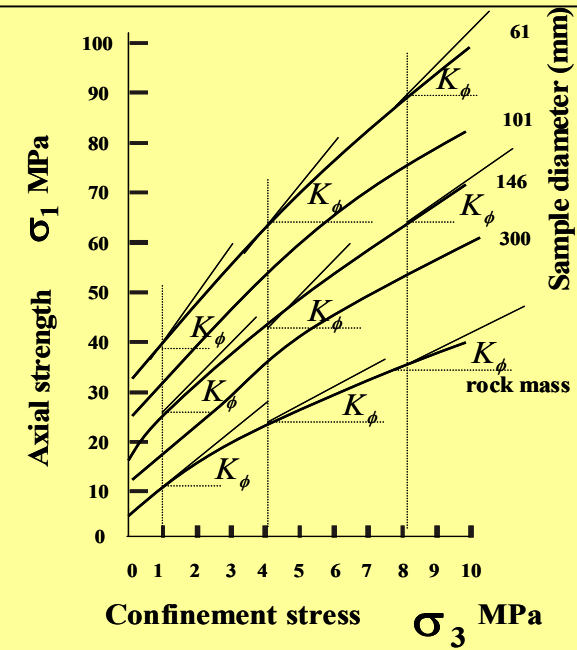
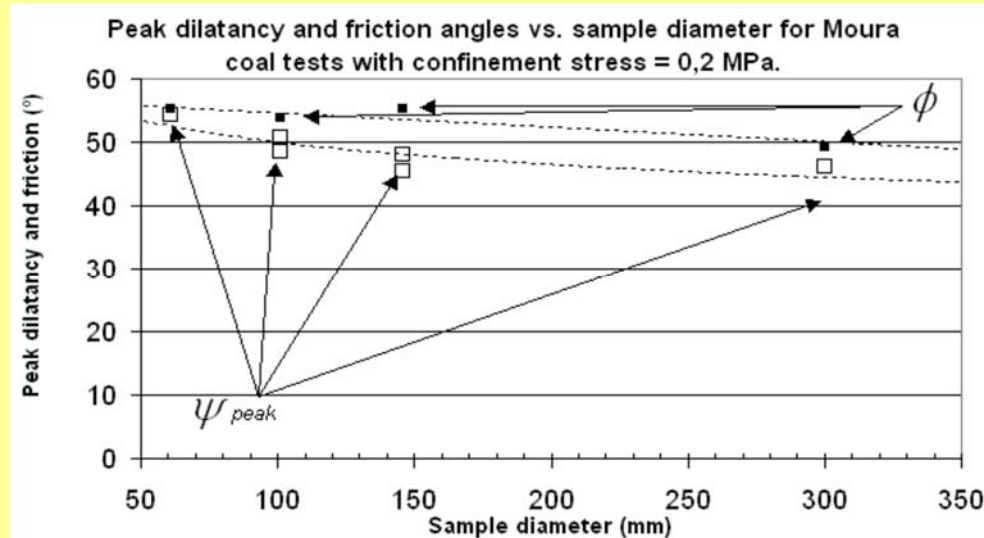
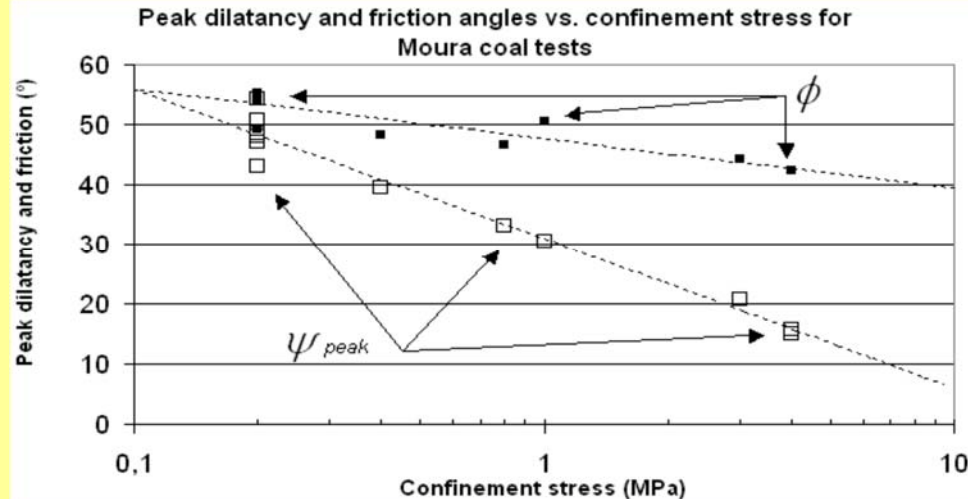
$$\psi = \arcsin \frac{\dot{\varepsilon}_v^p}{-2 \cdot \dot{\varepsilon}_1^p + \dot{\varepsilon}_v^p}$$

$$-\frac{d\varepsilon_3^p}{d\varepsilon_1^p} = \frac{1}{2} \cdot \frac{1 + \sin\psi}{1 - \sin\psi} = \frac{K_\psi}{2}$$

$$\gamma^p = \varepsilon_1^p - \varepsilon_3^p$$



## Representation of all peak dilatancy data vs. confinement stress



$$\sigma_1 = \sigma_3 + \sigma_{ci} \left( m_i \frac{\sigma_3}{\sigma_{ci}} + s \right)^a$$

$$\frac{d\sigma_1}{d\sigma_3} = 1 + a \cdot m_i \left( m_i \frac{\sigma_3}{\sigma_{ci}} + s \right)^{a-1}$$

$$K_\phi = \frac{d\sigma_1}{d\sigma_3} = \frac{1 + \sin \phi}{1 - \sin \phi}$$

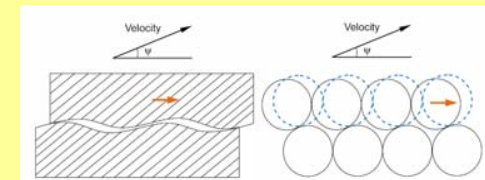
$$\phi = f(\sigma_3, \text{scale})$$

### DILTANCY MODEL: Peak dilatancy (stress-dependent)

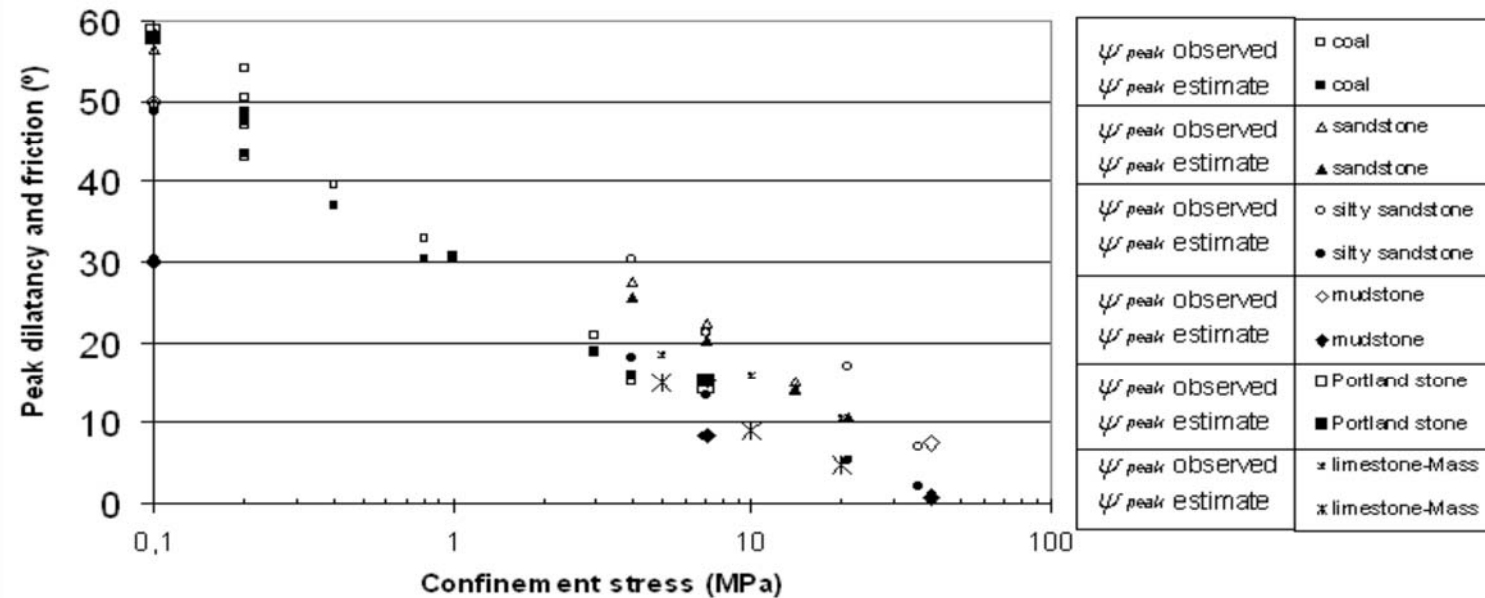
$$\psi_{peak} = \frac{\phi}{1 + \log_{10} \sigma_{ci}} \cdot \log_{10} \frac{\sigma_{ci}}{\sigma_3 + 0.1}$$



BARTON (Dilatancy in joints)



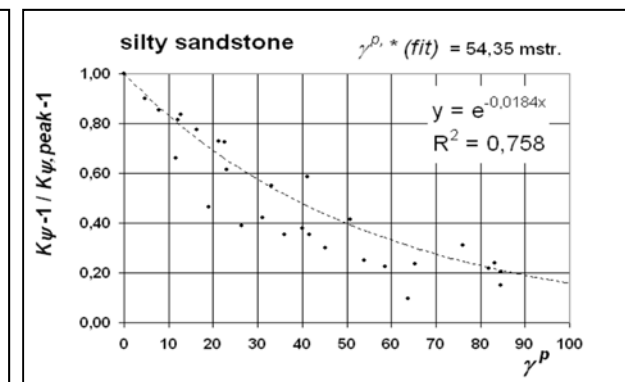
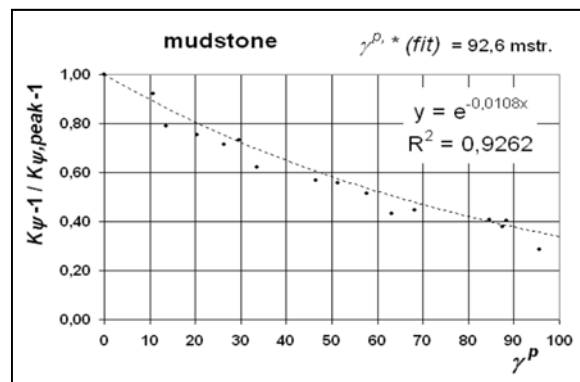
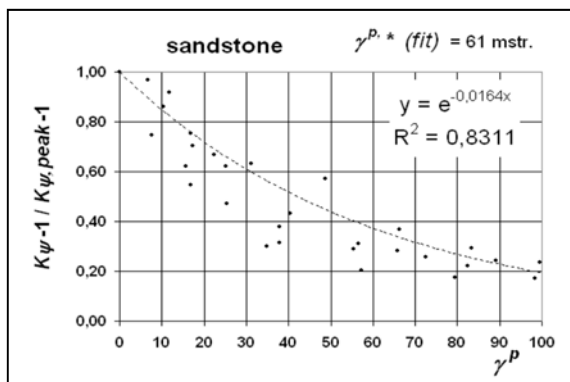
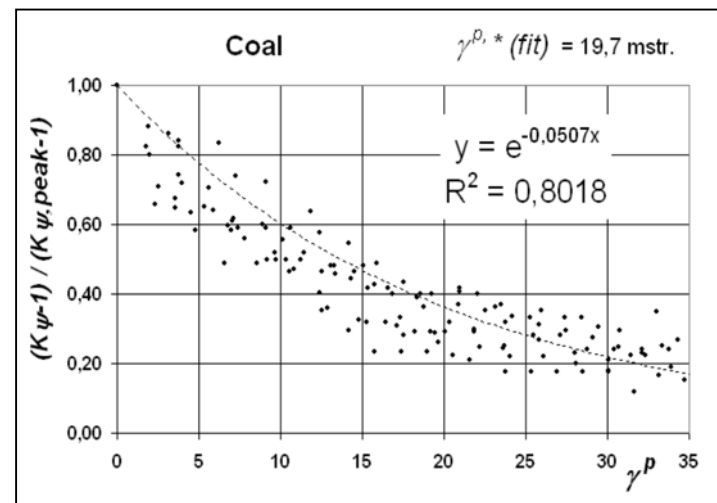
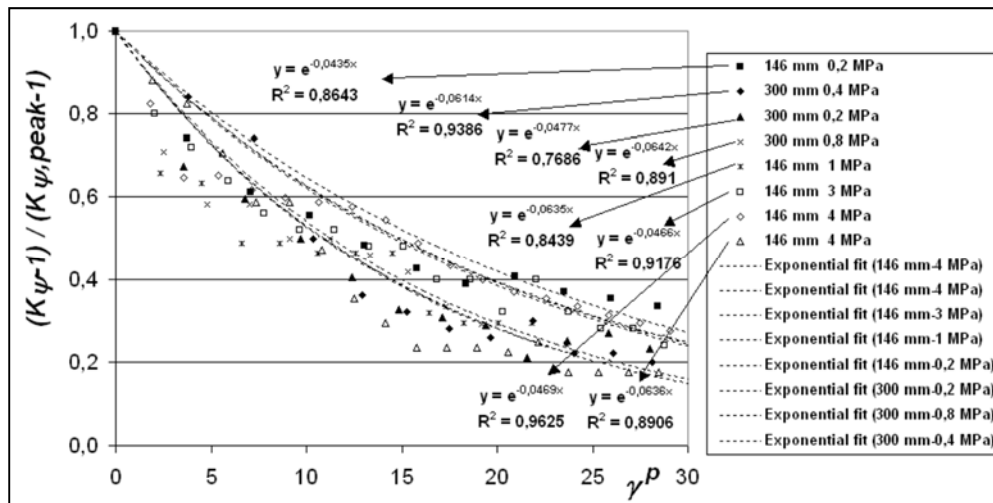
Peak dilatancy angles observed and calculated vs. confinement stress for different rocks  
 [15,39,40]



## DILATANCY MODEL: Evolving dilatancy (plastic-dependent)

$$K_\psi = 1 + (K_{\psi,peak} - 1) \cdot e^{-\frac{\gamma^p}{\gamma^{p,*}}}$$

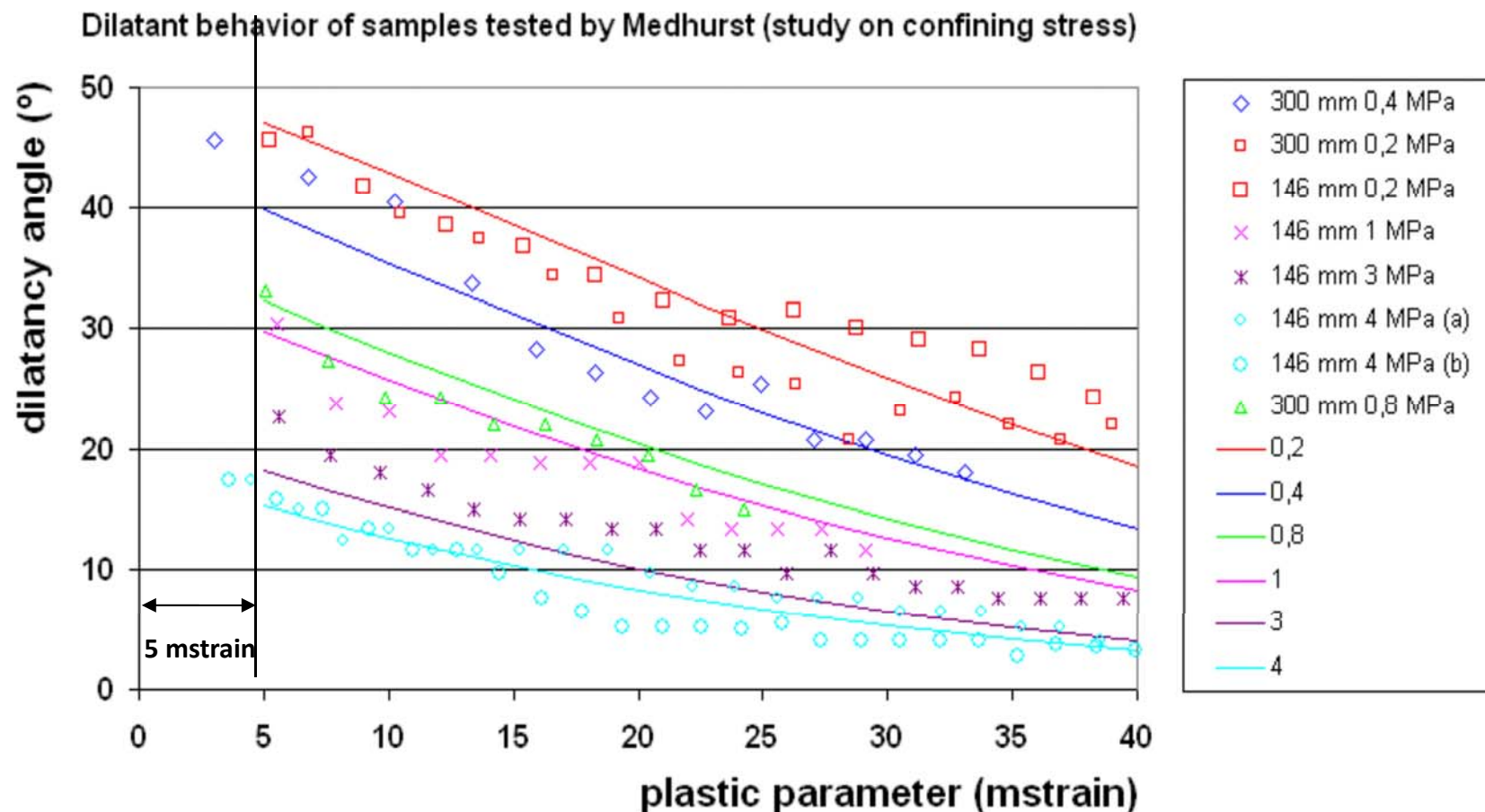
DETournay



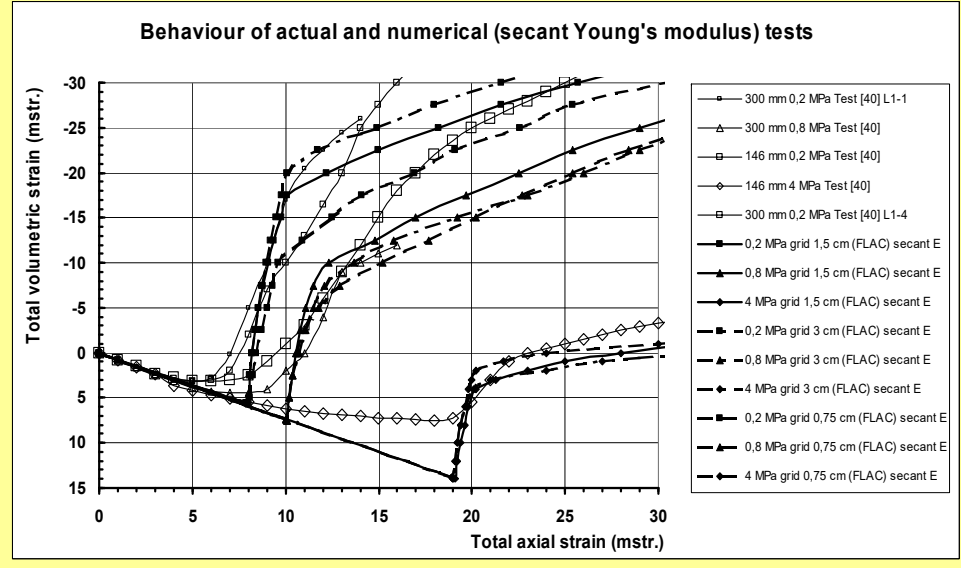
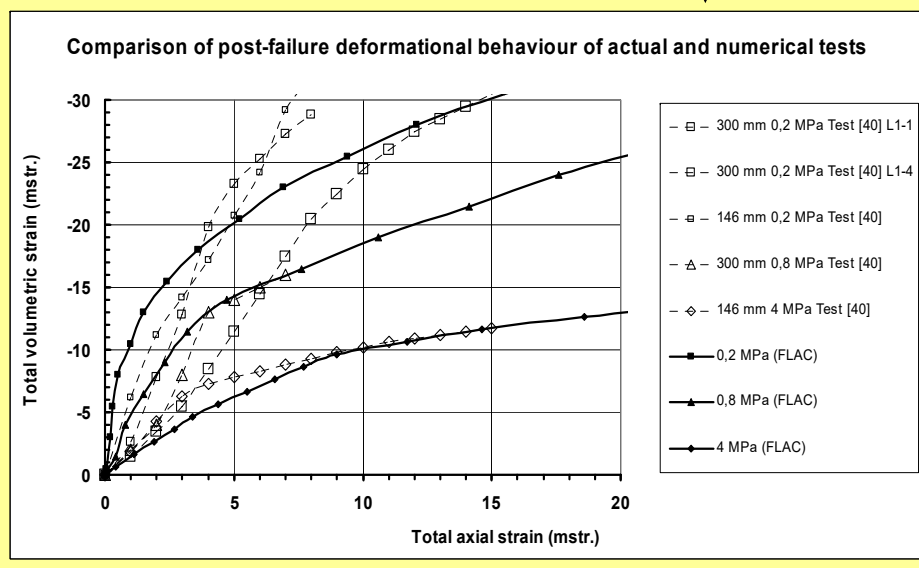
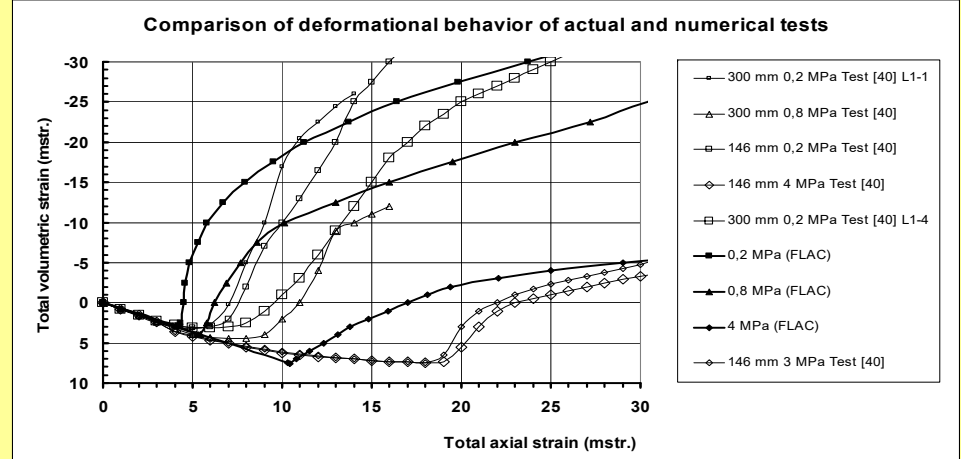
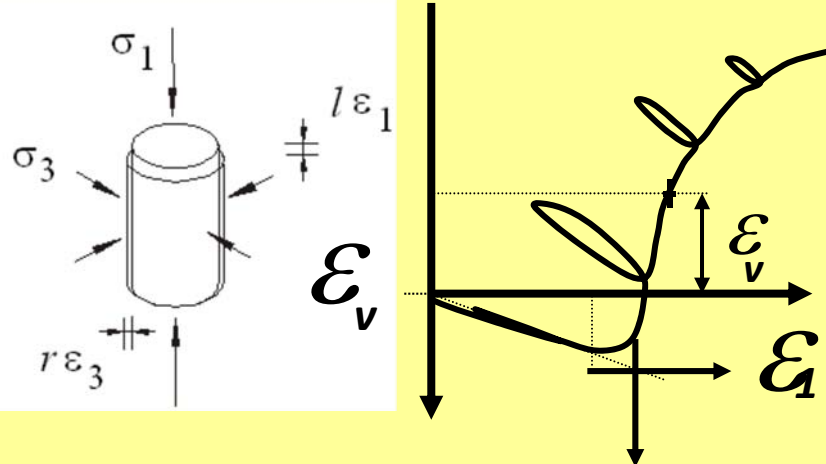
Detournay E (1986) Elastoplastic model of a deep tunnel for a rock with variable dilatancy. Rock Mech Rock Eng 19:99–108

## DILATANCY MODEL: fit to initial values

An offset of 5 mstrain is included to cope with non-elastic effect,  
a satisfactory level of agreement is found



## DILATANCY MODEL: application to triaxial tests (FLAC<sup>2D</sup>) -Validation ??



## CONCLUSIONS

$$\psi_{peak} = \frac{\phi}{1 + \log_{10} \sigma_{ci}} \cdot \log_{10} \frac{\sigma_{ci}}{\sigma_3 + 0.1}$$

$$K_\psi = 1 + (K_{\psi,peak} - 1) \cdot e^{-\frac{\gamma^p}{\gamma^{p*}}}$$

- A dilatancy model focusing rock & rock masses was presented, reflecting dependencies on confinement, plasticity and indirectly scale.
- Comparison of model results with actual test data shows good agreement.
- The model was simple (1 parameter), applicable to rock and rock masses and it can be implemented in NM.
- Preliminary results extend the applications to obtain more realistic GRC for tunnels.

### Zhao & Cai Dilatancy Model

In this model dilatancy was considered from CI and CD and it grows rapidly and then decays as in the A&A (2005) model.

$$\psi = ab[\exp(-b\gamma_p) - \exp(-c\gamma_p)]/(c-b)$$

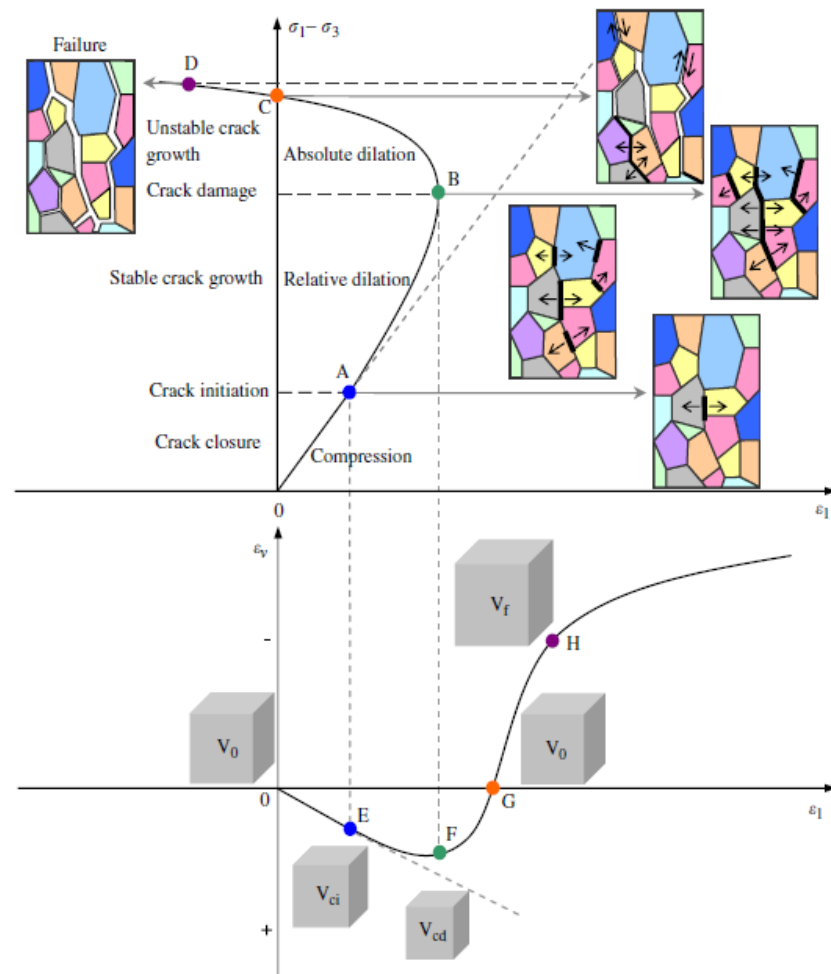
$$a = a_1 + a_2 \exp(-\sigma_3/a_3)$$

$$b = b_1 + b_2 \exp(-\sigma_3/b_3)$$

$$c = c_1 + c_2(\sigma_3)^{c_3}$$

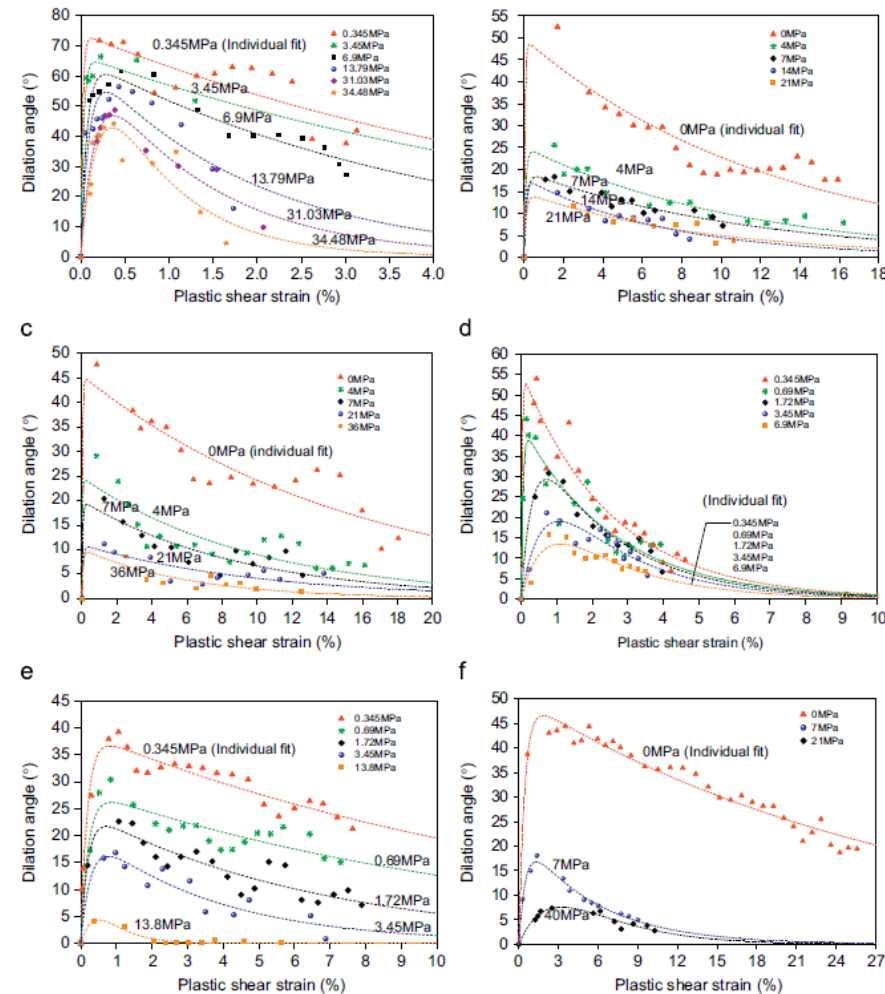
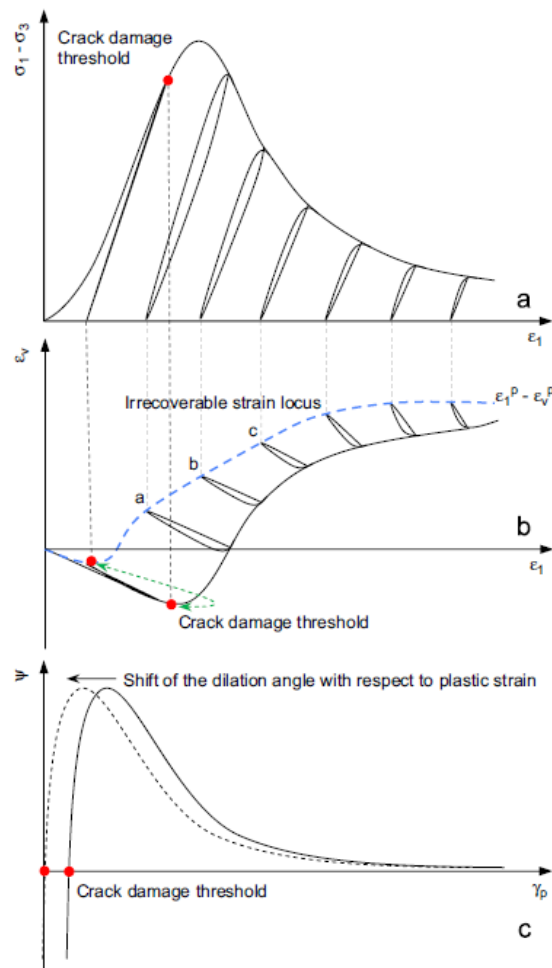
Fit coefficients for confining stress dependent  $a, b, c$  of seven rocks.

Rock type	$a$			$b$			$c$		
	$a_1$	$a_2$	$a_3$	$b_1$	$b_2$	$b_3$	$c_1$	$c_2$	(%)
Quartzite	63.17	11.92	2.80	5.83	36.25	6.77	0.14	1.14	1.23
Sandstone(strong)	14.63	34.90	3.40	4.06	15.56	5.54	0.08	0.40	0.58
Silty sandstone	10.34	34.76	4.90	10.14	17.77	16.26	0.07	1.13	0.55
Sandstone(weak)	20.93	35.28	2.34	0.99	44.39	0.73	0.37	3.54	0.47
Coal	20.03	35.64	0.89	10.47	26.58	1.31	0.15	17.5	0.82
Mudstone	17.19	32.40	3.37	0.09	2.23	23.6	0.03	8.75	0.25
Seatearth	12.57	27.23	2.09	1.49	4.02	6.62	0.07	2.90	1.60



X.G. Zhao, M. Cai. 2010. A mobilized dilation angle model for rocks International Journal of Rock Mechanics & Mining Sciences 47: 368–384

### Zhao & Cai Dilatancy Model



X.G. Zhao, M. Cai. 2010. A mobilized dilation angle model for rocks International Journal of Rock Mechanics & Mining Sciences 47: 368–384

### Zhao & Cai Dilatancy Model

- The method help to solve the problem of pre-peak dilatancy by adjusting the starting point of dilatancy at the CD stress
- The method is rather accurate, at the expense of needing 9 parameters (without know physical meaning) which are fitted when a god number of data is available. In this sense it goes against the Occam's razor principle (the simple, the better).
- Numerical models better represent sample behaviour since an appropriate decay function for cohesion and friction was input.
- The model focus intact rock but forget rock masses.

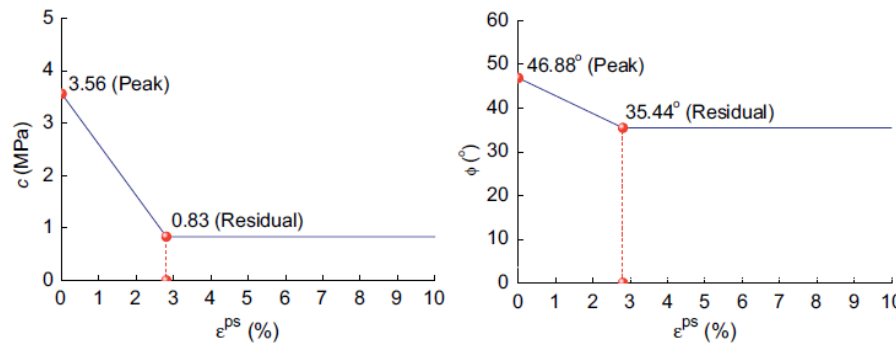
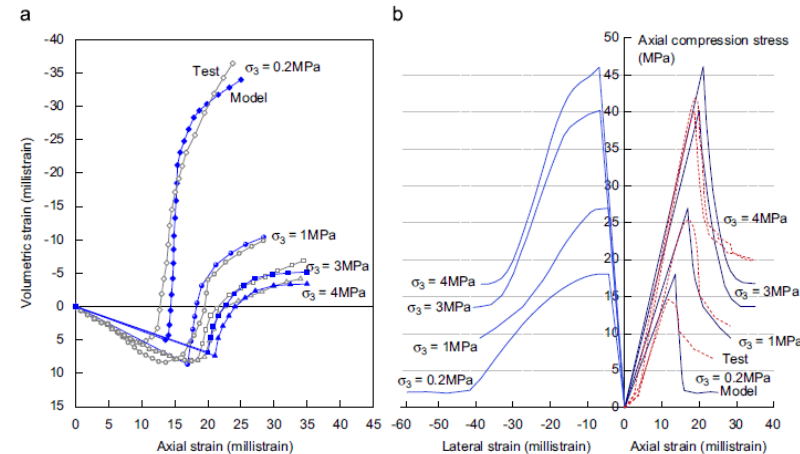


Fig. 15. Illustration of the  $c$  and  $\phi$  as a bilinear decay function of plastic strain.



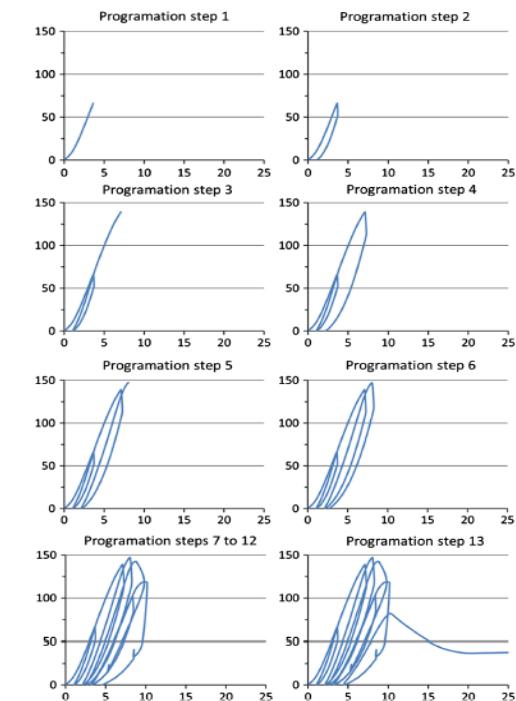
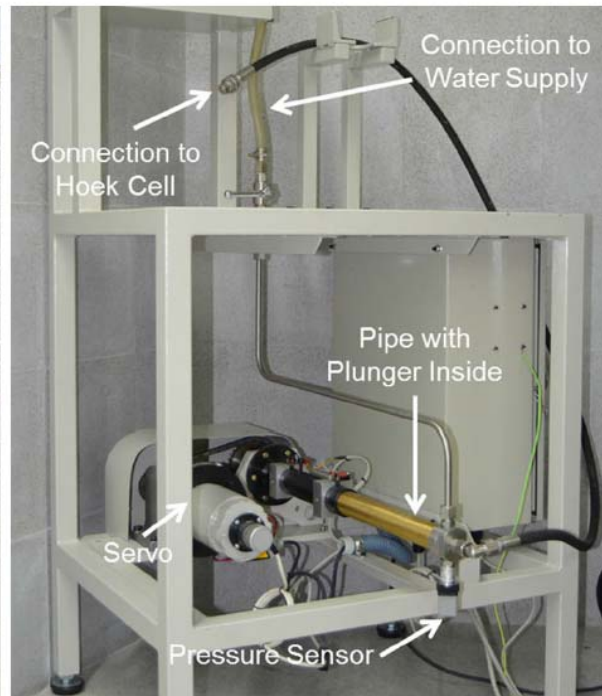
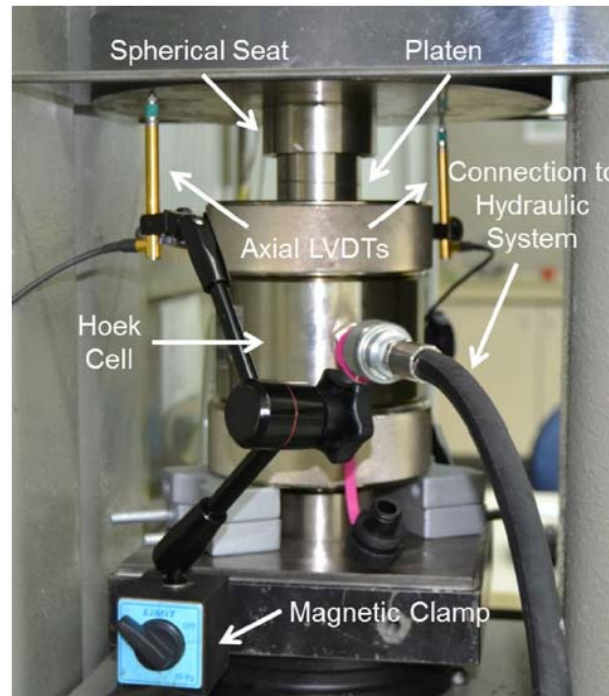
X.G. Zhao, M. Cai. 2010. A mobilized dilation angle model for rocks International Journal of Rock Mechanics & Mining Sciences 47: 368–384

### Additional developments in UVIGO lab

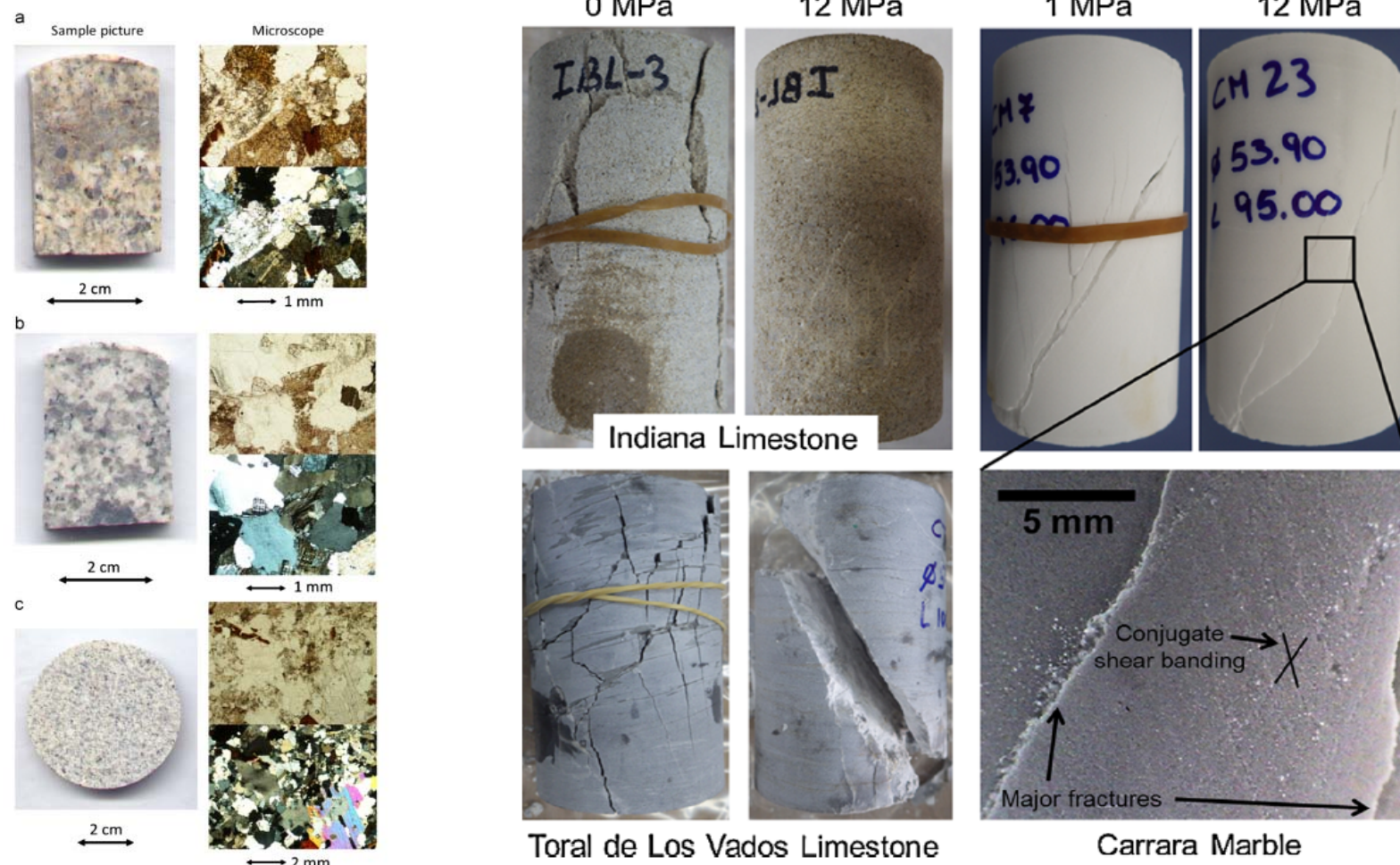
We develop a system in our lab to carry out tests measuring post-failure deformation. To control deformation we tend to use loading-unloading cycles.

We carry out this type of tests in 3 granites and then some sedimentary and metamorphic rocks.

Results often did not fit the A&A model. Obviously they fit y the Z&C model.



### Additional developments in UVIGO lab

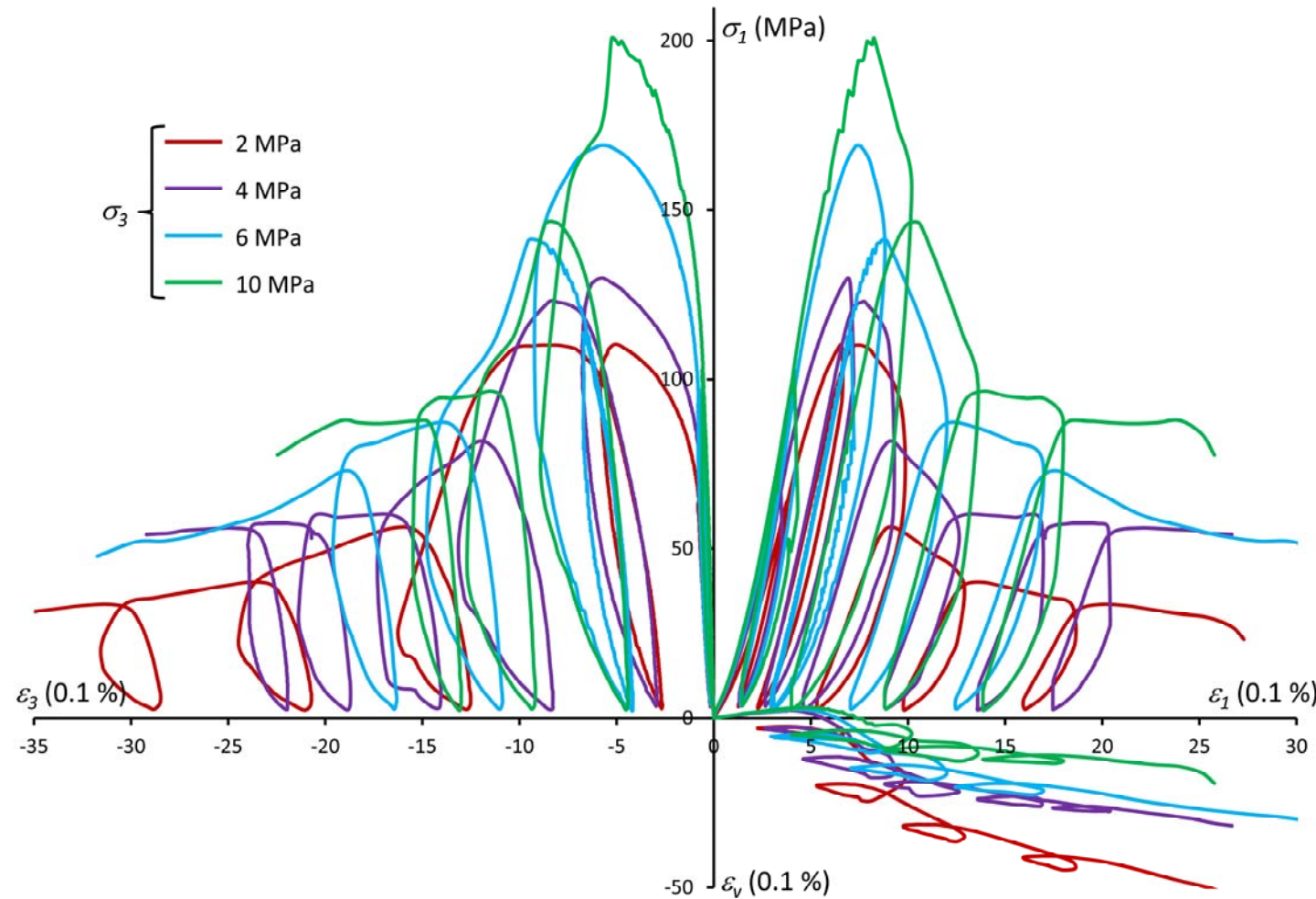


Arzúa J, Alejano LR. 2013. Dilation in granite according to servo-controlled strength tests. Int J Rock Mech Min Sci 61:43–56.

Walton G, Arzua J, Alejano LR, Diederichs MS. 2015. A laboratory-testing-based study on the strength, deform-ability, and dilatancy of Carbonate Rocks at Low Confinement. Rock Mech Rock Eng (2015) 48:941–958.

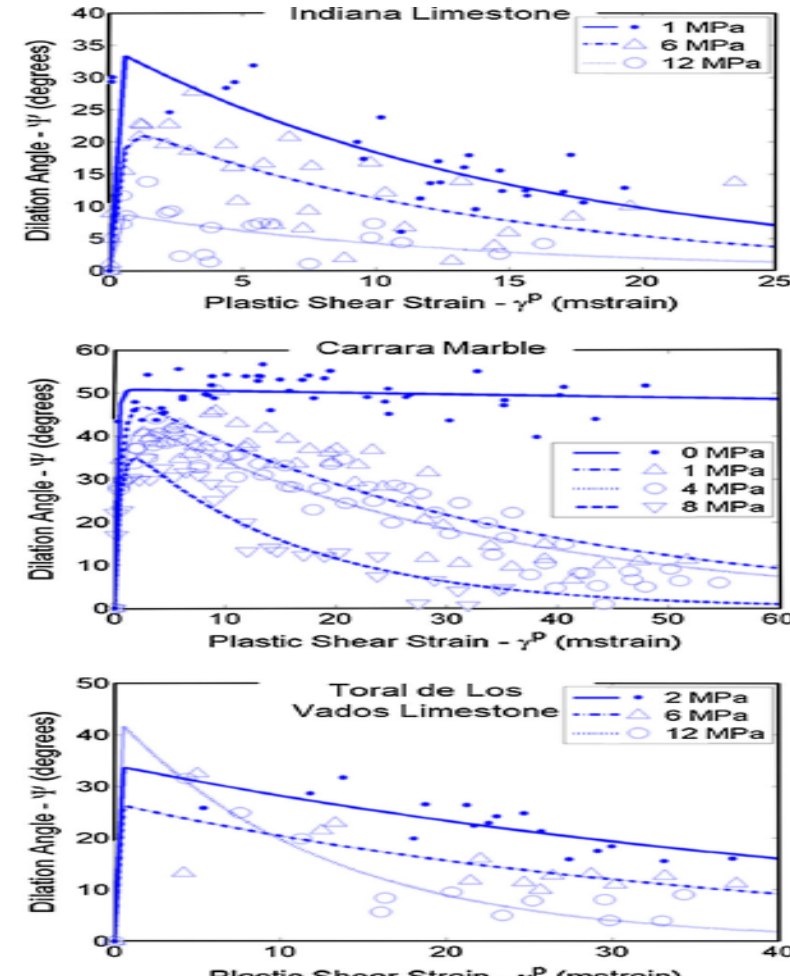
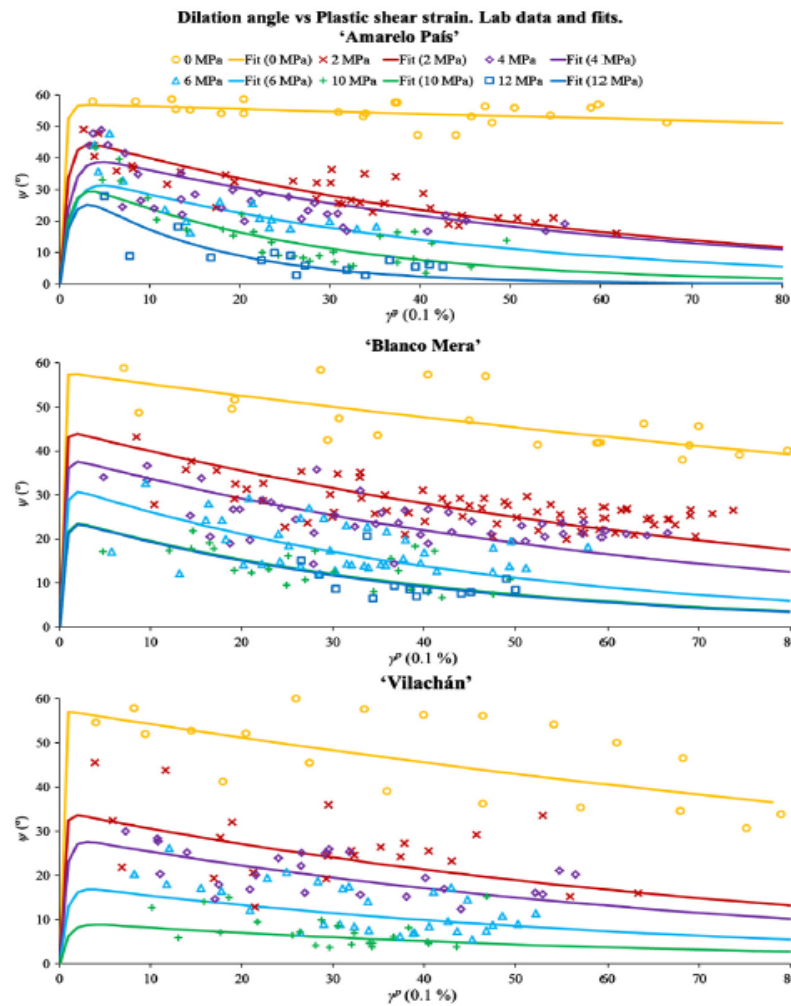
### Additional developments in UVIGO lab

#### Complete stress-strain curves (Amarelo País)



Arzúa J, Alejano LR. 2013. Dilation in granite according to servo-controlled strength tests. Int J Rock Mech Min Sci 61:43–56

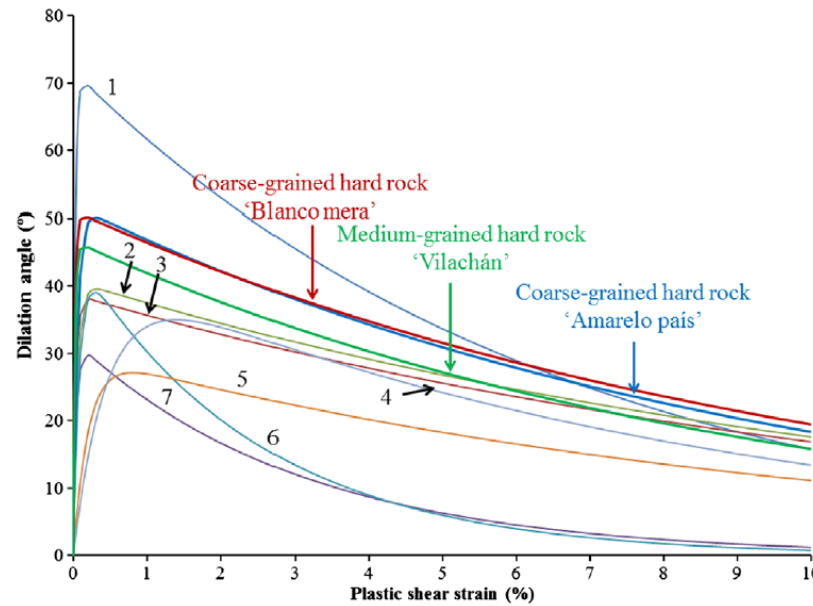
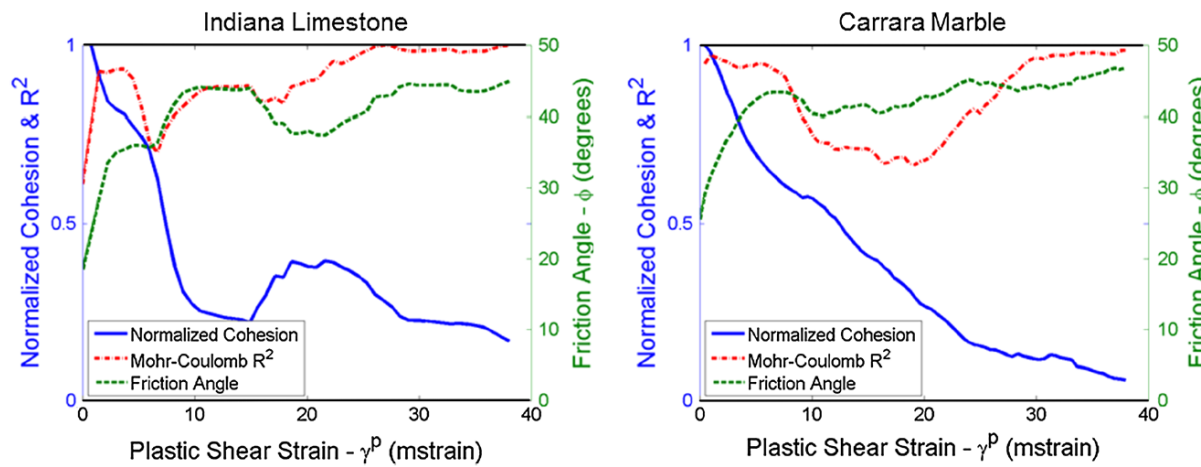
### Additional developments in UVIGO lab



Arzúa J, Alejano LR. 2013. Dilation in granite according to servo-controlled strength tests. Int J Rock Mech Min Sci 61:43–56.

Walton G, Arzua J, Alejano LR, Diederichs MS. 2015. A laboratory-testing-based study on the strength, deform-ability, and dilatancy of Carbonate Rocks at Low Confinement. Rock Mech Rock Eng (2015) 48:941–958.

## 2. THE DECADE 2005-2015 – TESTING IN OUR LAB



Walton G, Arzua J, Alejano LR, Diederichs MS. 2015. A laboratory-testing-based study on the strength, deformability, and dilatancy of Carbonate Rocks at Low Confinement. *Rock Mech Rock Eng* (2015) 48:941–958.

### Walton & Diederichs Model

$$\psi_{peak}(\sigma_3) = \begin{cases} \text{For sedimentary rocks:} \\ \frac{\phi_{peak}}{1 + \log_{10}(\sigma_{ci})} \cdot \log_{10}\left(\frac{\sigma_{ci}}{\sigma_3 + 0.1}\right) \\ \\ \text{For crystalline rocks:} \\ \begin{cases} \phi_{peak} \cdot \left(1 - \frac{\beta'}{e^{-\left(\frac{1-\beta_0-\beta'}{\beta'}\right)}} \cdot \sigma_3\right) \text{ when } \sigma_3 < e^{-\left(\frac{1-\beta_0-\beta'}{\beta'}\right)} \\ \phi_{peak} \cdot (\beta_0 - \beta' \cdot \ln(\sigma_3)) \text{ when } \sigma_3 > e^{-\left(\frac{1-\beta_0-\beta'}{\beta'}\right)} \end{cases} \\ \\ \psi(\sigma_3, \gamma^p) = \begin{cases} \frac{\alpha \cdot \gamma^p \cdot \psi_{peak}}{e^{\left(\frac{\alpha-1}{\alpha}\right)} \gamma_m} \text{ when } \gamma^p < \gamma_m \cdot e^{\left(\frac{\alpha-1}{\alpha}\right)} \\ \psi_{peak} \cdot \left(\alpha \cdot \ln\left(\frac{\gamma^p}{\gamma_m}\right) + 1\right) \text{ when } \gamma_m \cdot e^{\left(\frac{\alpha-1}{\alpha}\right)} \leq \gamma^p < \gamma_m \\ \psi_{peak} \cdot e^{\left(\frac{-(\gamma^p - \gamma_m)}{\gamma^*}\right)} \text{ when } \gamma^p \geq \gamma_m \end{cases} \end{cases}$$

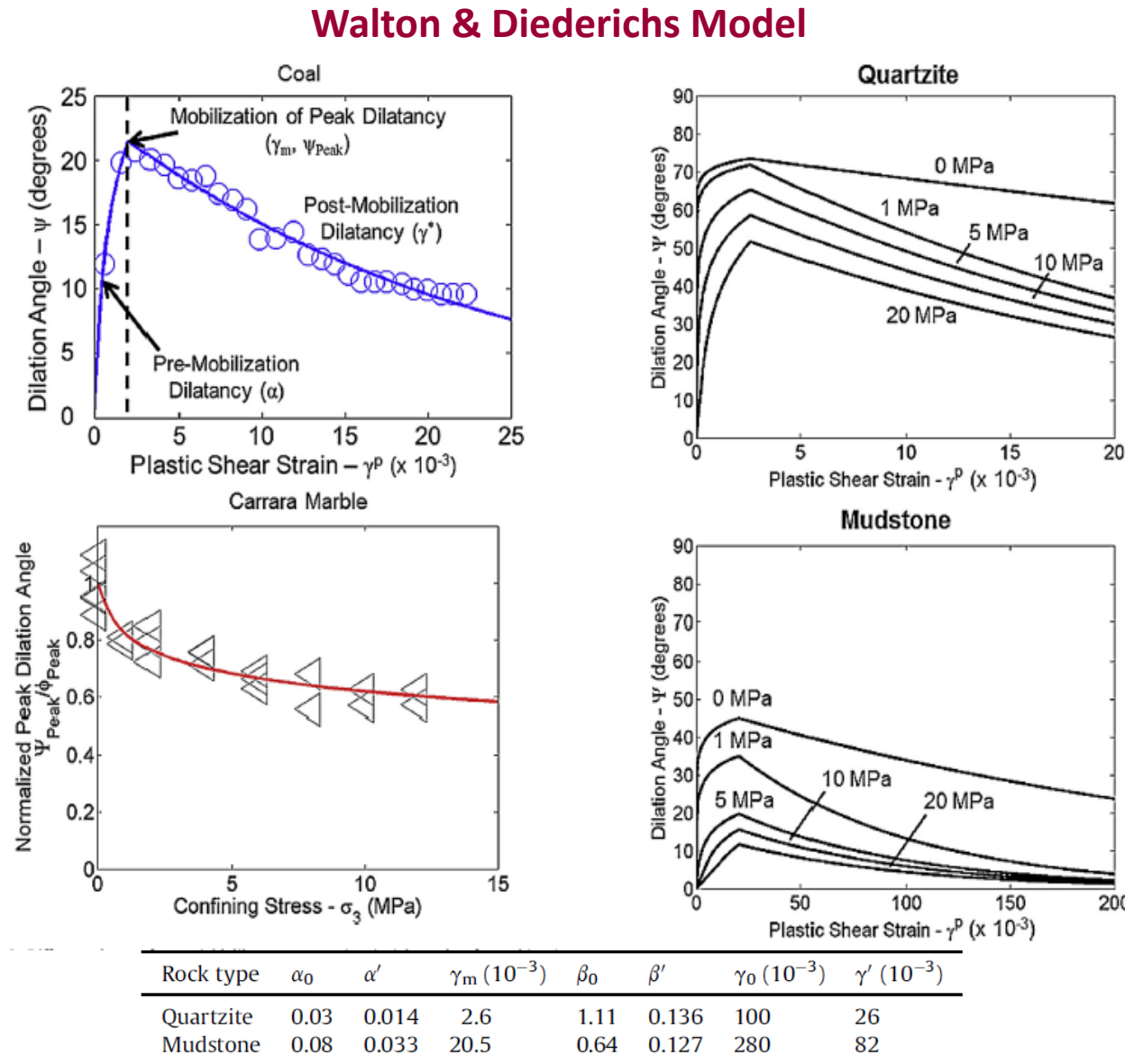
Model mathematically more complex than Z&C, using less parameters (6-7 with more physical meaning, instead of 9), adapted for CI, CD, but applicable to rock (in-situ brittle rock), not to rock masses.

$$\beta', \beta_0, \gamma', \gamma_0, \gamma_m, \alpha \& \alpha'$$

$$\gamma^* = \begin{cases} \gamma_0 \text{ when } \sigma_3 = 0 \\ \gamma' \text{ when } \sigma_3 \neq 0 \end{cases}$$

$$\alpha = \alpha_o + \alpha' \cdot \sigma_3$$

Different phases of post-yield dilatancy as seen in triaxial test data for coal (top) and confinement dependency of the peak dilation angle ( $\psi_{\text{Peak}}$ ) for Carrara Marble (bottom).

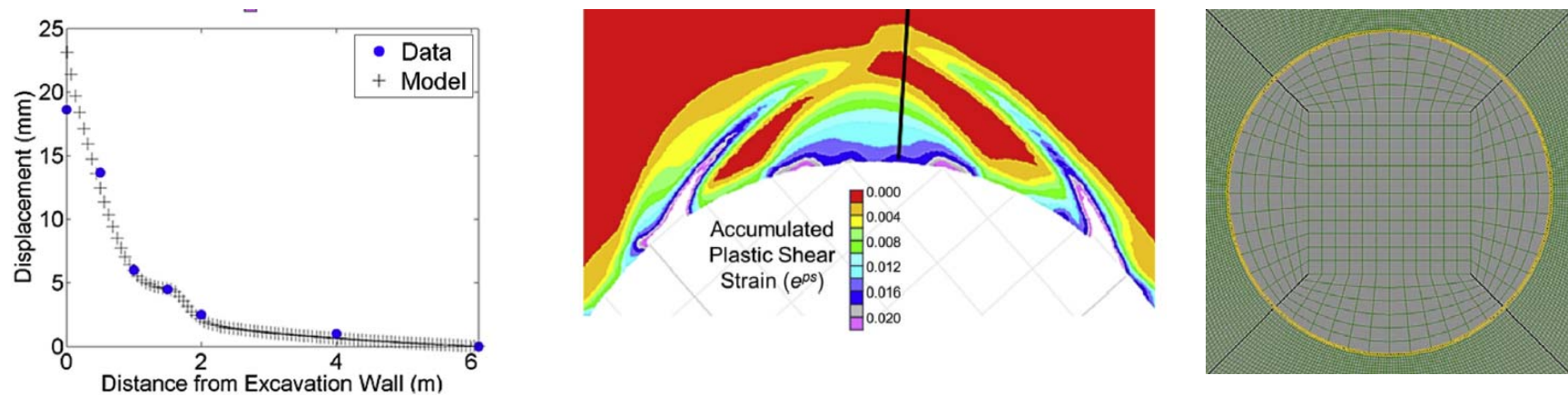


Walton G, Diederichs MS. 2015. A new model for the dilation of brittle rocks based on laboratory compression test data with separate treatment of dilatancy mobilization and decay. Gotech Geol Eng 33:661–679

WD dilation angle model results for Witwatersrand quartzite (top) and mudstone (bottom) with confining stresses and parameter values shown in table below,

### Walton & Diederichs Model

Using several case studies, the ability of an appropriate mobilized dilation model combined with a CWFS strength model to replicate observed brittle deformation in situ was shown. Although there is still uncertainty associated with exact parameter values obtained from the back analyses performed due to the lack of in situ data available, the applicability of the mobilized dilation angle was shown.



Arizona mine shaft case study: extremely fine mesh used to model strain localization, contours of plastic shear strain with extensometer location indicated, and comparison of model results and extensometer data

Back analyzed CWFS material parameters for the foliated quartzite present at 1582 m depth in the Silver Shaft.

Peak cohesion, $c$ (MPa)	Initial friction angle, $\phi_i$ ( $^\circ$ )	Plastic shear strain ( $e^{ps}$ ) to residual cohesion ( $10^{-3}$ )	Plastic shear strain ( $e^{ps}$ ) to peak friction ( $10^{-3}$ )	Residual cohesion, $c_r$ (MPa)	Peak friction angle, $\phi_p$ ( $^\circ$ )	$\alpha_0$	$\alpha'$	$\beta_0$	$\beta'$	$e_m^{ps}$ ( $10^{-3}$ )	$e_0^{ps}$ ( $10^{-3}$ )	$e^{ps'}$ ( $10^{-3}$ )
35	0	1	2	0.8	55	0.05	0.01	1	0.1	0.5	7.5	7.5

Walton G, Diederichs MS, Alejano LR, Arzúa J. 2014a. Verification of a laboratory-based dilation model for in situ conditions using continuum models. *J Rock Mech Geotech Eng* 6:522–534.

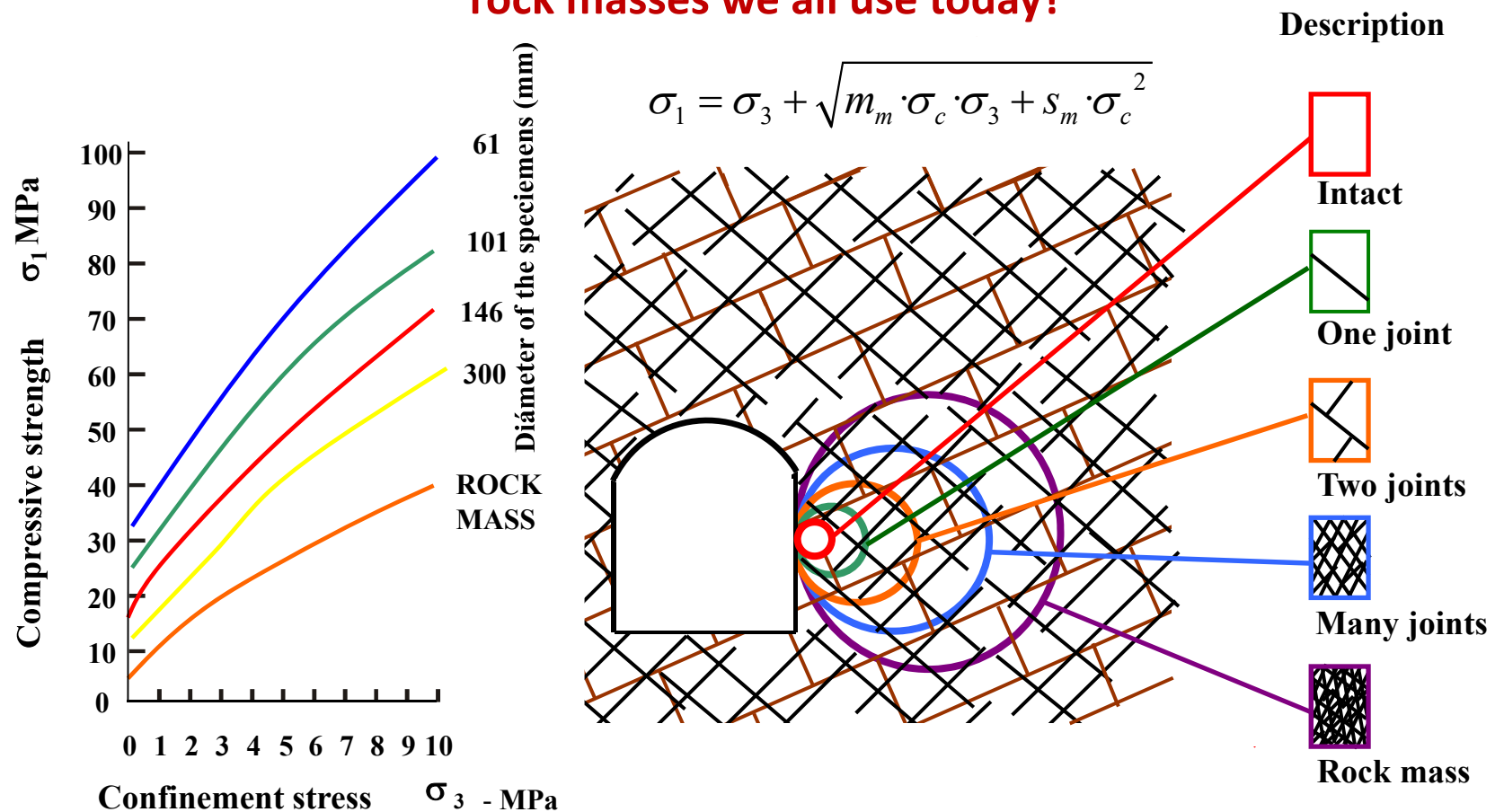
# CONCLUSIONS

- Over the original Alejano & Alonso (2005) dilatancy models, two new models focusing rocks were proposed (Zhao & Cai model (2010) and (Walton and Diederichs 2015)).
- Both were interesting; one is more accurate but it is more black-box type, does not permit to interpret the mechanisms behind. The other has less parameters of more physical meaning, and it is particularly developed focused typical brittle spalling behaviour in combination with CWFS evolving failure criteria.
- Both are interesting but both are much less simple than A&A model and are not thought to be extended to rock mass scale (average quality rock masses), since they need many parameters fitted starting from lab test data.
- How to proceed towards understanding what happens at the rock mass scale? In 1960s we knew how to estimate intact rock strength, but NOT ROCK MASS STRENGTH. Now we know how to estimate rock dilatancy, but NOT ROCK MASS DILATANCY.

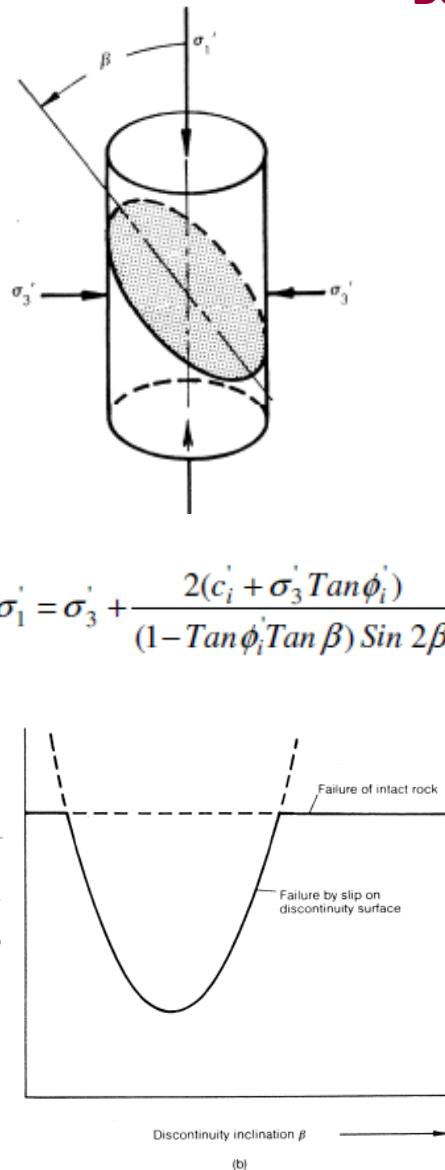
#### Some concepts

In 1970s we knew how to estimate intact rock strength, but NOT ROCK MASS STRENGTH.  
 Now we know how to estimate rock dilatancy, but NOT ROCK MASS DILATANCY.

**How professors Hoek & Brown come to propose their failure criterion for rock masses we all use today?**



#### Behind Hoek & Brown failure criterion



$$\sigma_1' = \sigma_3' + \frac{2(c_i' + \sigma_3' \tan \phi_i')}{(1 - \tan \phi_i' \tan \beta) \sin 2\beta}$$

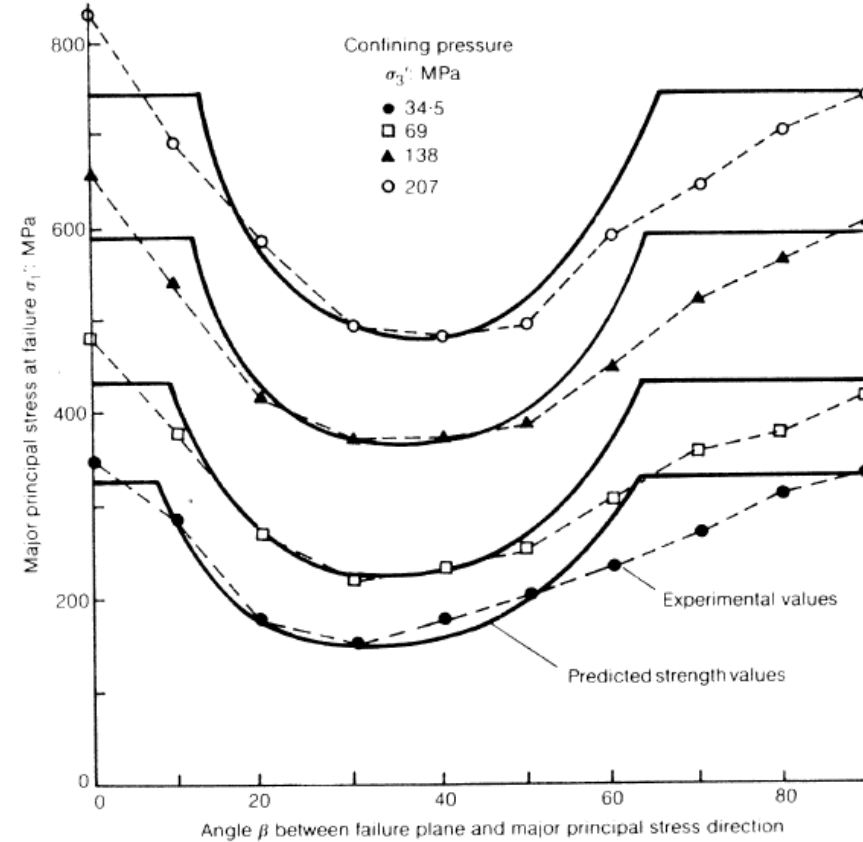
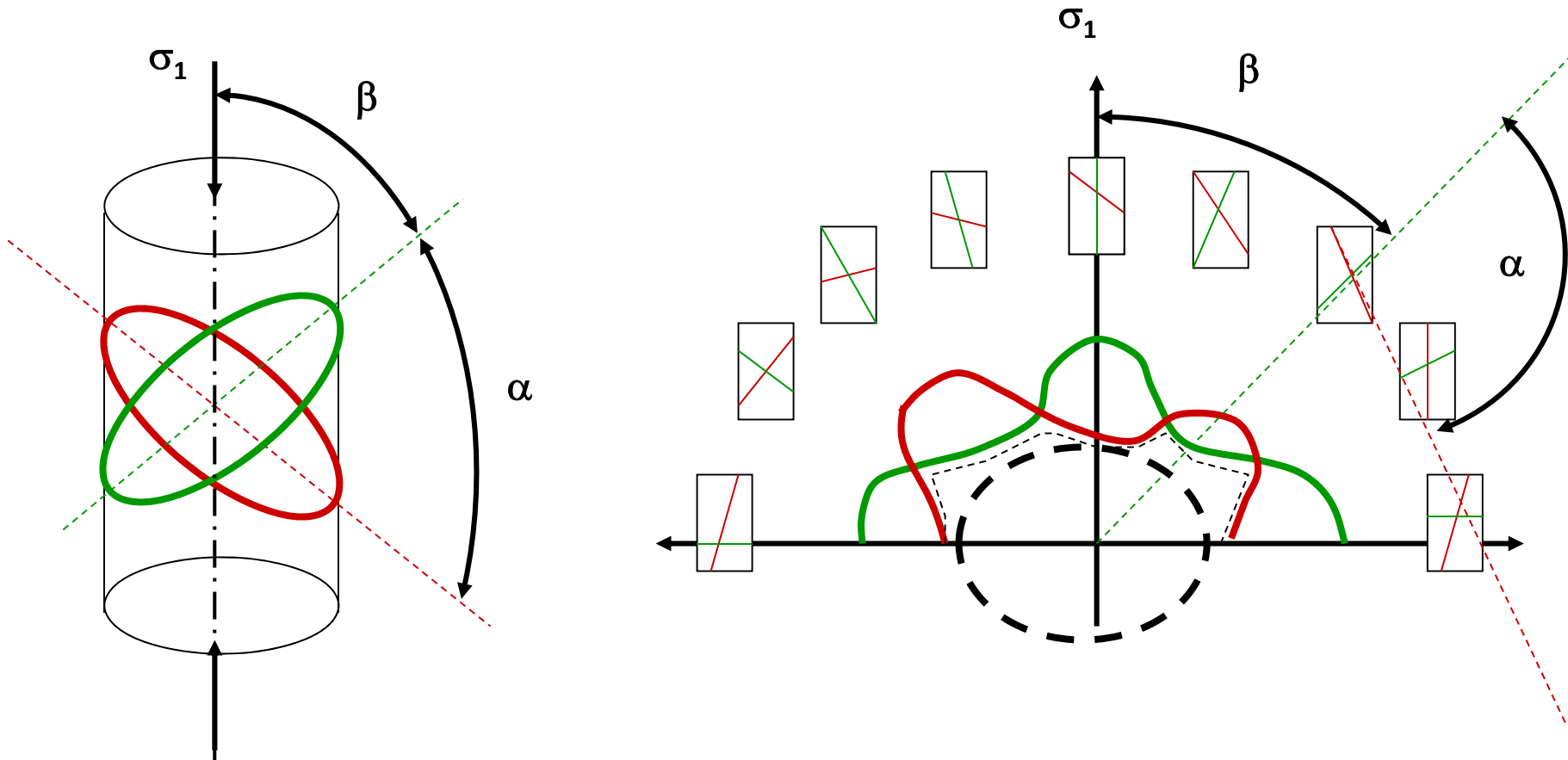


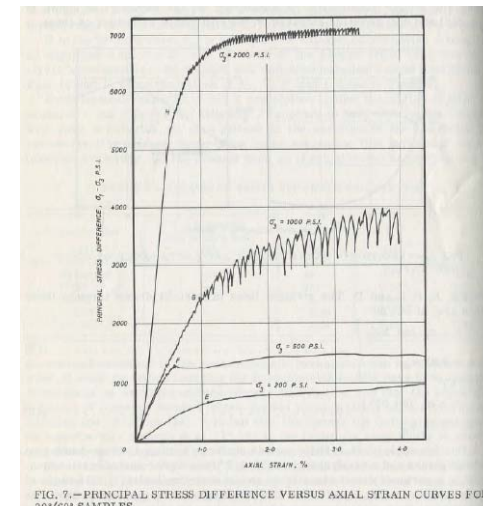
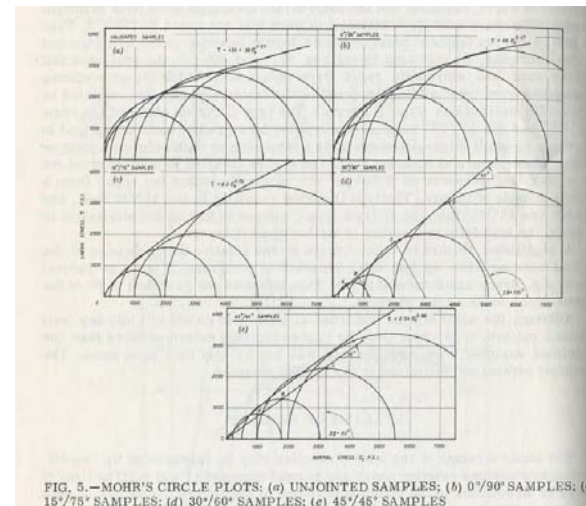
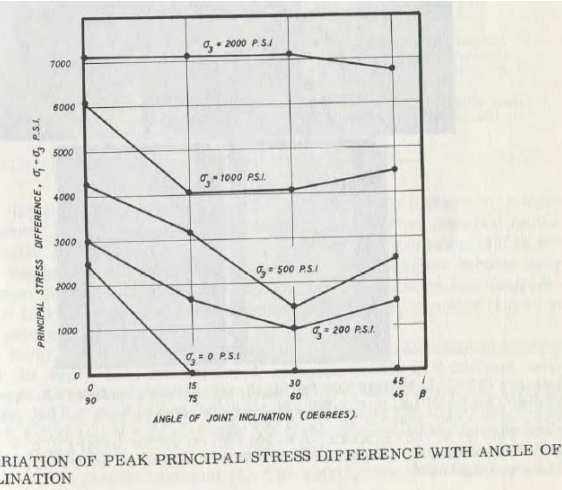
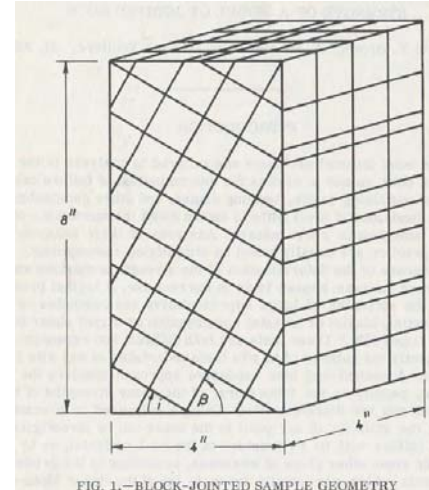
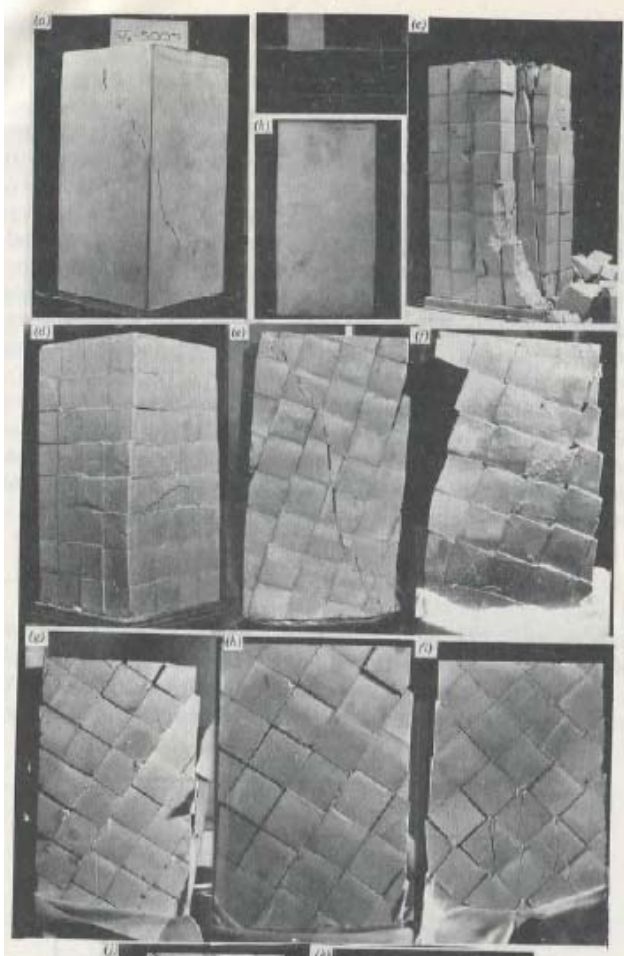
Figure 12 : Triaxial test results for slate with different failure plane inclinations, obtained by McLamore and Gray (1967), compared with strength predictions from equations 3 and 14.

#### Behind Hoek & Brown failure criterion



Variation of the uniaxial compressive strength of a specimen with two joints

#### Behind Hoek & Brown failure criterion



## Behind Hoek & Brown failure criterion

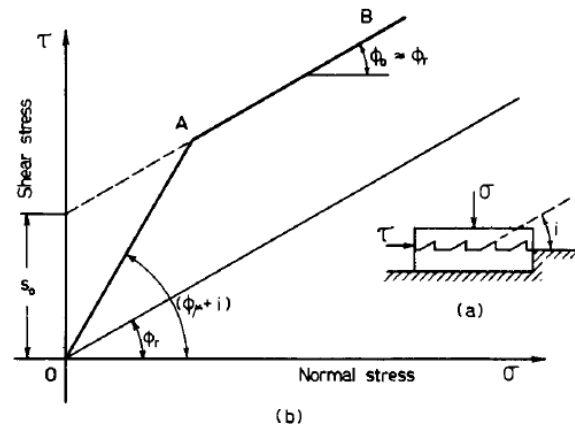


Fig. 1—Bilinear failure envelope for multiple inclined surfaces according to Patton.<sup>4</sup>

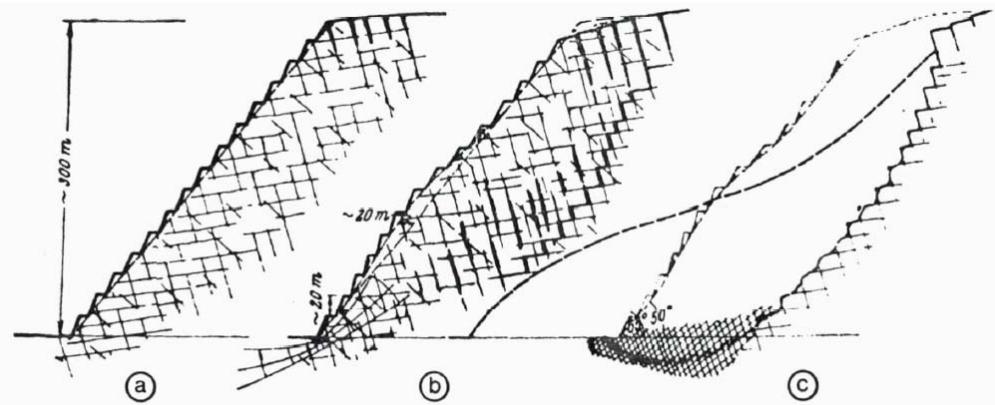
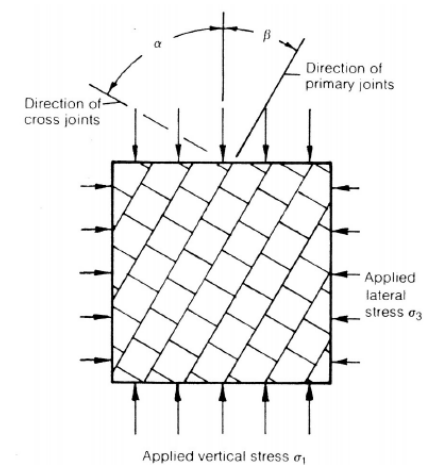
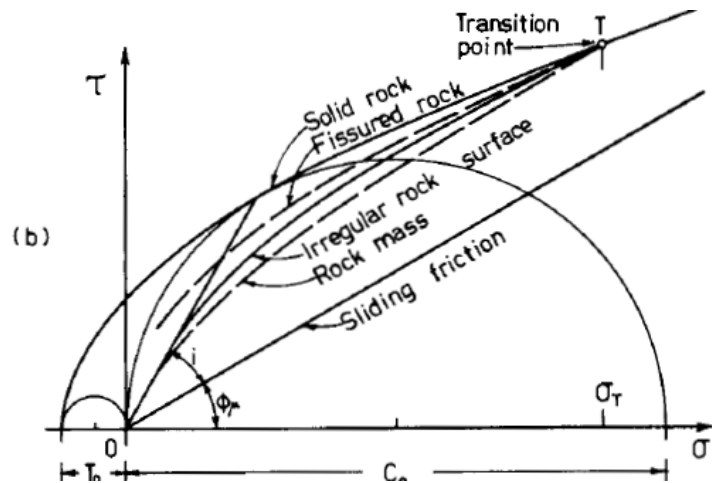
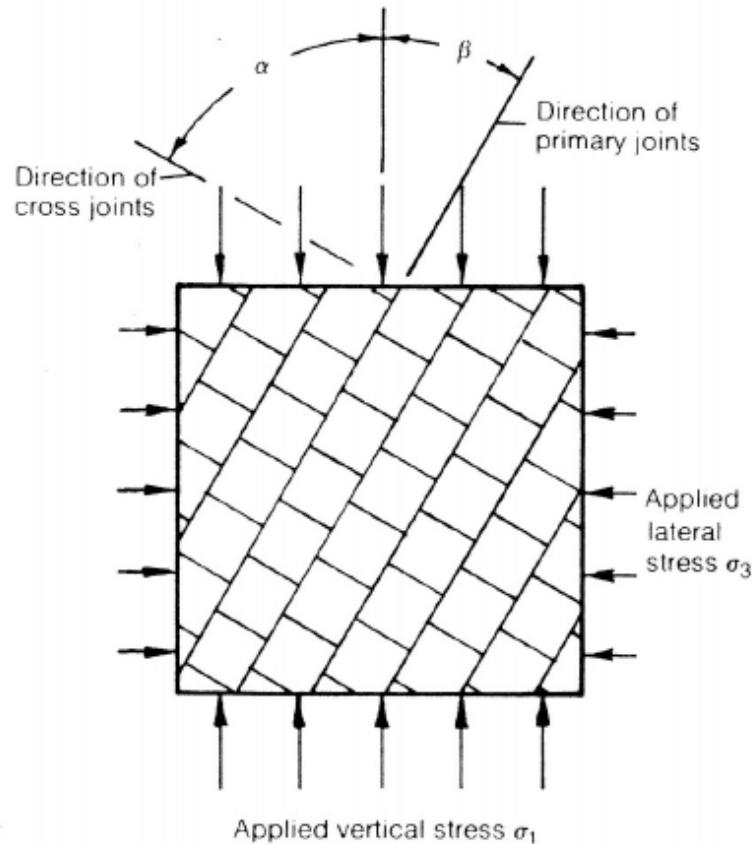


FIGURE 1 — Trois phases de la rupture progressive d'un talus rocheux, d'après Müller (1963):

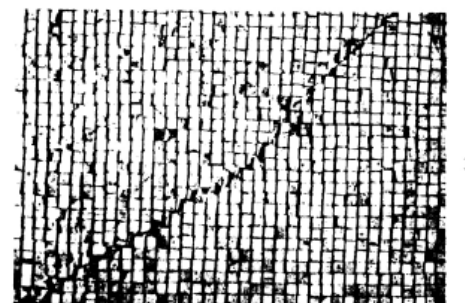
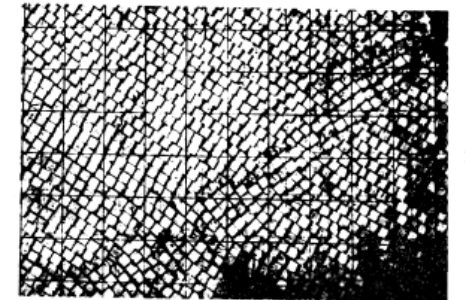


Ladanyi B, Archambault G (1972) Évaluation de la résistance au cisaillement d'un massif rocheux fragmenté. In: Proceedings of the 24th international geological congress, Montreal; 1972; vol 130: 249–260

#### Behind Hoek & Brown failure criterion

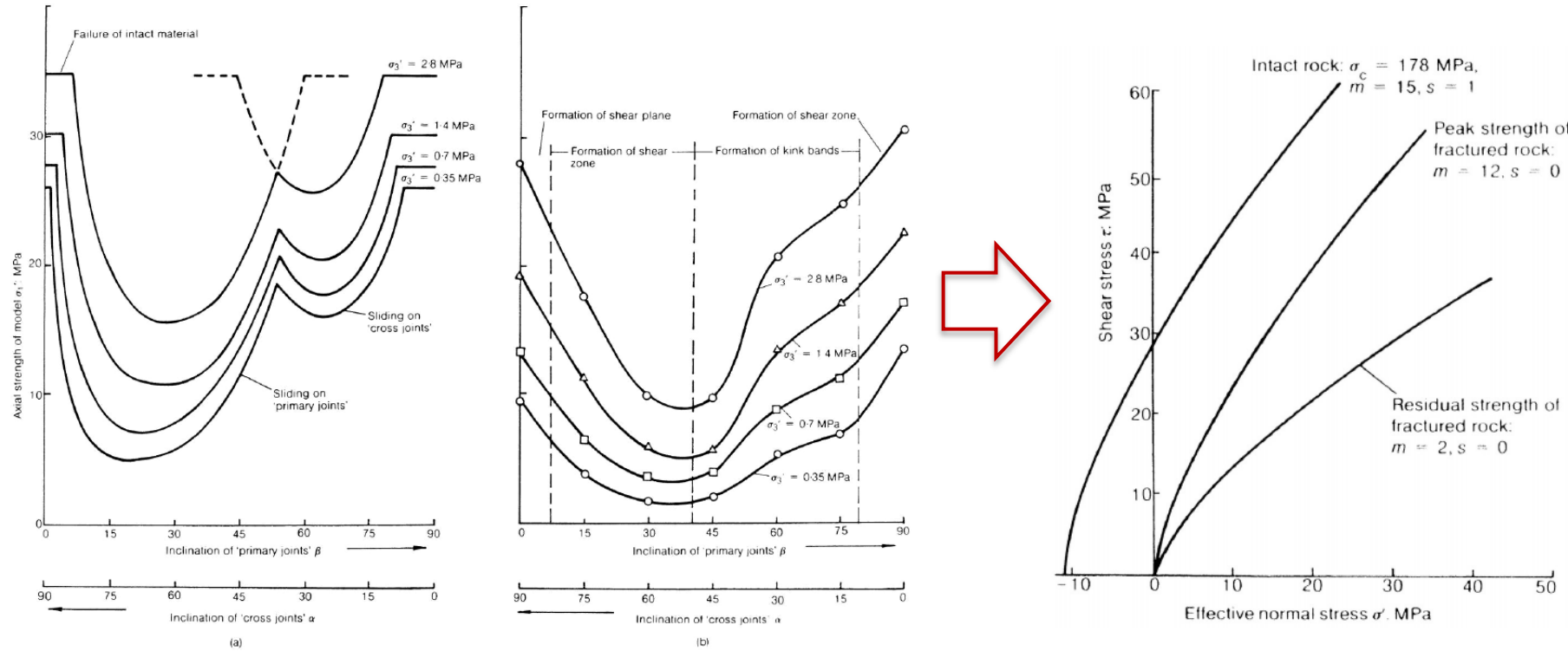


Configuration of brickwall model tested by Ladanyi and Archambault (1972)



Ladanyi B, Archambault G (1972) Évaluation de la résistance au cisaillement d'un massif rocheux fragmenté. In: Proceedings of the 24th international geological congress, Montreal; 1972; vol 130: 249–260

#### Behind Hoek & Brown failure criterion

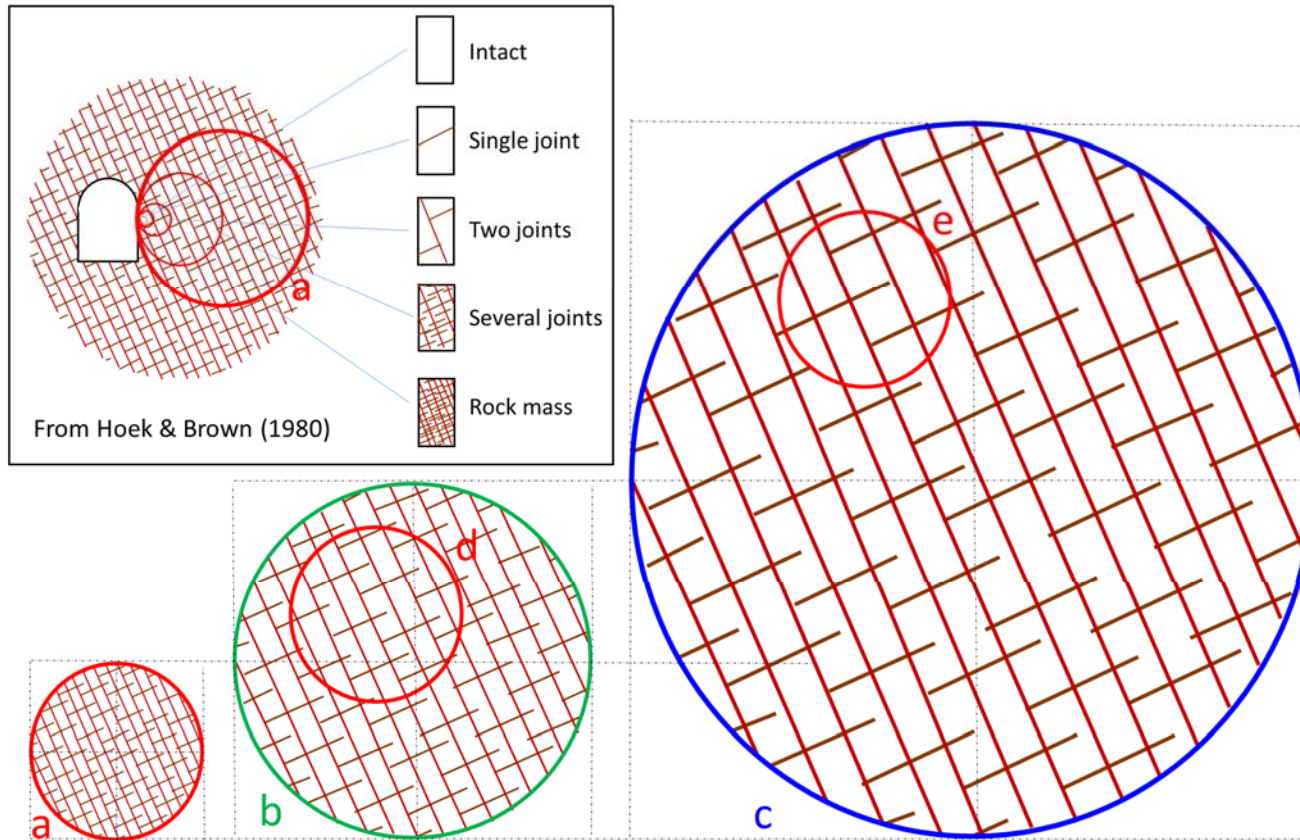


Comparison between a) predicted and b) observed strength of brickwall model tested by Ladanyi & Archambault (1972). From Hoek (1983). This figure explains how the sharply defined predicted transitions between different failure modes do not occur in practice. This illuminated Professors Hoek & Brown to propose the extension of their failure criterion to rock masses.

**Can we use jointed samples to study rock mass behavior ?**

### Behind Hoek & Brown failure criterion

Can we follow something similar to study also post-failure behavior ?



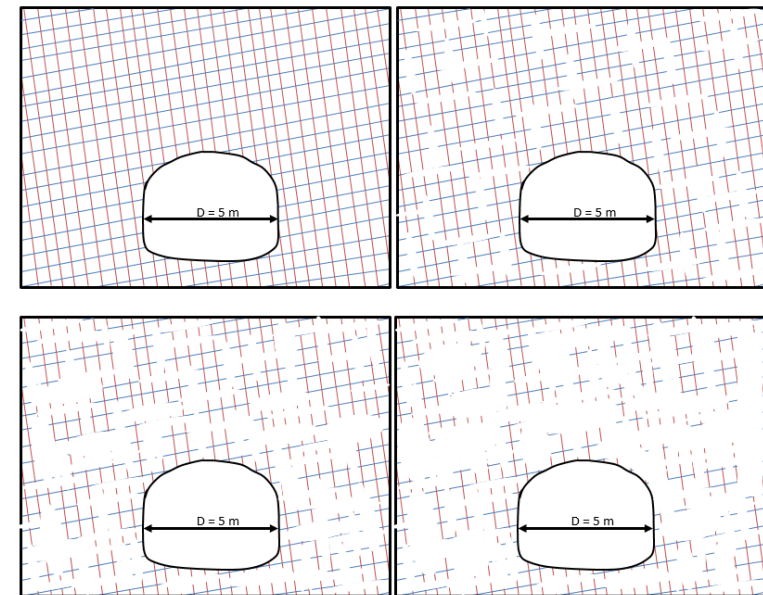
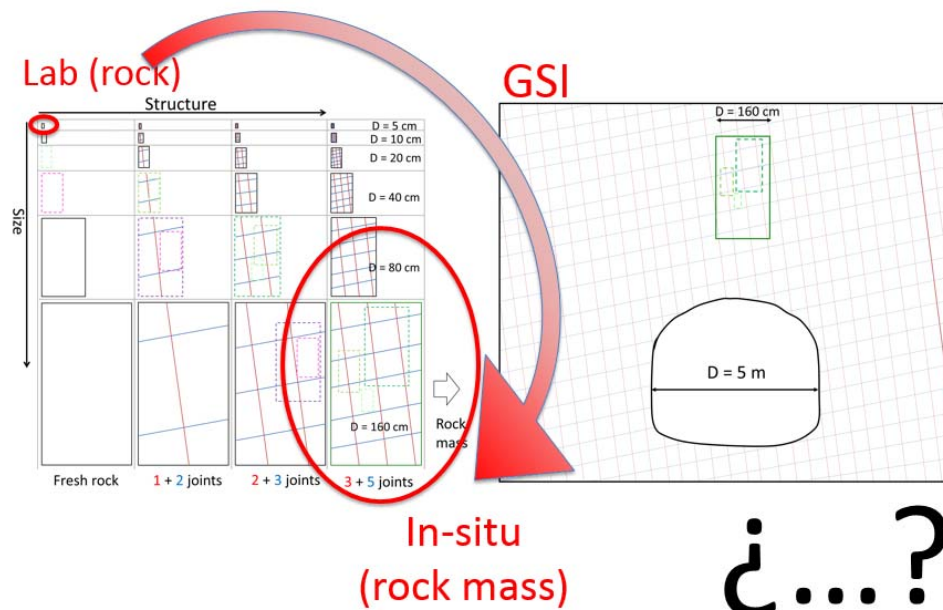
Scale and structure in rock masses. a, rock mass sample representative of rock mass behavior at the engineering scale; b and c, homothetic transformation of circle a by doubling and quadrupling its size; d and e, rock mass samples of the same size as a but with original structures corresponding to b and c.

Alejano LR, Arzúa J, Bozorgzadeh N, Harrison JP. (2017) Triaxial strength and deformability of intact and increasingly jointed granite samples. Int J Rock Mech Min Sci 95:87–103

### Some concepts

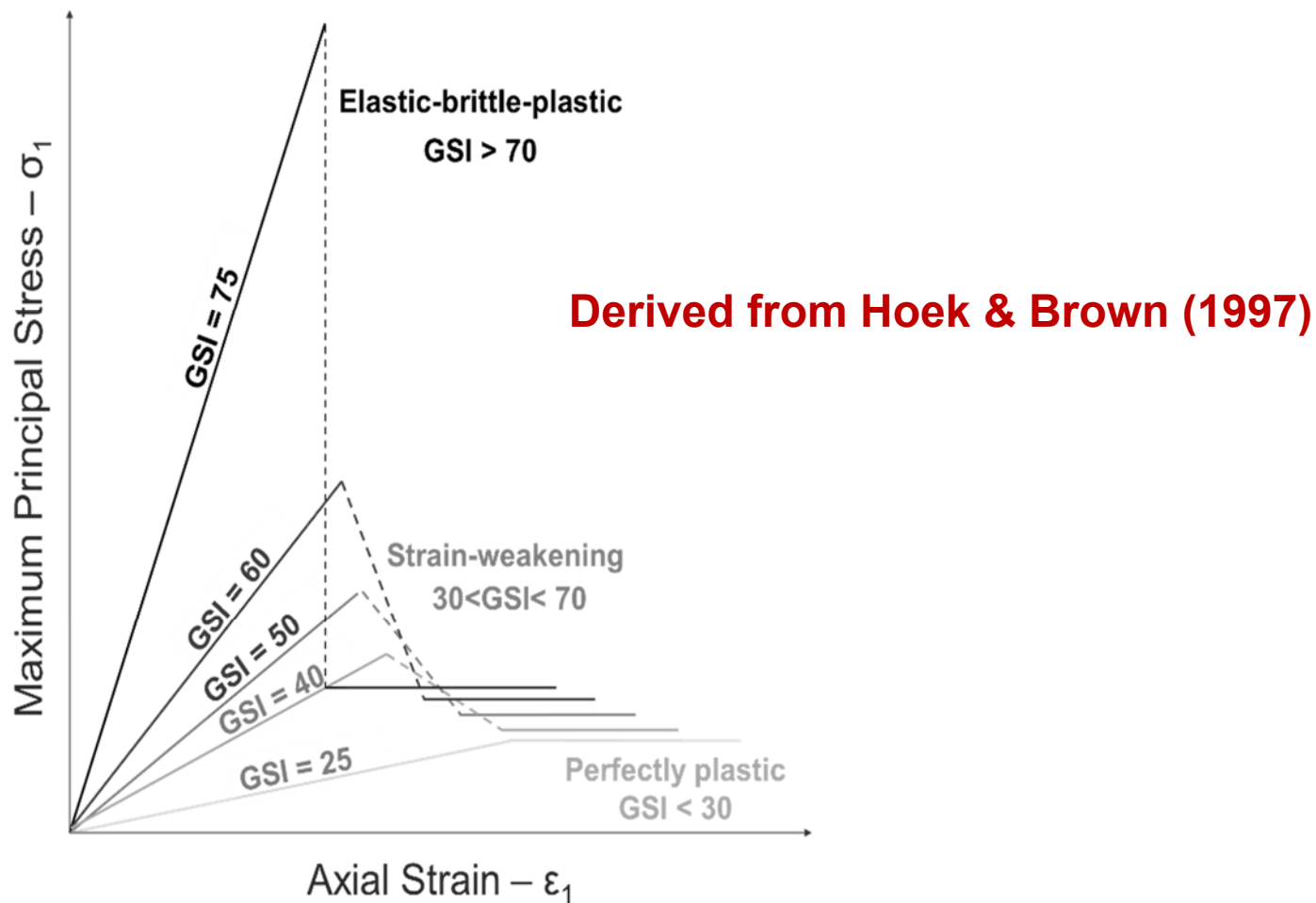
A procedure to estimate of the mechanical properties of a rock mass at different scales is still not available. It is necessary to postulate and verify methods of estimating rock mass properties from those of the constituent elements (rock + structure (joints in the rock) + scale).

The GSI approach can be convenient at large scales (over a REV), but it certainly does not work at mine pillar scale. It should be thought on the relevance of the different features contributing to rock mass behaviour variation at different scales, particularly in post-failure.



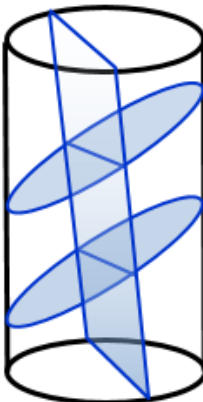
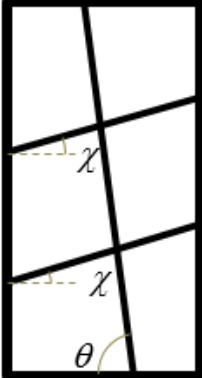
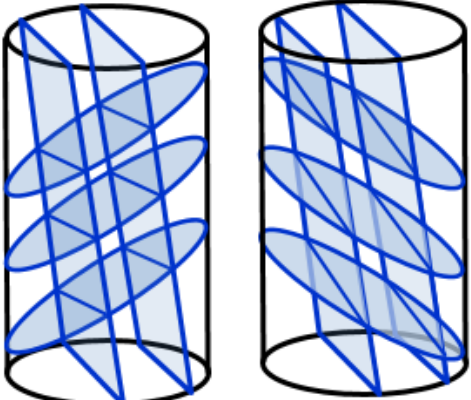
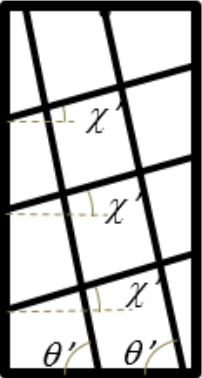
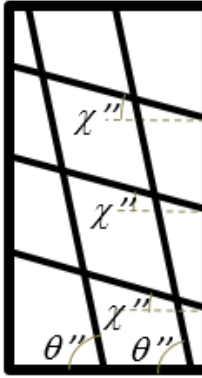
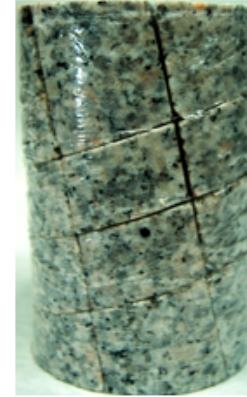
### Some concepts

Can we distinguish the role of scale and the role of jointing?



Hoek E, Brown ET. Practical estimates of rock mass strength. Int J Rock Mech Min Sci Geomech Abstr. 1997;34:1165–1186.

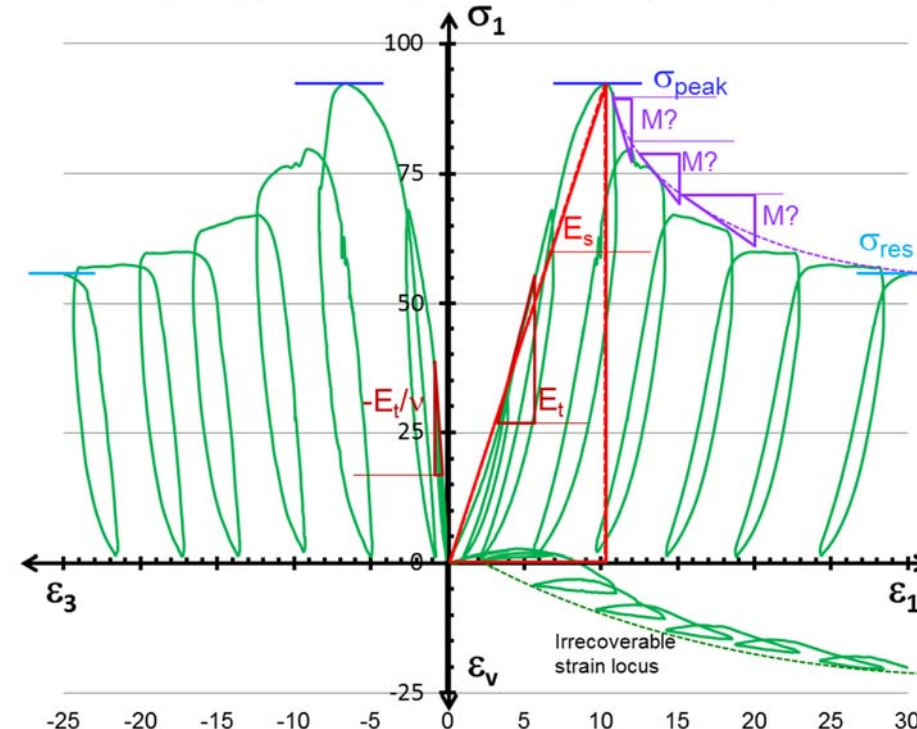
### Laboratory tests

	3D sketches	Cross-cut sections	Pictures
a)		$\theta = 85.0 \pm 1.9^\circ$ $\chi = 23.6 \pm 0.8^\circ$ 	
b)		$\theta' = 78.4 \pm 1.0^\circ$ $\chi' = 22.7 \pm 1.0^\circ$  $\theta'' = 77.2 \pm 1.0^\circ$ $\chi'' = 22.9 \pm 0.5^\circ$ 	

Alejano LR, Arzúa J, Bozorgzadeh N, Harrison JP. (2017) Triaxial strength and deformability of intact and increasingly jointed granite samples. Int J Rock Mech Min Sci 95:87–103

### Laboratory tests

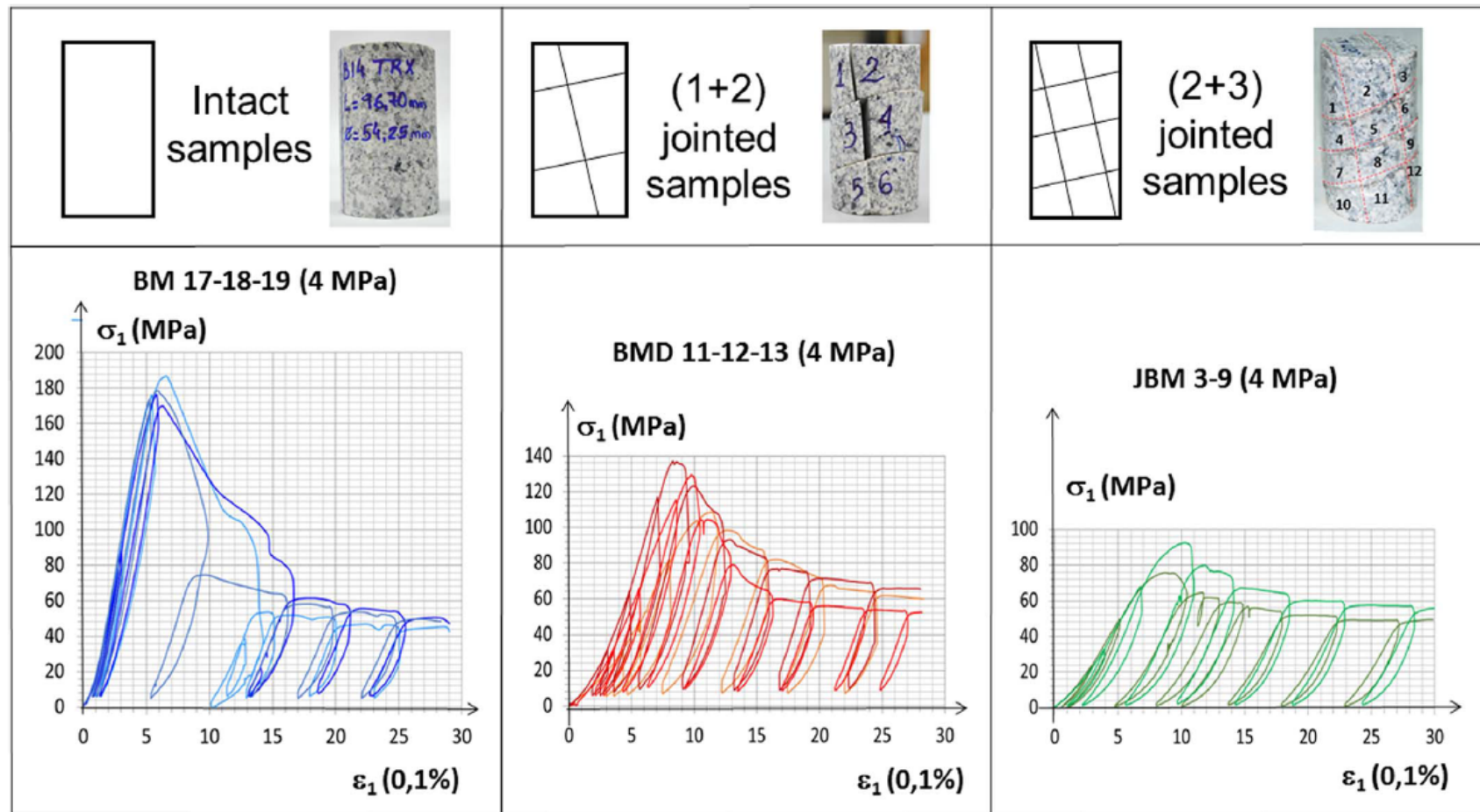
Complete Stress (MPa) - Strain (0.1 %) curve  
 (3 + 2) jointed sample JBM9 (for  $\sigma_3 = 4$  MPa)



Complete stress-strain curve resulting from a confined ( $\sigma_3=4$  MPa) compressive strength test on a 2+3 jointed specimen with unloading-reloading cycles. Also shown is how key parameters were obtained.

Alejano LR, Arzúa J, Bozorgzadeh N, Harrison JP. (2017) Triaxial strength and deformability of intact and increasingly jointed granite samples. Int J Rock Mech Min Sci 95:87–103

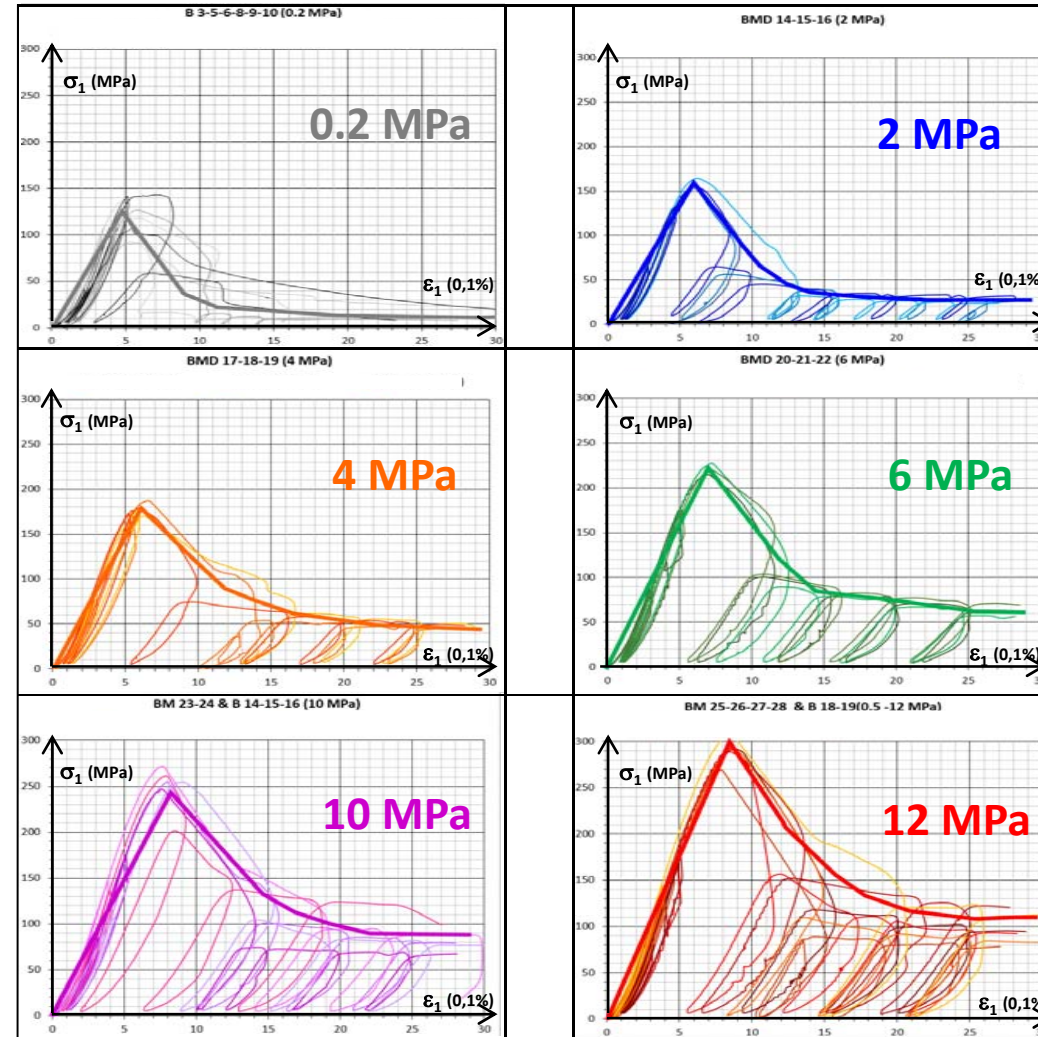
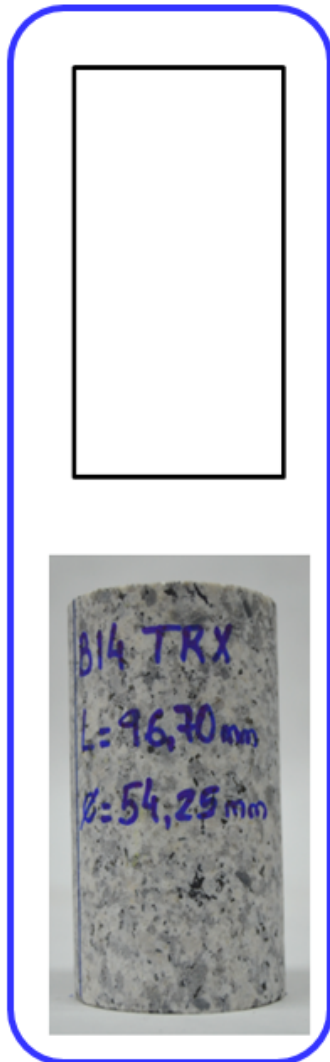
### Laboratory tests



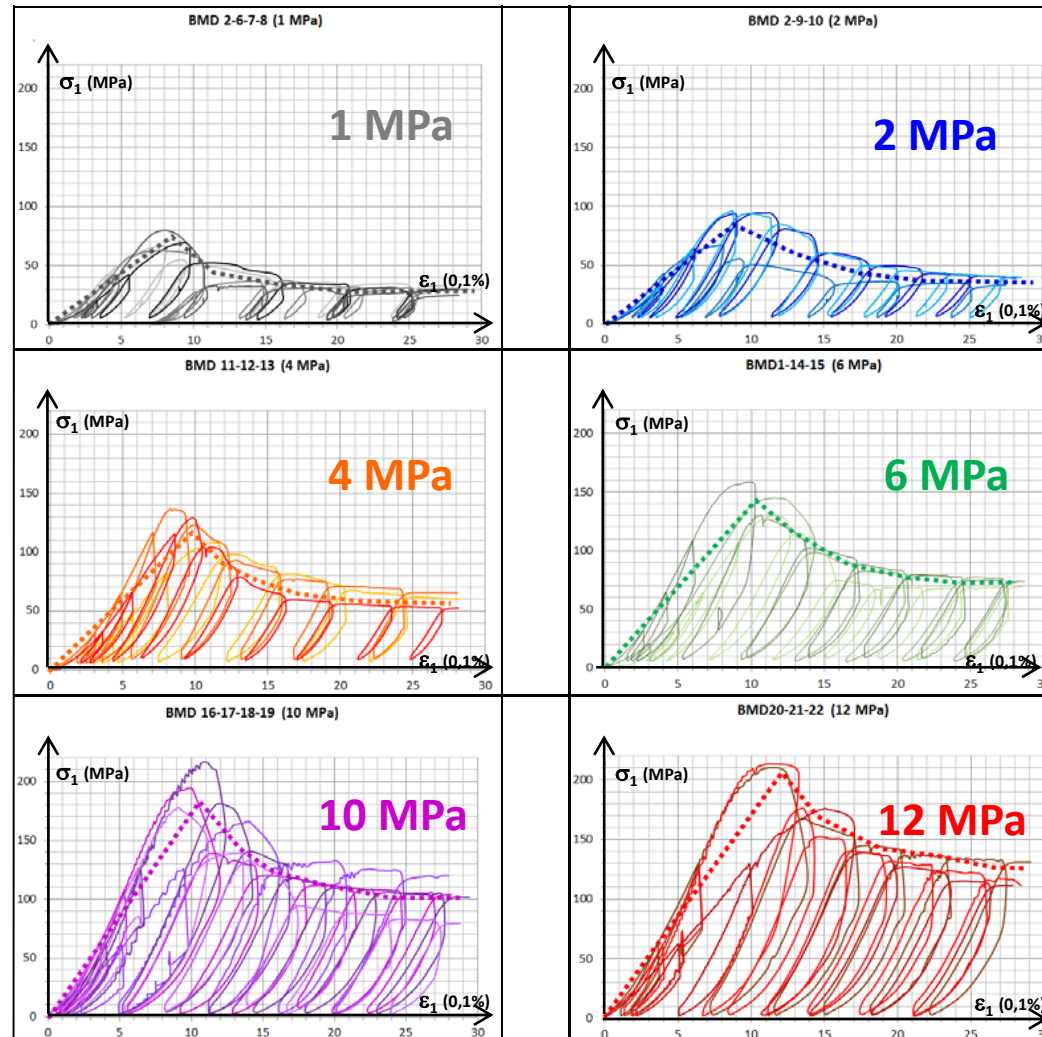
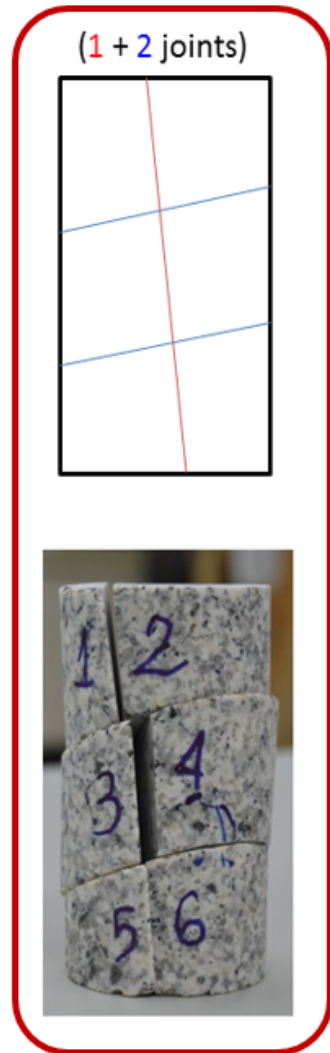
Axial stress-axial strain curves with unloading-loading cycles for triaxial testing at different confinement stress values for intact, (1+2) and (2+3) jointed samples.

Alejano LR, Arzúa J, Bozorgzadeh N, Harrison JP. (2017) Triaxial strength and deformability of intact and increasingly jointed granite samples. Int J Rock Mech Min Sci 95:87–103

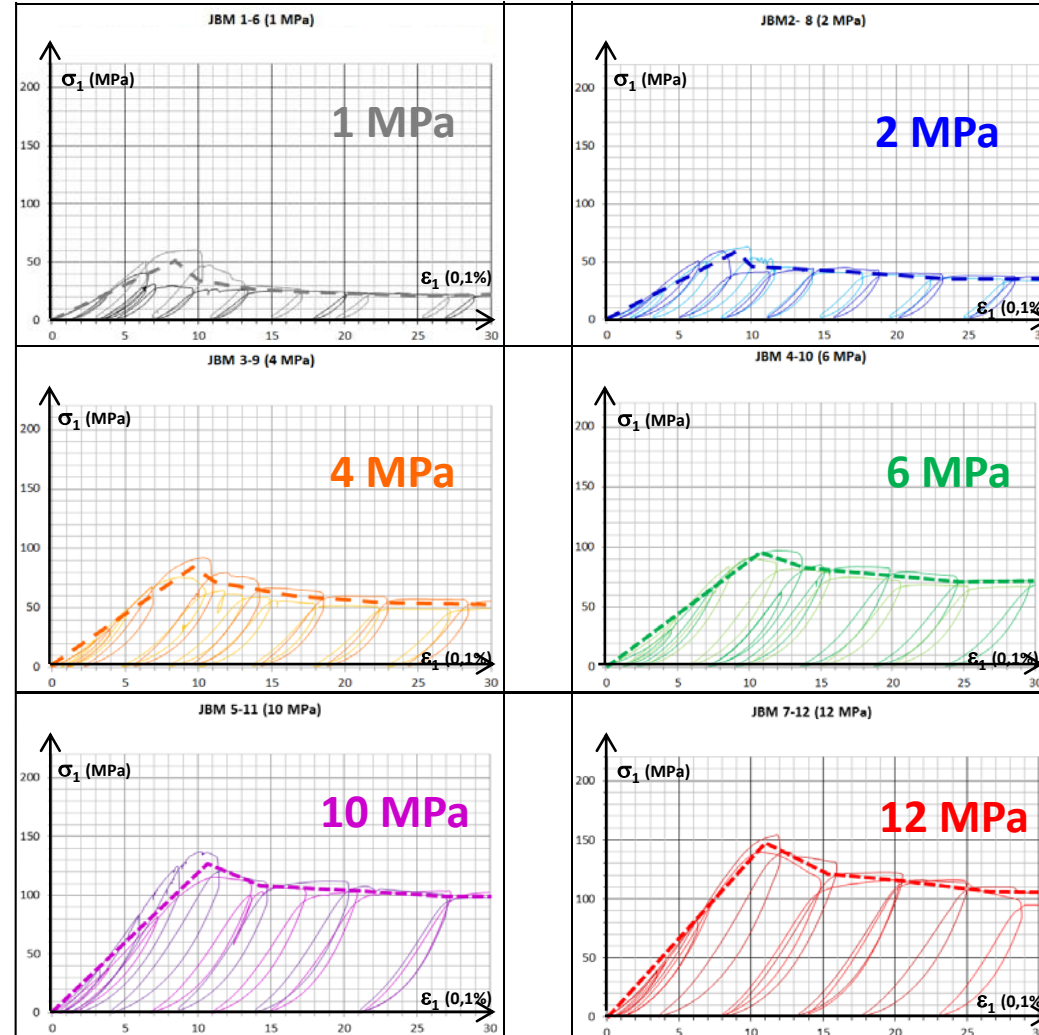
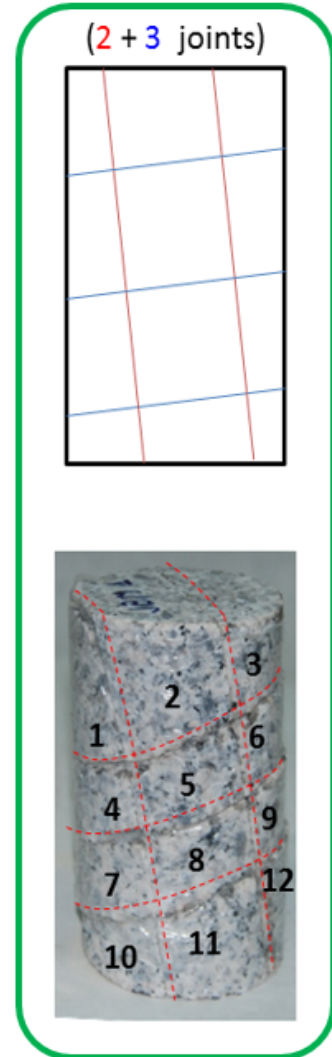
### Laboratory tests



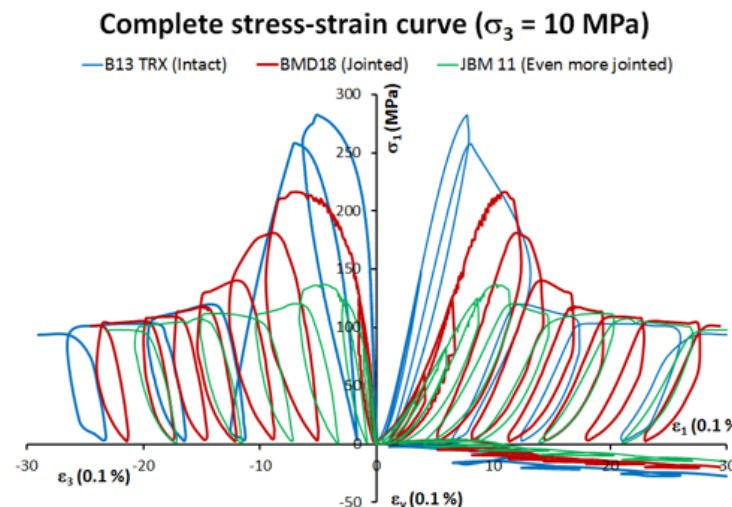
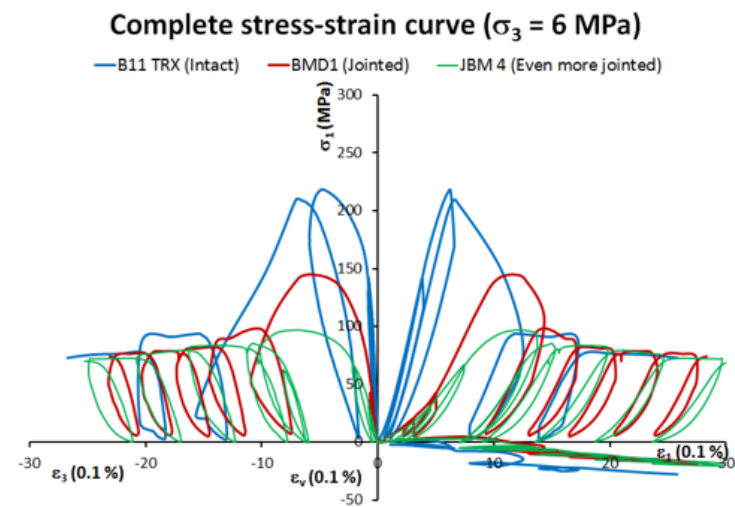
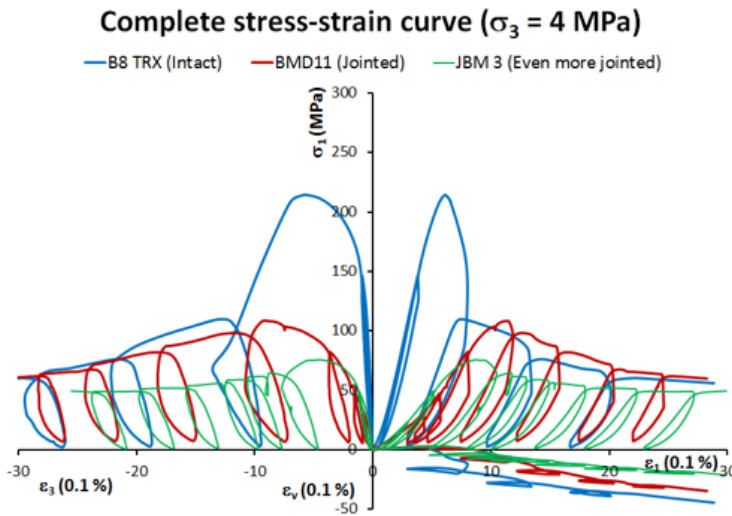
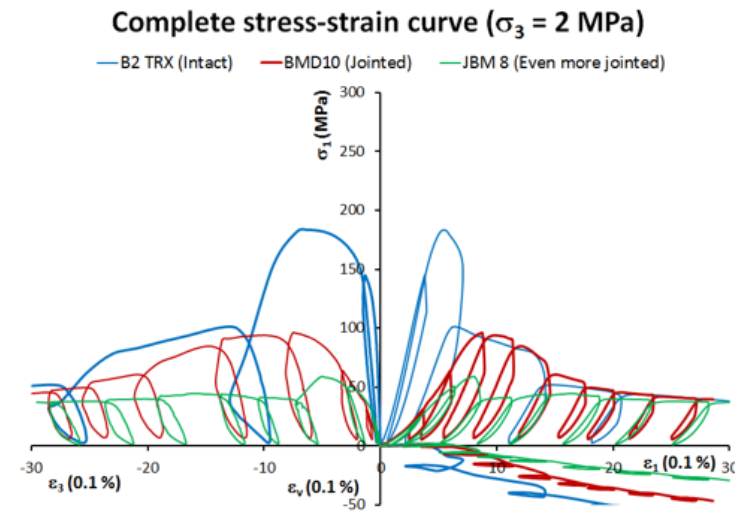
### Laboratory tests



### Laboratory tests



### Laboratory tests – response at various confinement levels for all type samples



Alejano LR, Arzúa J, Bozorgzadeh N, Harrison JP. (2017) Triaxial strength and deformability of intact and increasingly jointed granite samples. Int J Rock Mech Min Sci 95:87–103

### Laboratory tests – Broken samples

a)

Image of fresh Blanco  
 Mera granite  
 specimen B6RCS after  
 testing under  
 unconfined  
 conditions.

Axial splitting  
 associated to  
 significant dilation is  
 observed.



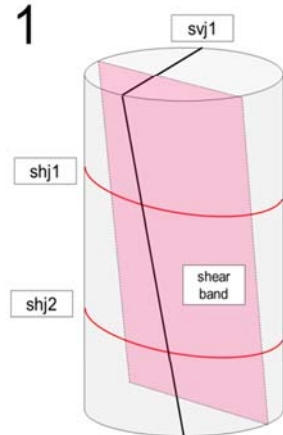
b)

Image of fresh Blanco  
 Mera granite  
 specimen B13TRX  
 after testing under  
 confined conditions  
 $(\sigma_3 = 10 \text{ MPa})$ .

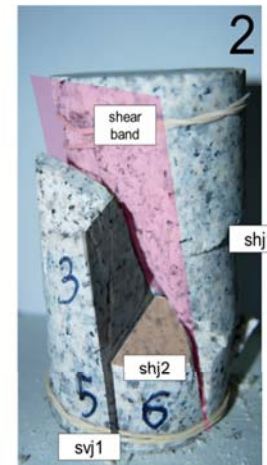
A shear band  
 associated to  
 moderate dilation is  
 observed.



1

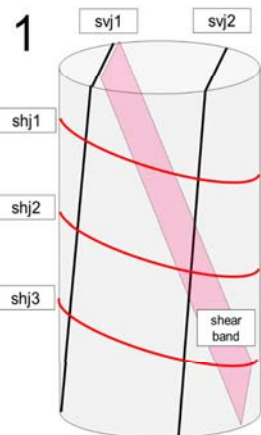


c)

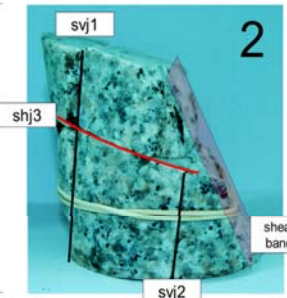


Sketch of a (1 + 2) jointed sample, where joints (svj1, shj1 and shj2) are marked and the observed shear band and rock sample after testing for confine pressure of 4 MPa.

1

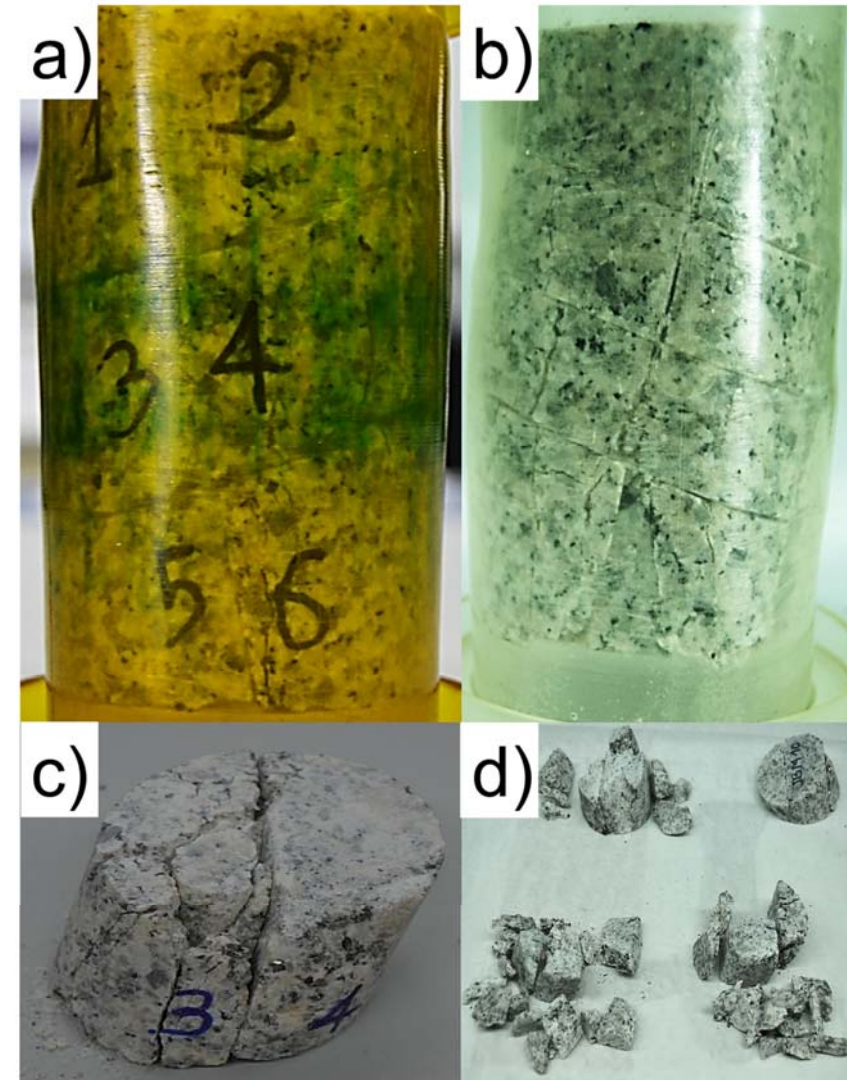
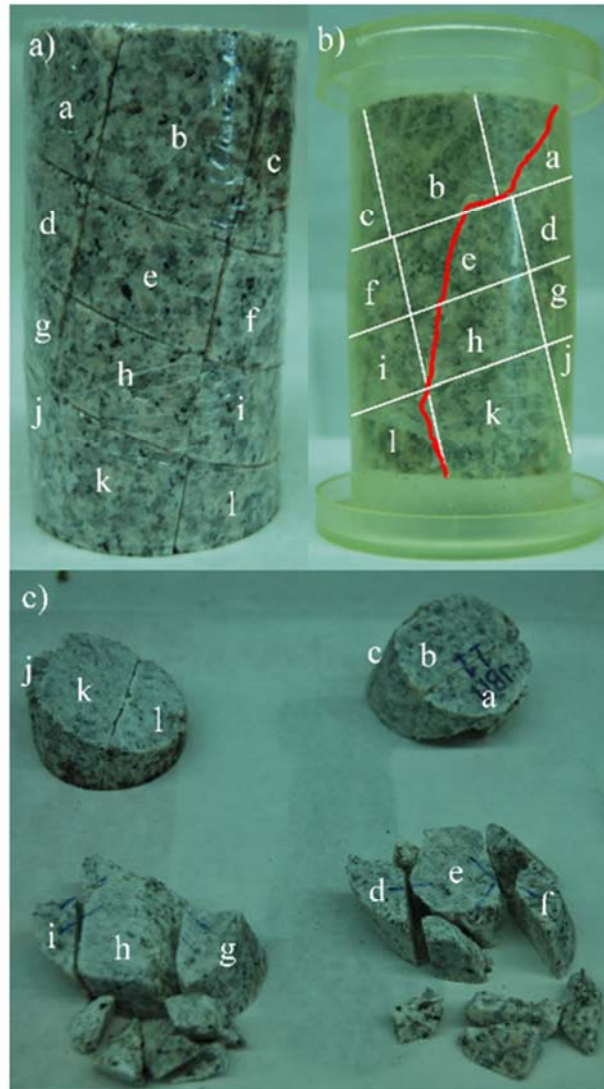


d)



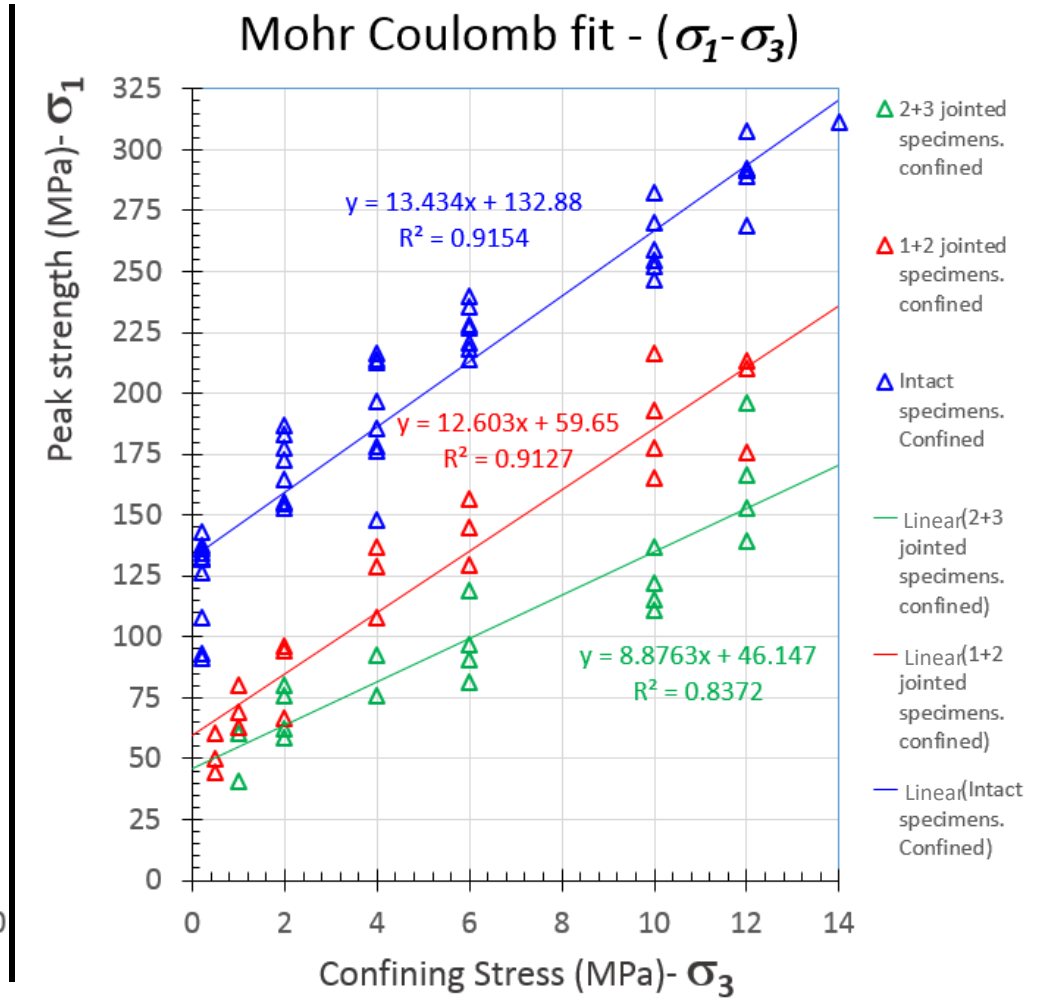
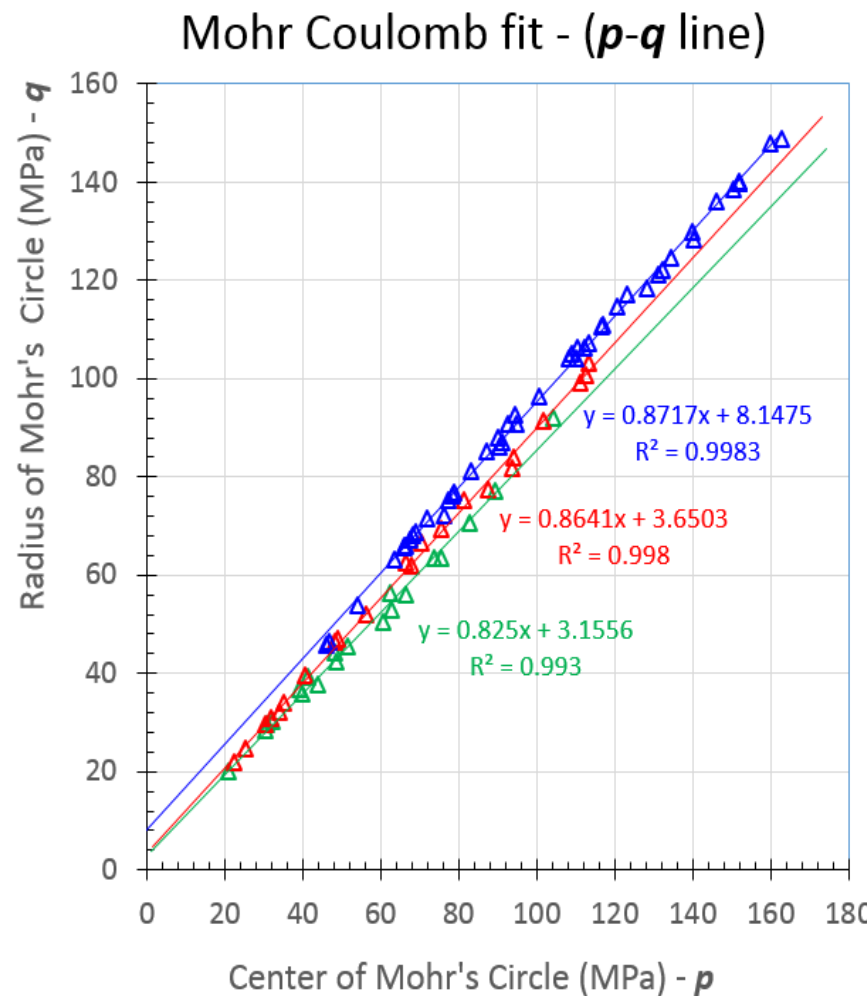
Sketch of a (2 + 3) jointed sample, where joints (svj1, svj2, shj1, shj2 and shj3) are marked and observed shear band and rock sample after testing ( $\sigma_3 = 4 \text{ MPa}$ ).

### Laboratory tests – Broken samples



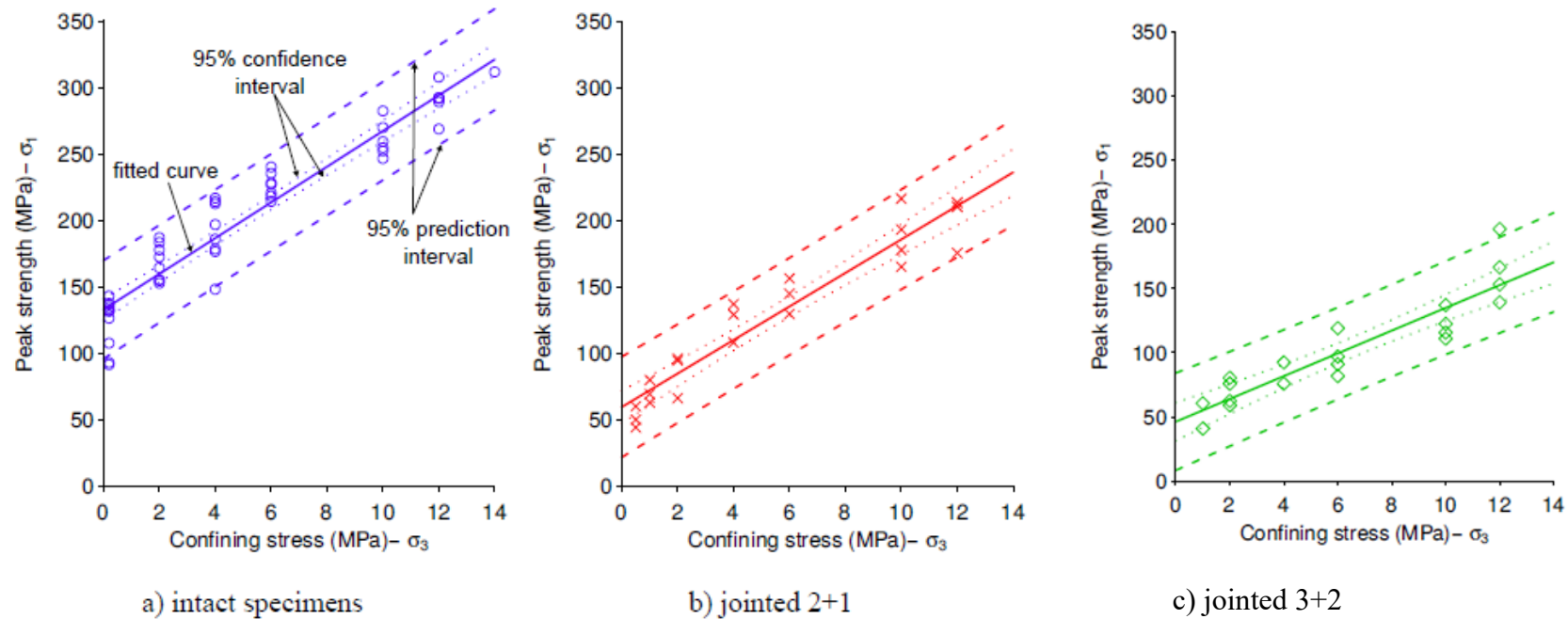
Alejano LR, Arzúa J, Bozorgzadeh N, Harrison JP. (2017) Triaxial strength and deformability of intact and increasingly jointed granite samples. *Int J Rock Mech Min Sci* 95:87–103

### Laboratory tests – Peak strength (M-C)



Alejano LR, Arzúa J, Bozorgzadeh N, Harrison JP. (2017) Triaxial strength and deformability of intact and increasingly jointed granite samples. *Int J Rock Mech Min Sci* 95:87–103

### Laboratory tests – Peak strength (M-C)

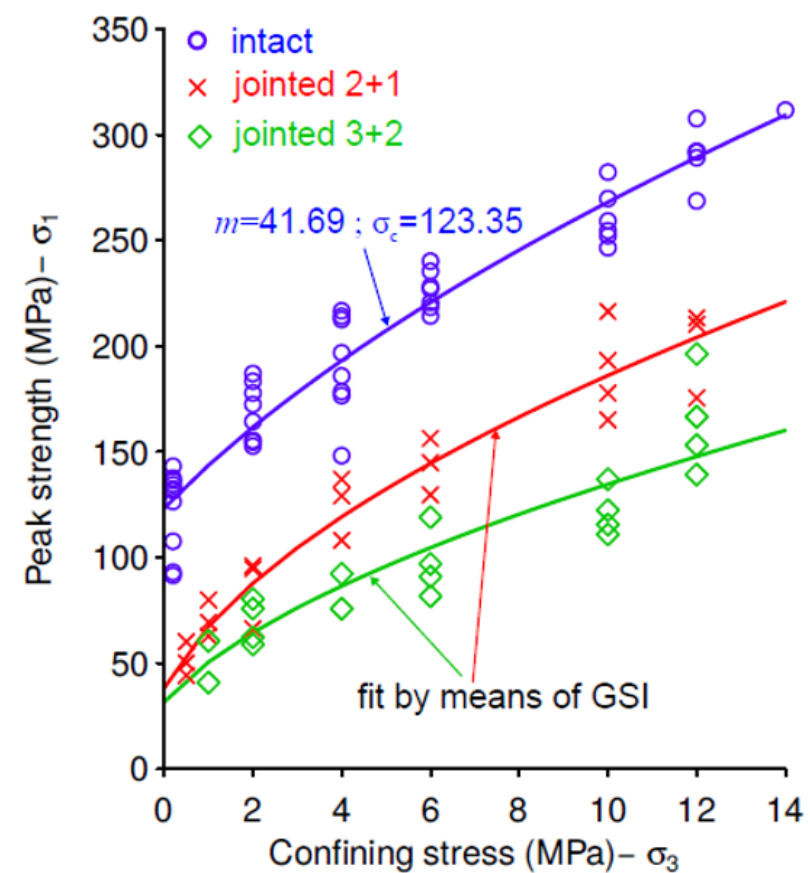
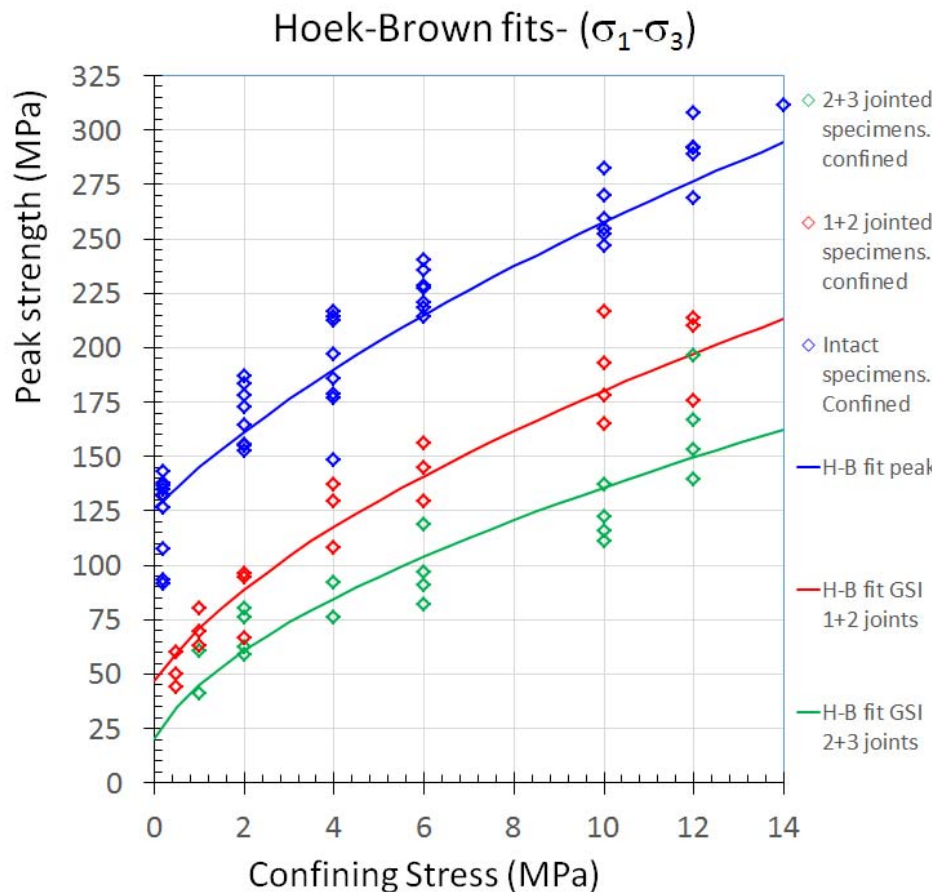


Mohr-Coulomb failure peak strength criterion parameters derived from fittings in the  $\sigma_1-\sigma_3$  space and corresponding 95% confidence intervals for every parameter.

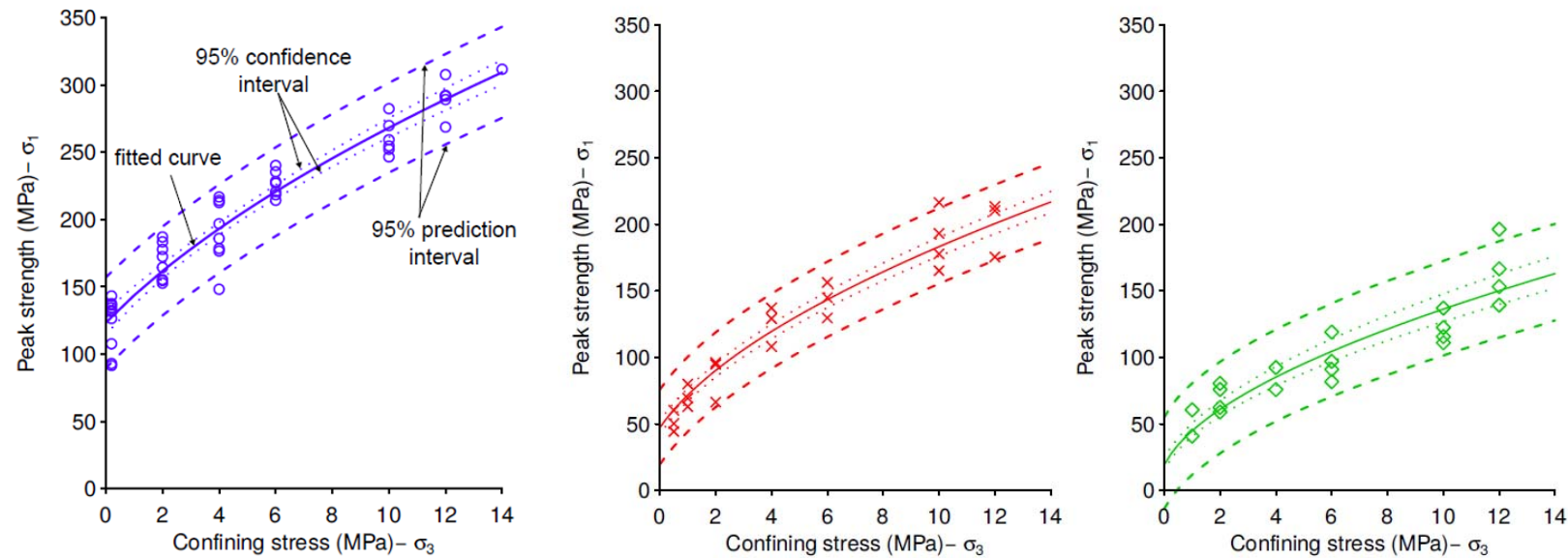
Parameter	Intact		1+2 jointed		2+3 jointed	
	Estimate	95% CI	Estimate	95% CI	Estimate	95% CI
$\sigma_c^{pk}$ (MPa)	132.88	(124.73,141.02)	59.65	(47.37,71.93)	46.15	(31.32,60.97)
$K_\phi$	13.43	(12.21,14.66)	12.60	(10.78,14.42)	8.88	(6.94, 10.81)
$\phi$ (°)	59.48	(58.06,60.72)	58.54	(56.13,60.49)	46.15	(31.32,60.97)
c (MPa)	18.13	(16.39,20.05)	8.40	(6.31, 10.82)	7.74	(4.82,11.42)
$\tan(\alpha)$	0.86	(0.85,0.87)	0.85	(0.83, 0.87)	0.78	(0.75, 0.83)
b	9.20	(8.03,10.58)	4.38	(3.13, 6.00)	4.67	(2.70, 7.54)
$\varsigma_{\sigma 1}$ (MPa)	17.91	—	17.14	—	16.63	—
$R^2$	0.9154	—	0.9127	—	0.8372	—

Alejano LR, Arzúa J, Bozorgzadeh N, Harrison JP. (2017) Triaxial strength and deformability of intact and increasingly jointed granite samples. Int J Rock Mech Min Sci 95:87–103

### Laboratory tests – Peak strength (H-B)



### Laboratory tests – Peak strength (H-B)



Generalized Hoek-Brown failure criterion with fitted GSI and parameters derived from fitting strength results reduced to 70%.

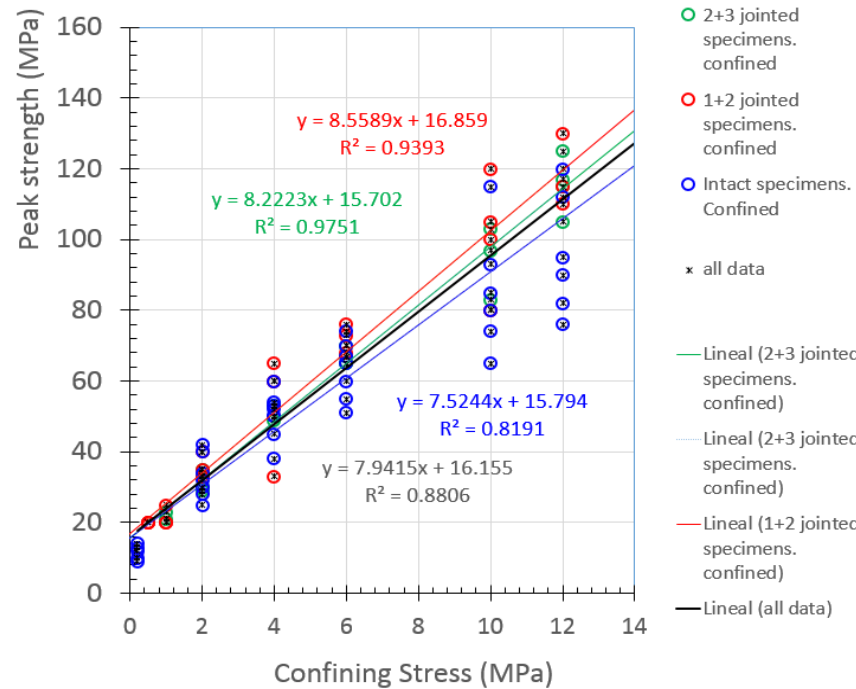
Parameter	SPECIMENS			
	1+2 jointed	95% CI	2+3 jointed	95% CI
Generalized Hoek-Brown failure criterion with fixed $\sigma_{ci}$ and $m_i$ , fitted GSI and scaled down strength				
$\sigma_{ci}$ (MPa)	<u>123.35</u>	–	<u>123.35</u>	–
$m_i$	<u>41.69</u>	–	<u>41.69</u>	–
$D$	<u>0</u>	–	<u>0</u>	–
GSI *	<b>64.90</b>	(62.59, 67.86)	<b>45.89</b>	(41.26, 50.19)
$m_b$ from GSI (Eq. (5))	12.08	(10.96, 13.23)	6.04	(5.12, 7.04)
$a$ from GSI (Eq. (5))	0.5020	(0.5023, 0.5016)	0.5080	(0.5104, 0.5056)
$s$ from GSI (Eq. (5))	0.0212	(0.0157, 0.0281)	0.0024	(0.0015, 0.0039)
$\xi_{\sigma_1}$ (MPa)	10.49	–	12.48	–

Asterisks indicate fitted parameters and underlining indicates fixed parameters (all other values are derived).

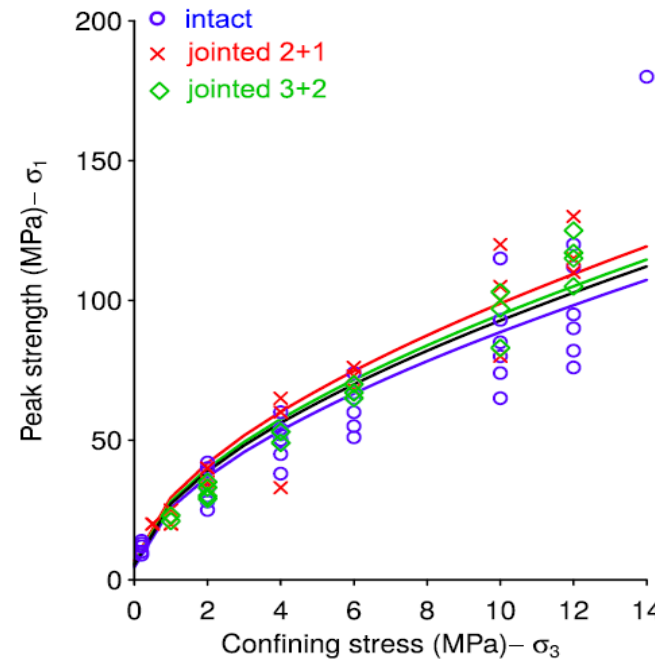
Alejano LR, Arzúa J, Bozorgzadeh N, Harrison JP. (2017) Triaxial strength and deformability of intact and increasingly jointed granite samples. Int J Rock Mech Min Sci 95:87–103

### Laboratory tests – Residual strength – Practically equal in all cases\*

Mohr Coulomb fit- ( $\sigma_1 - \sigma_3$ ) - residual



Hoek-Brown ( $\sigma_1 - \sigma_3$ ) - residual

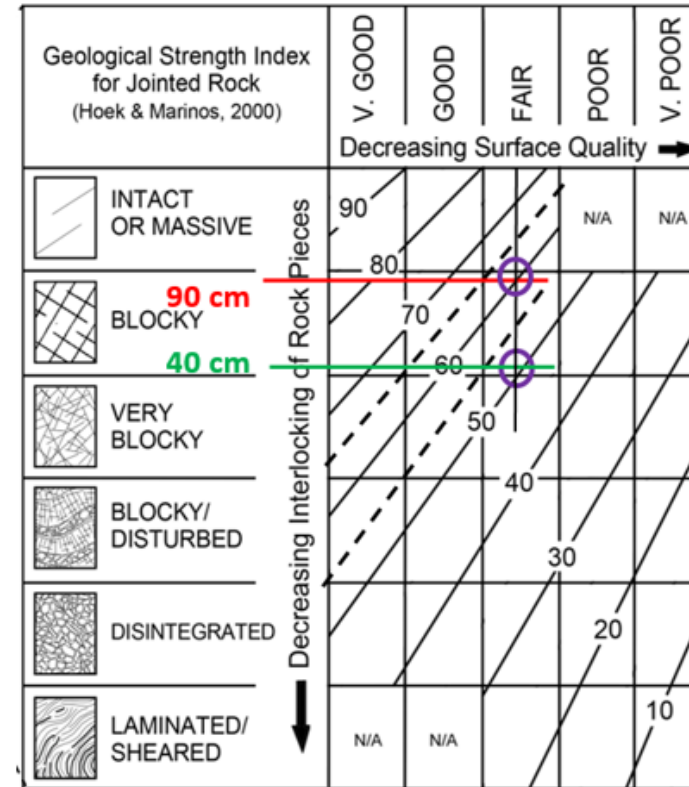
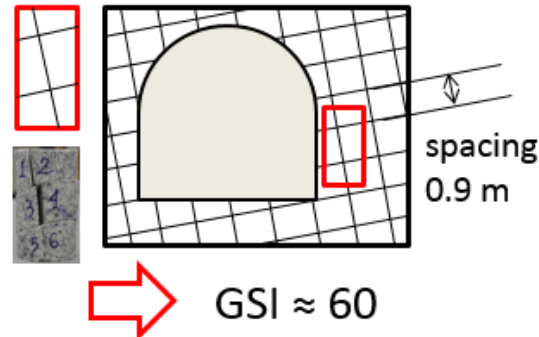


Parameter	Intact	Jointed 1+2	Jointed 2+3	All data
	Estimate	Estimate	Estimate	Estimate
$\sigma_c^{pk}$ (MPa)	15.79	16.86	15.70	16.15
$K_\phi$	7.52	8.56	8.22	7.94
$\phi$ (°)	49.94	52.26	52.26	50.92
c (MPa)	2.88	2.88	2.88	2.87

	Parameter	SPECIMENS			
		Intact	1+2 jointed	2+3 jointed	All
Generalized Hoek-Brown failure criterion with fixed $\sigma_{ci}$ and $m_i$ and fitted $GSI$ and $D$	$\sigma_{ci}$ (MPa)	123.35	123.35	123.35	123.35
	$m_i$	41.69	41.69	41.69	41.69
	$D^*$	0	0	0	0
	$GSI^*$	41.72	48.25	45.78	44.44
	$m_b$ from $GSI$ and $D$ (Eq. (6))	5.22	6.58	6.01	5.73

Alejano LR, Arzúa J, Bozorgzadeh N, Harrison JP. (2017) Triaxial strength and deformability of intact and increasingly jointed granite samples. Int J Rock Mech Min Sci 95:87–103

### Laboratory tests – Residual strength – Practically equal in all cases\*



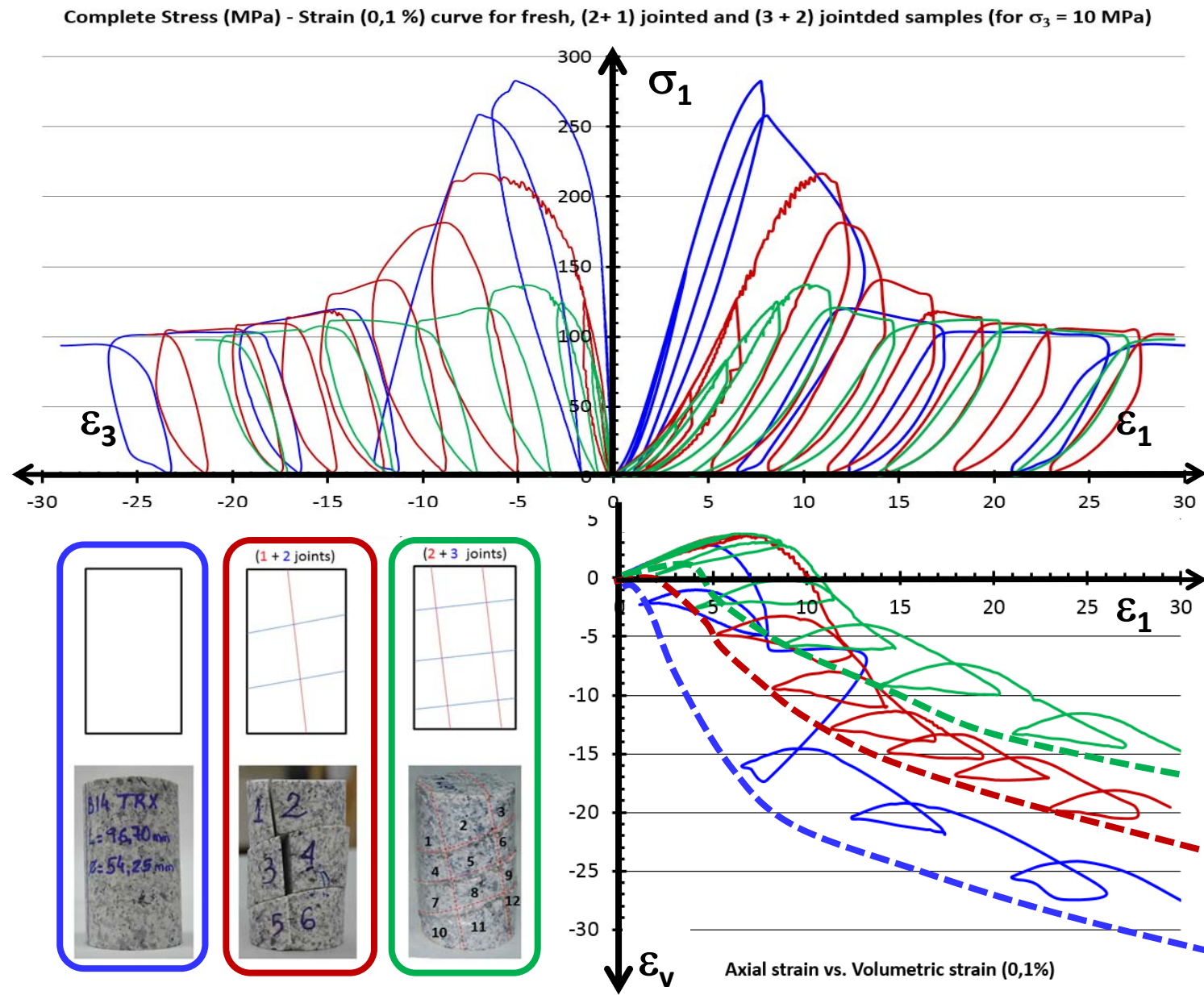
For a standard 4-m diameter tunnel excavated in a granite rock mass with a regular pattern of normal discontinuities and fair surface quality, a GSI of around 60 would be obtained for spacing of 0.9 m and of around 50 for spacing of 0.4 m. If we could test a specimen with a diameter of 1 m and a height of 2 m for both these cases, the structure would be homothetic to jointed samples. The stress-strain response of these samples would be representative of the rock mass at the scale of the tunnel. Once corrected for scale (70%) our results seem to represent this behavior.

## Conclusions regarding strength

- A number of triaxial tests have been carried out on fresh and artificially jointed granite samples. Results show that scale effects on (hard) rock mass behavior seems to be associated more relevantly to rock structure than to sample size.
- Peak strength clearly depends on jointing. Residual strength does not seem to be much affected by the degree of initial jointing, in line with Gao & Kang (2017). This suggests that rock mass residual strength could be estimated from laboratory tests.
- Small samples with a structure homothetic to large-scale rock masses could thus provide useful information on rock mass behavior at the engineering scale.
- Correlations of fracturing in terms of fracture intensity,  $J_v$ , block volume, R.Q.D. or GSI are looked for to understand strength in terms of rock structure and scale.
- Further laboratory studies of different rocks with different jointing patterns would contribute to identifying which components of strength reduction from laboratory to engineering site are related to sample size and to rock structure.

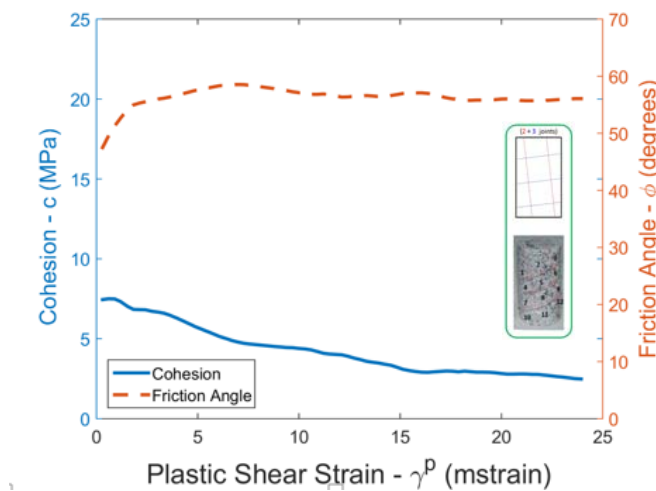
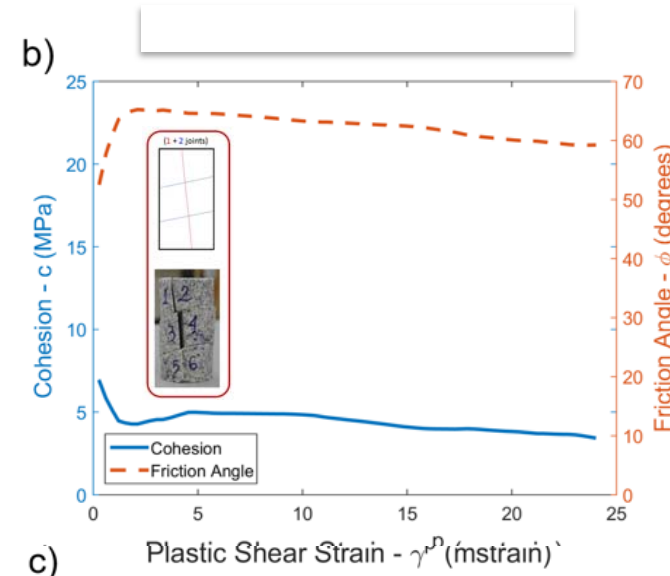
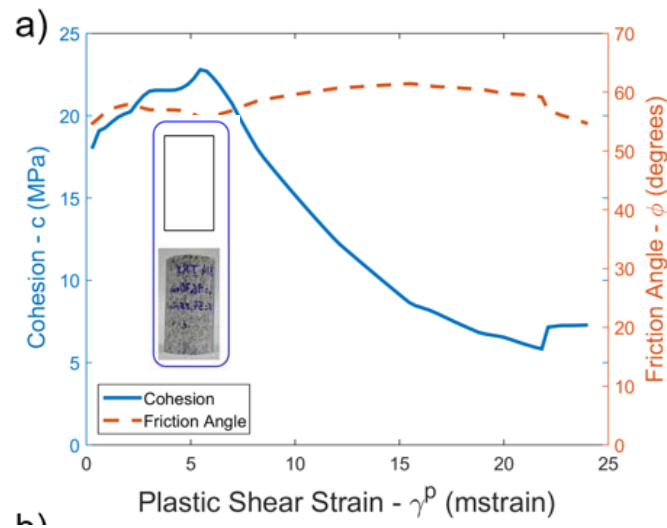
Alejano LR, Arzúa J, Bozorgzadeh N, Harrison JP. (2017) Triaxial strength and deformability of intact and increasingly jointed granite samples. Int J Rock Mech Min Sci 95:87–104.

Gao FQ, Kang HP. Effects of pre-existing discontinuities on the residual strength of rock mass – insight from a discrete element method simulation. J Struct Geol. 2016;85:40–50.



### Post-failure Strength

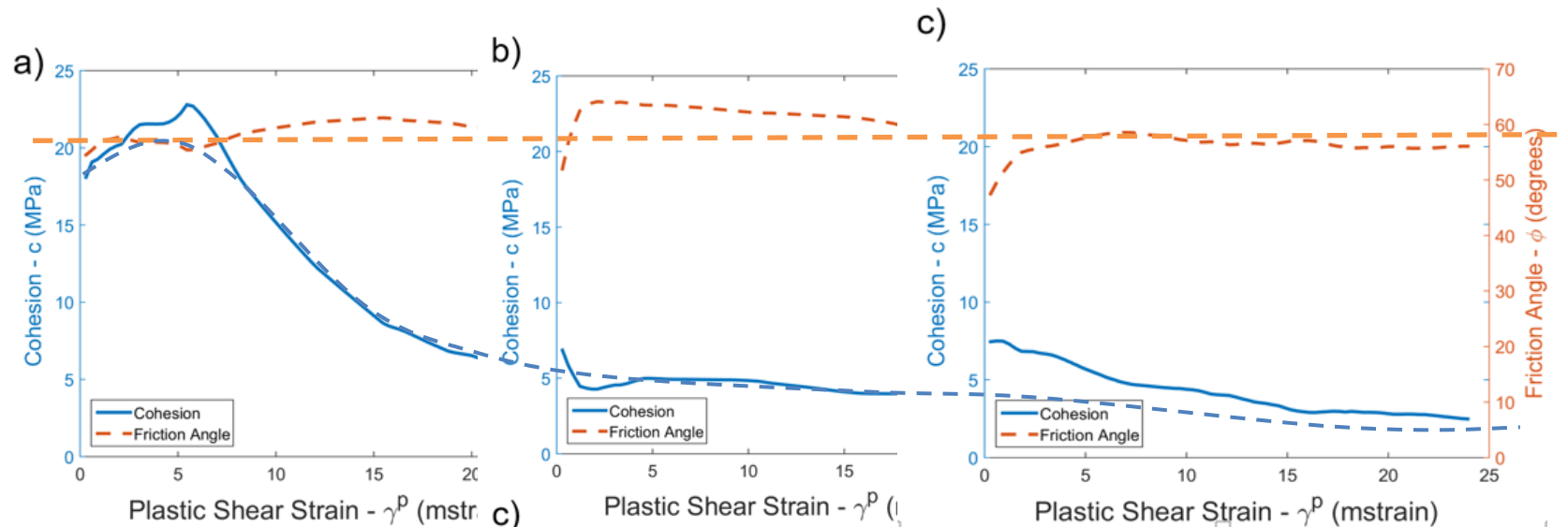
Cohesion and friction profiles as a function of plastic shear strain for (a) intact samples, (b) samples with 1+2 joints, and (c) samples with 2+3 joints.



The intact rock roughly followed the cohesion-weakening-friction-strengthening model for brittle rock strength, as proposed by Martin (1997). Similar profiles are evident for the jointed samples, although the initial cohesion for these samples was significantly lower than in the intact case.

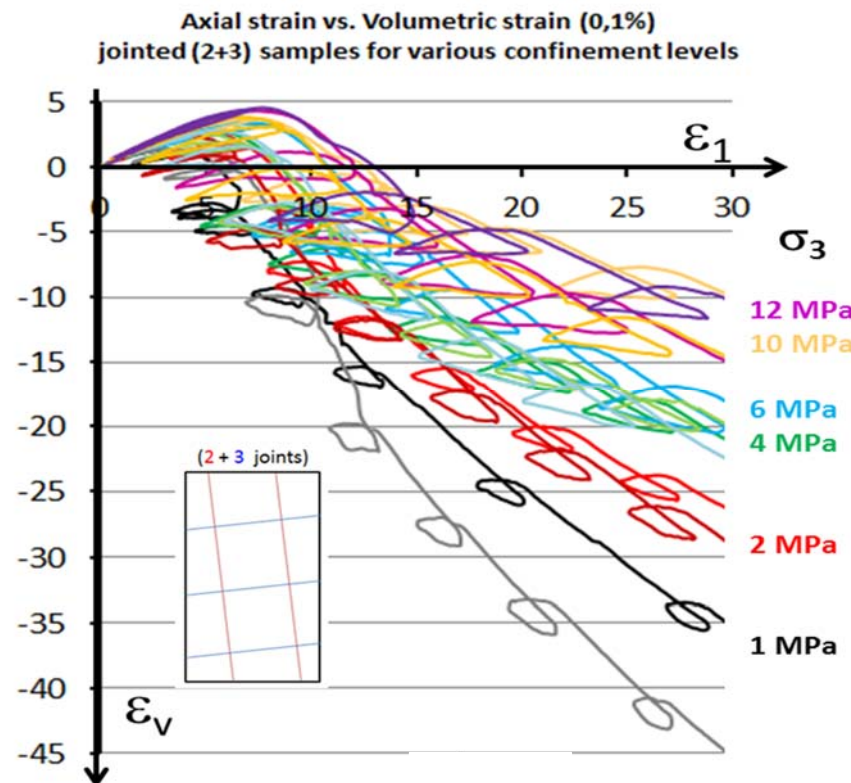
## Post-failure Strength

**Can a trend as the one proposed below be proposed ?**



### Dilatancy

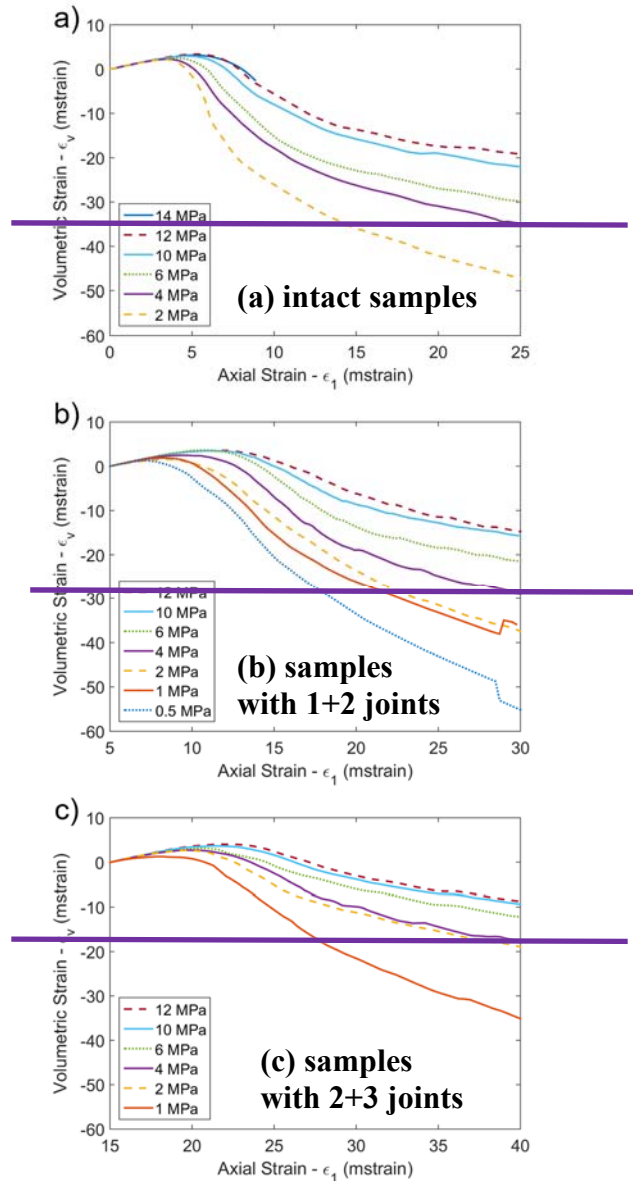
Axial strain Vs. Volumetric strain (0.1%) (2+3) jointed specimens for various confinements



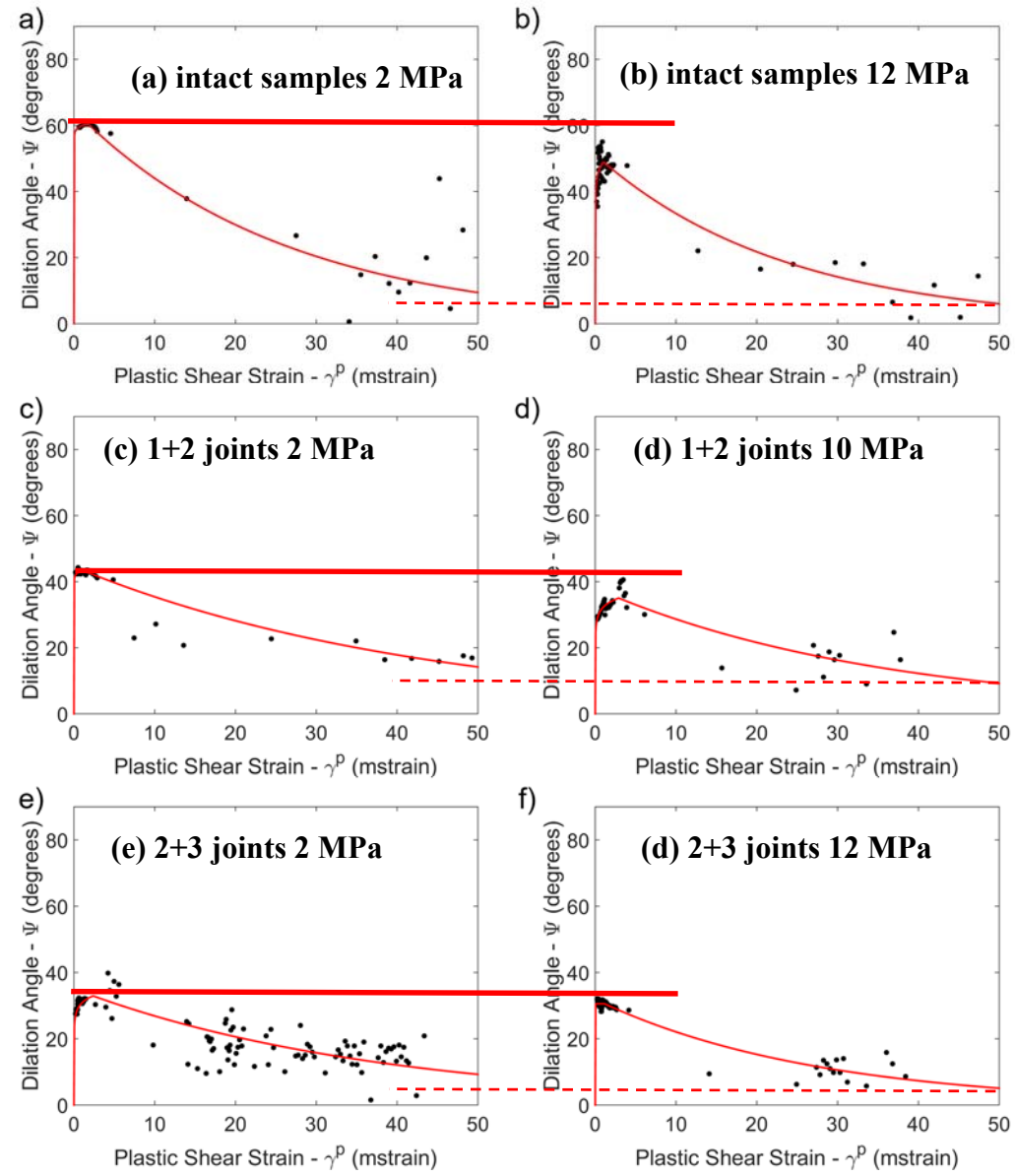
Dilation is largely dependent on confinement and level of plasticity suffered by the sample. This was already remarked (implemented )in models A&A (2005), Z&C (2010) or W&D (2015).

It does not seem to be accurate enough to model underground excavations (at least in average to good quality rock masses) implementing constant dilation.

### Averaged volumetric strain curves



### Representative dilation data and W-D model fits



### Conclusions regarding dilatancy

Dilation seems to be sensible to the level of jointing.

More fractured rock samples tend to dilate not so much as fresh rock or good quality rock masses.

This can be associated to the presence of planar joints less rough than newly formed shear bands.

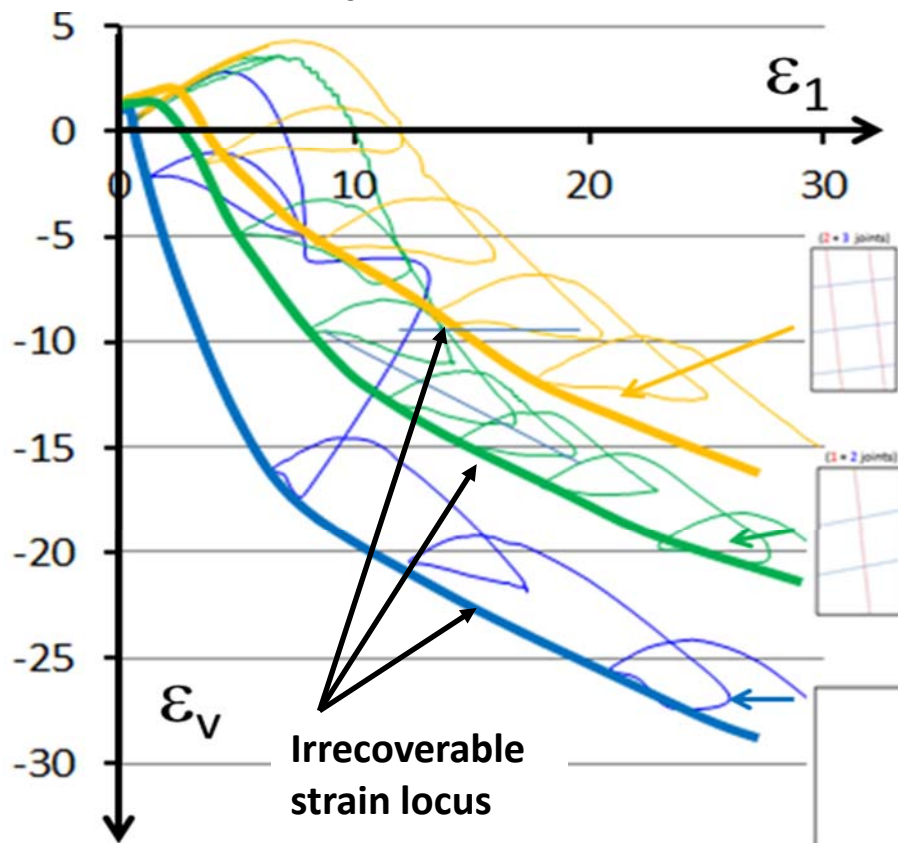
This trend is also in line with Hoek & Brown (1997) guidelines for rock mass dilation estimate.

A rock based dilatancy model (Walton & Diederichs, 2015) can be fit.

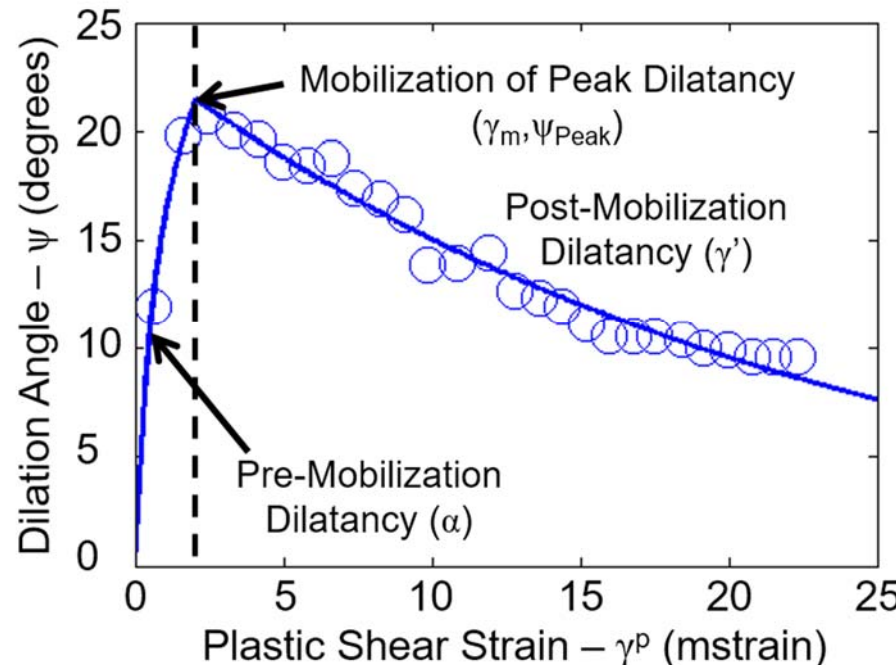
Axial strain Vs. Volumetric strain (0.1%)

Fresh, (1+2) joints and (2+3) joints

$\sigma_3 = 10 \text{ MPa}$



### Dilatancy – Walton & Diederichs (2015) model



A typical dilation angle profile obtained from a triaxial test.

If the pre-mobilization and post-mobilization model parameters ( $\alpha$  and  $\gamma'$ , respectively) are considered constant as a function of confining stress, only five parameters are required to define the model for all  $\gamma_p, \sigma_3$  conditions ( $\alpha, \gamma_m, \beta', \beta_0, \gamma'$ ).

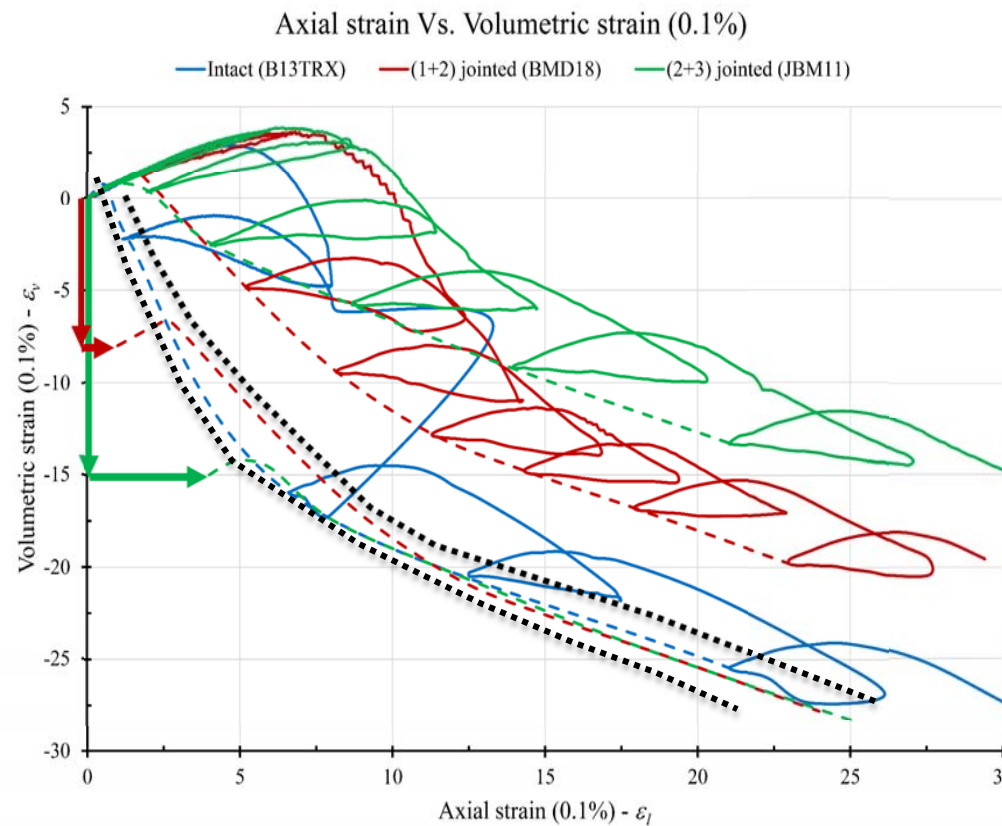
	$\alpha$	$\gamma_m$ (mstrain)	$\beta_0$	$\beta'$	$\gamma'_1$ (mstrain)	$\gamma'_2$ (mstrain)
Intact	0–0.1	1–4	0.99	0.107	– 12.2	51.6
1 + 2 Jointed	0–0.1	2–5	0.71	0.044	– 14.6	67.8
2 + 3 Jointed	0–0.1	2–4	0.63	0.045	– 14.5	68.4

## Dilatancy

Can a trend as the one proposed below be proposed ?

Moving the origin of the irrecoverable strain locus of the jointed samples in the axe of vol. str. and in the axe of axial strain some values (associated to damage or fracturing):

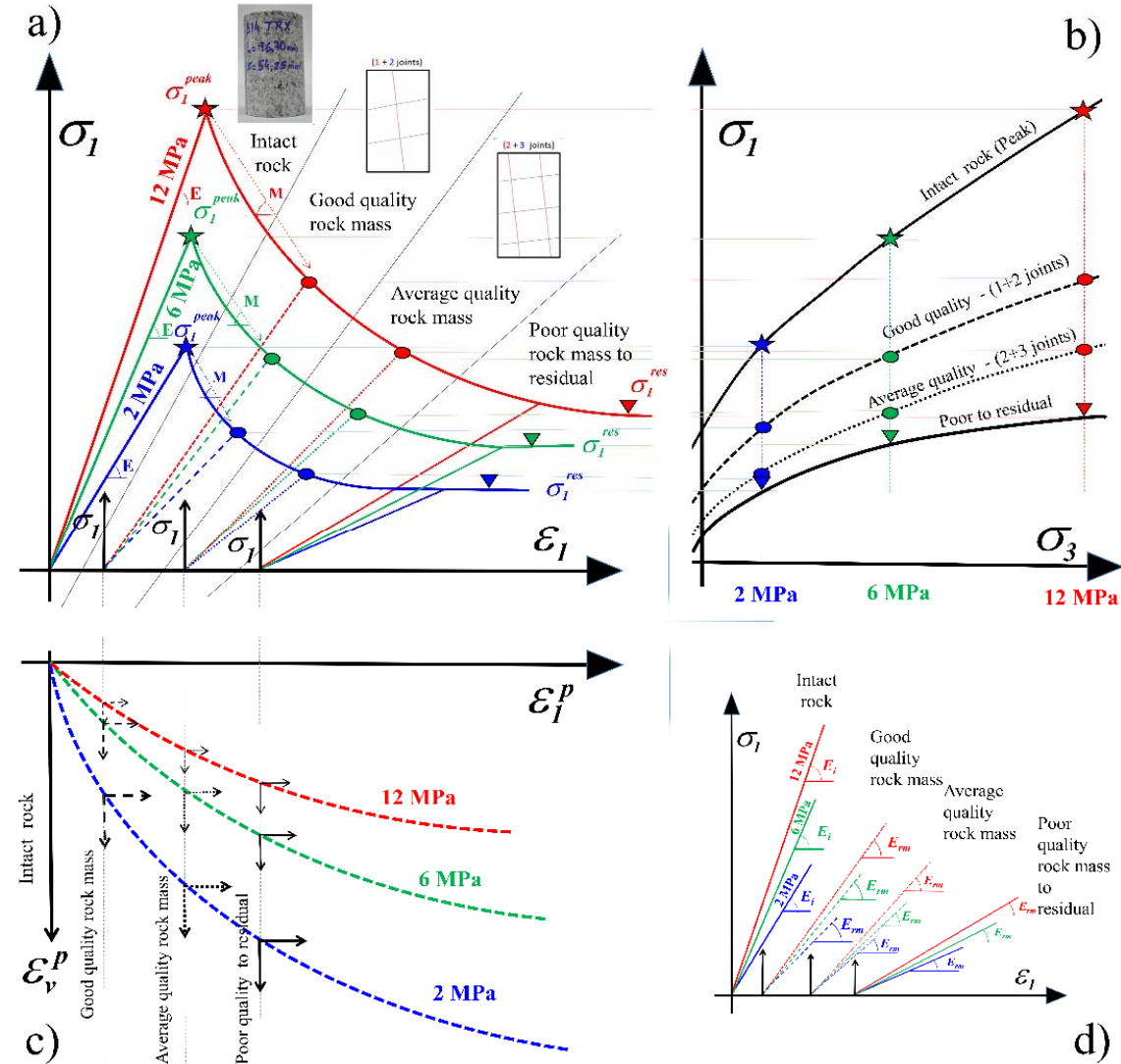
The irrecoverable stain locus is bracketed in rather limited zone.



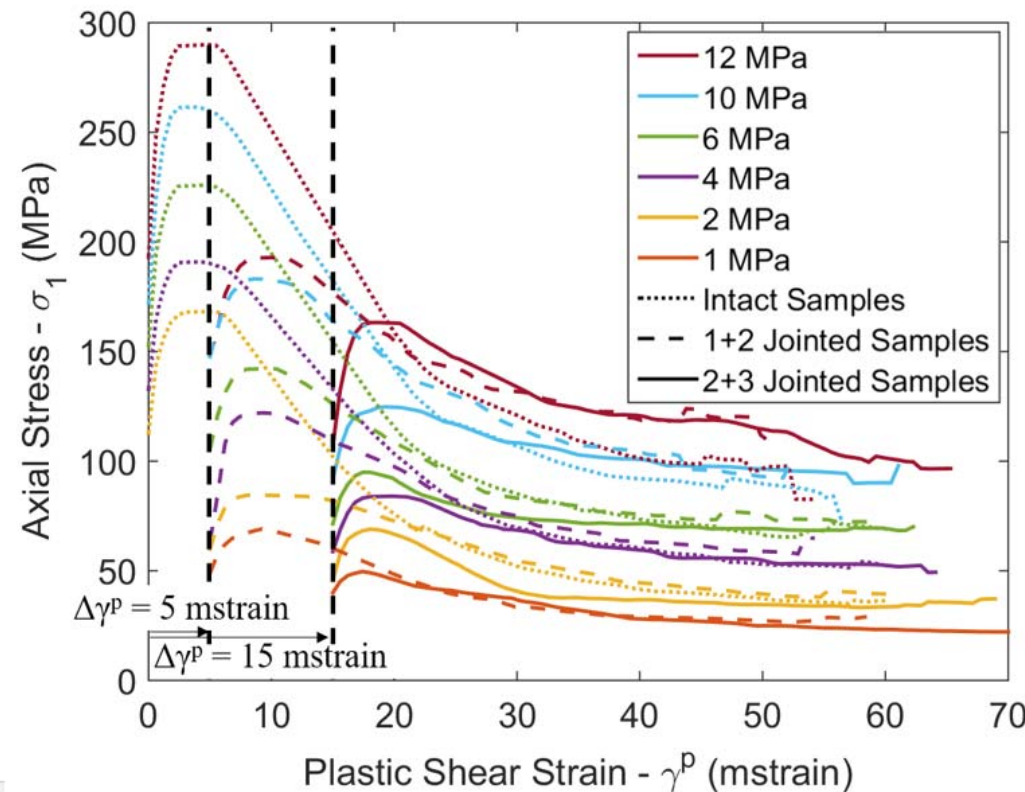
Walton G, Alejano LR, Arzua J, Markley T. 2018. Crack Damage Parameters and Dilatancy of Artificially Jointed Granite Samples Under Triaxial Compression. Rock Mechanics and Rock Engineering.

### Discussion: a conceptual model interpretative basis regarding rock mass behaviour

A conceptual model on how different aspects of rock mass behavior change as increasing degrees of jointing are added to the rock mass (either natural joints in a field-scale rock mass or artificial joints in the rock mass analogs presented in this study). It is suggested that the presence of such discrete weakness planes is roughly equivalent to having incurred prior inelastic strains, reflected in shifts along the strain axes of each plot and resulting in weakening, softening, reduced brittleness and reduced dilatancy.

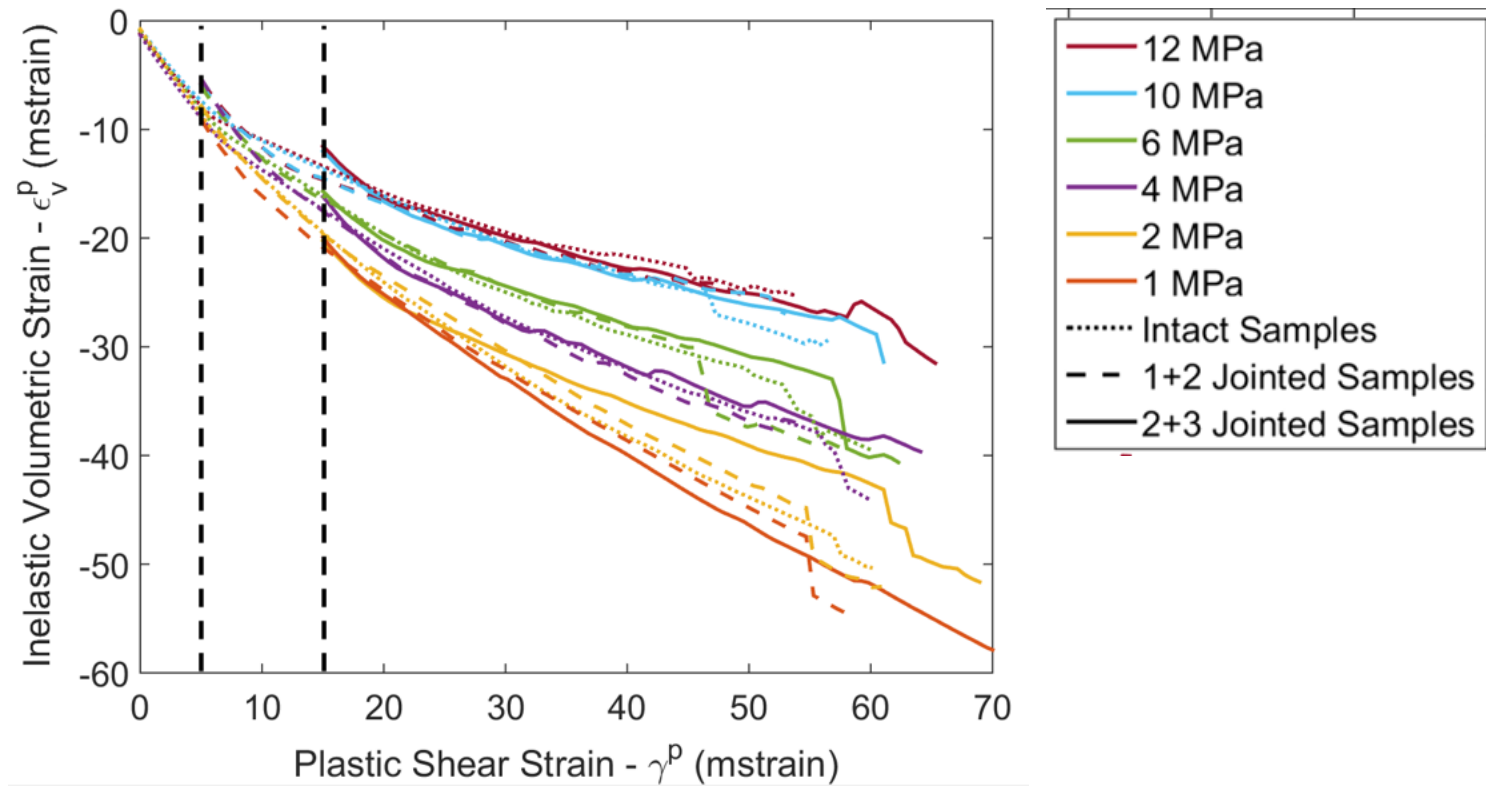


### Discussion: a conceptual model interpretative basis regarding rock mass behaviour



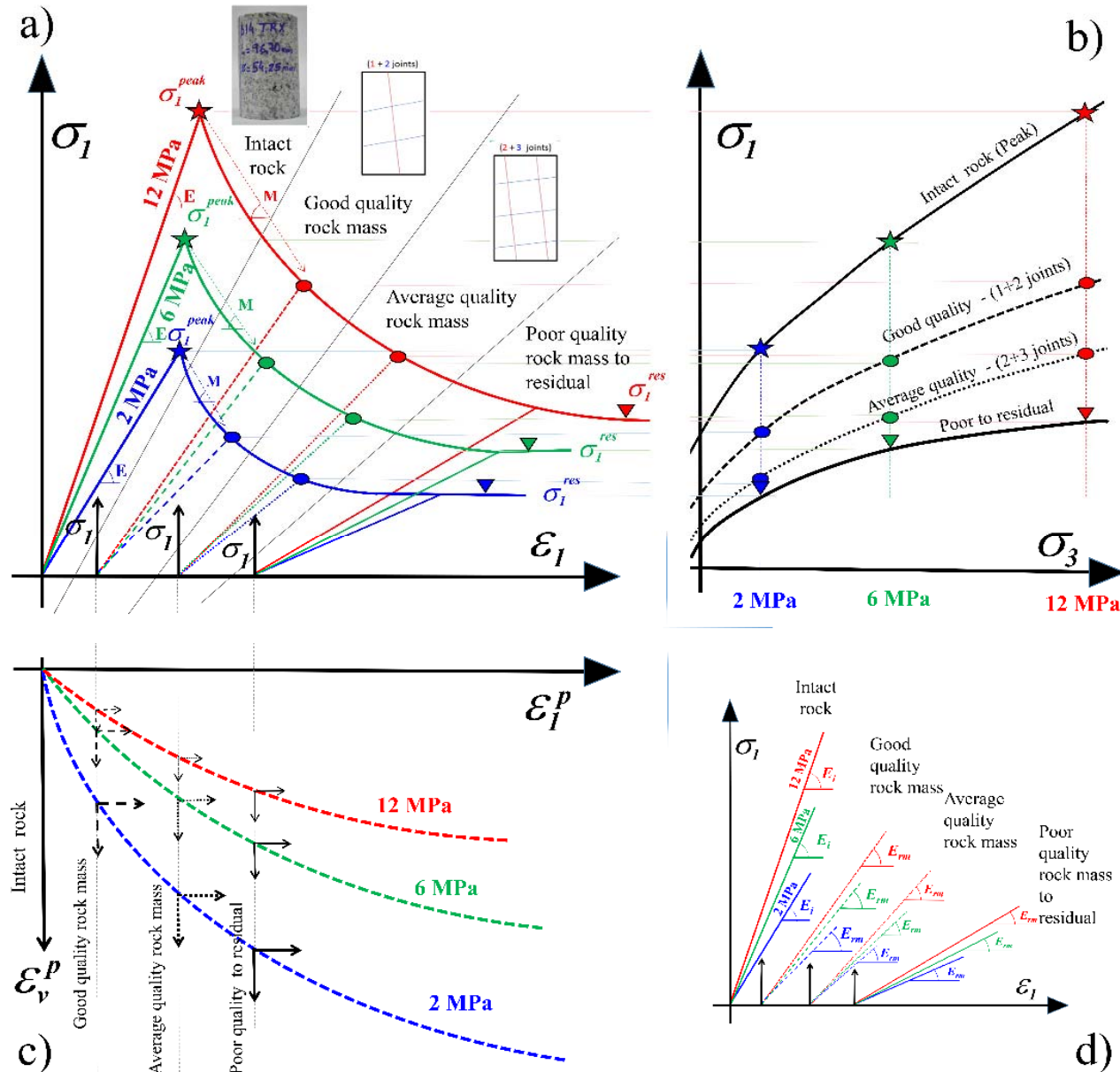
Averaged profiles of axial stress versus plastic shear strain for each confining stress. A consistent 5 mstrain shift has been applied to the plastic shear strain of the 1+2 samples, and a consistent 15 mstrain shift has been applied to the plastic shear strain of the 2+3 samples.

### Discussion: a conceptual model interpretative basis regarding rock mass behaviour



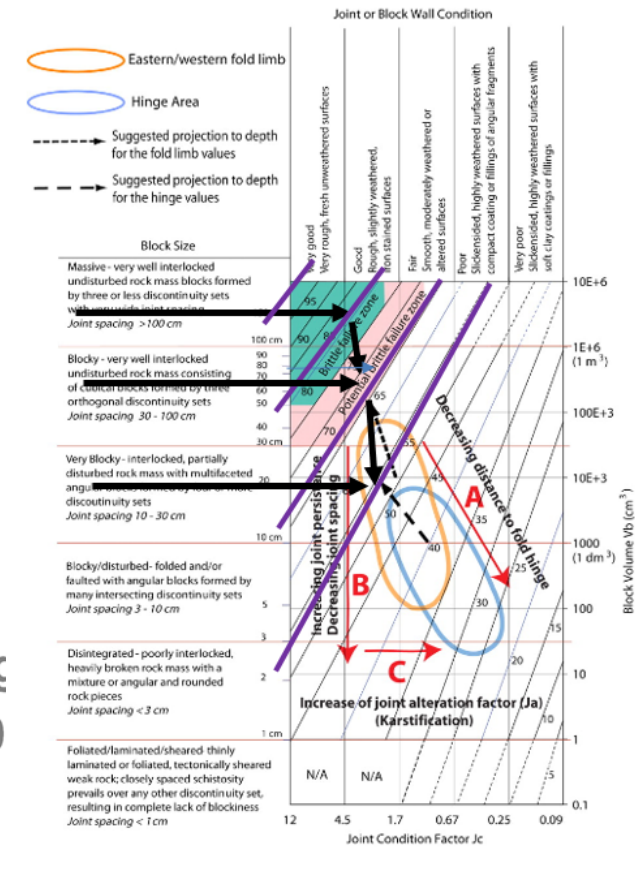
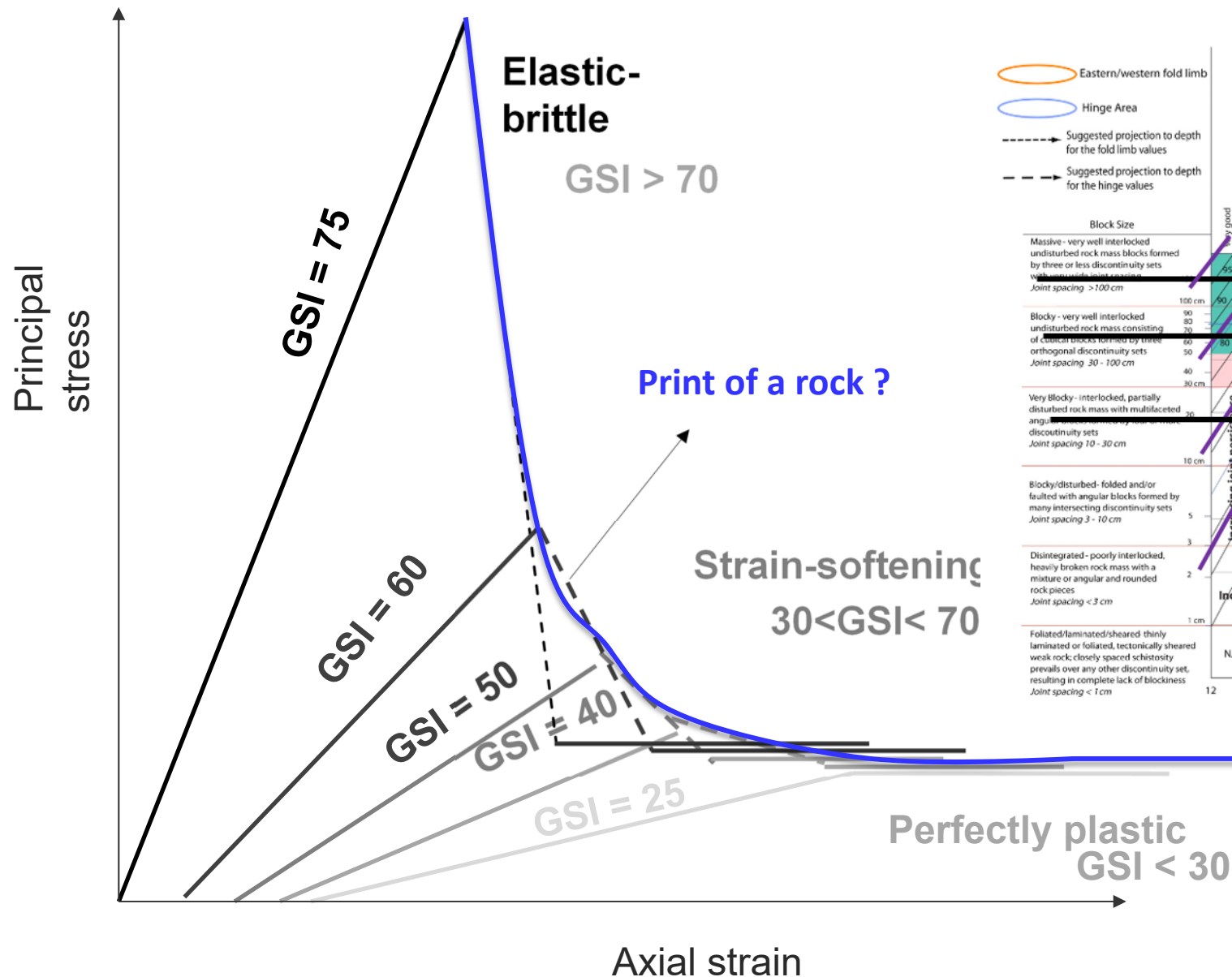
Averaged profiles of inelastic volumetric strain vs. plastic shear strain for each  $\sigma_3$ . A 5 mstrain shift has been applied to the plastic shear strain of the 1+2 samples, and a 15 mstrain shift has been applied to the plastic shear strain of the 2+3 samples. Vertical shifts have been applied to the inelastic vol. str. data depending on the  $\sigma_3$  (larger shifts applied at low  $\sigma_3$  ).

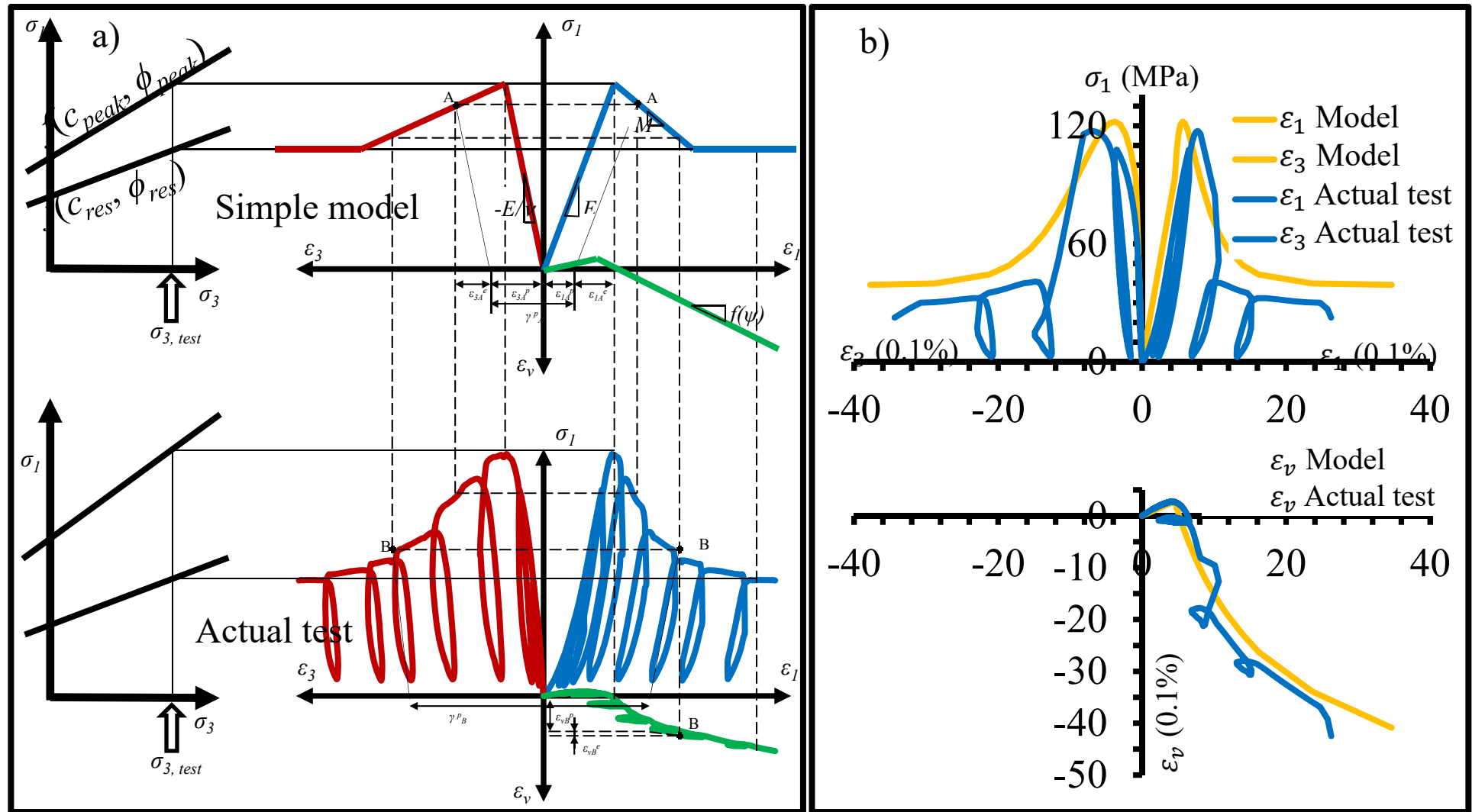
## 5. A CONCEPTUAL MODEL OF ROCK MASS BEHAVIOUR



## 5. A CONCEPTUAL MODEL OF ROCK MASS BEHAVIOUR

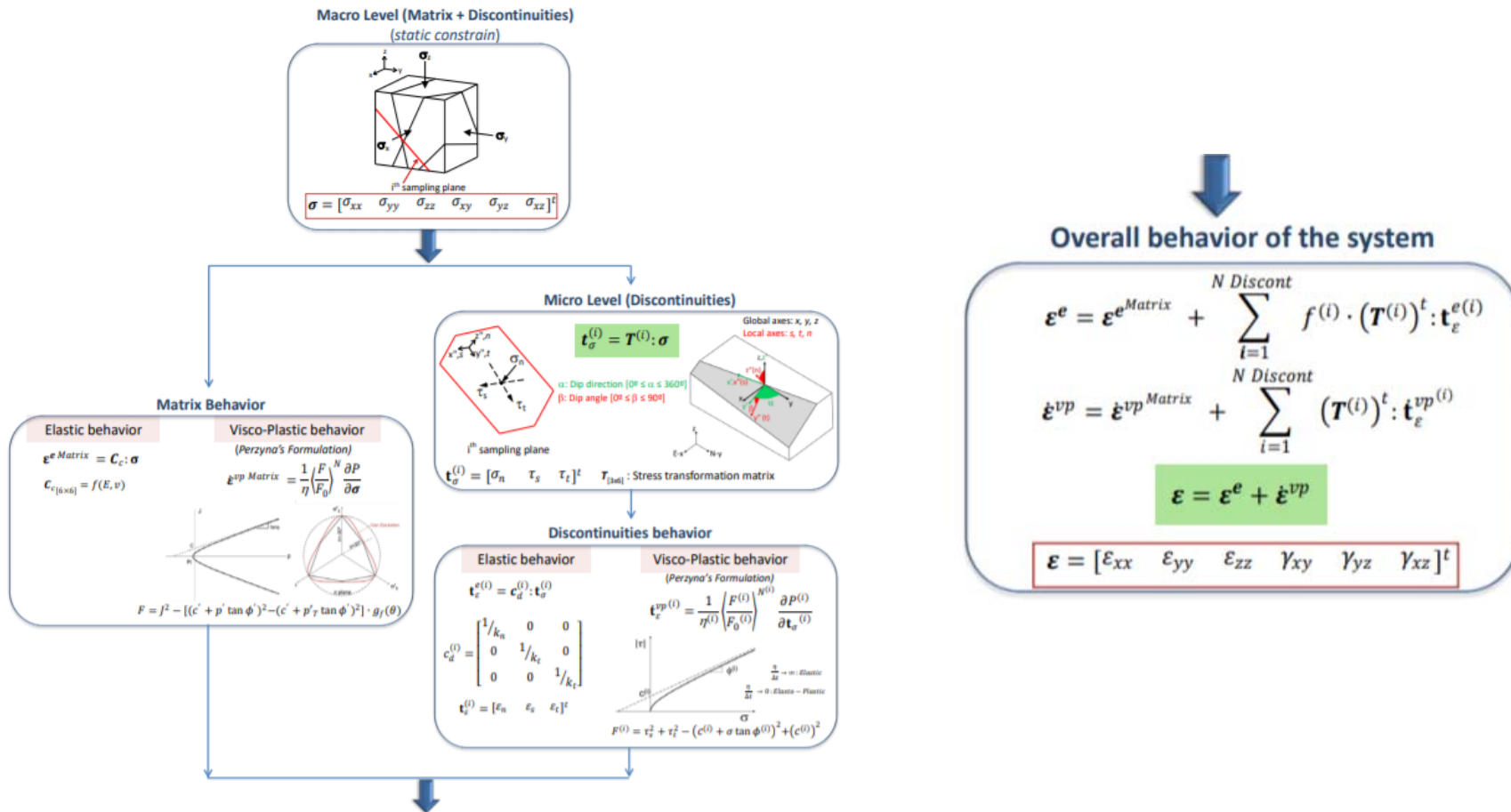
Jean Mandel Lecture 2020:  
 Rock post-failure behavior  
 L.R. Alejano, Spain



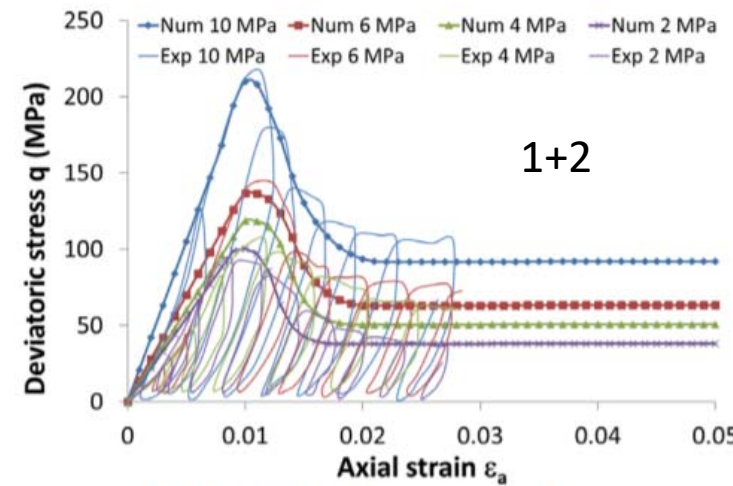
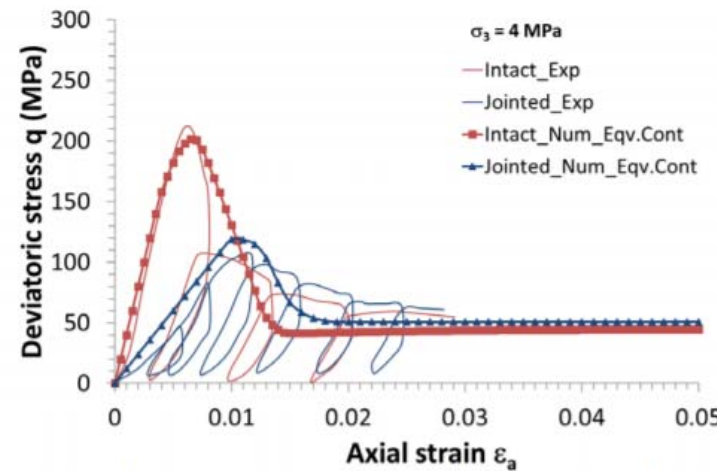
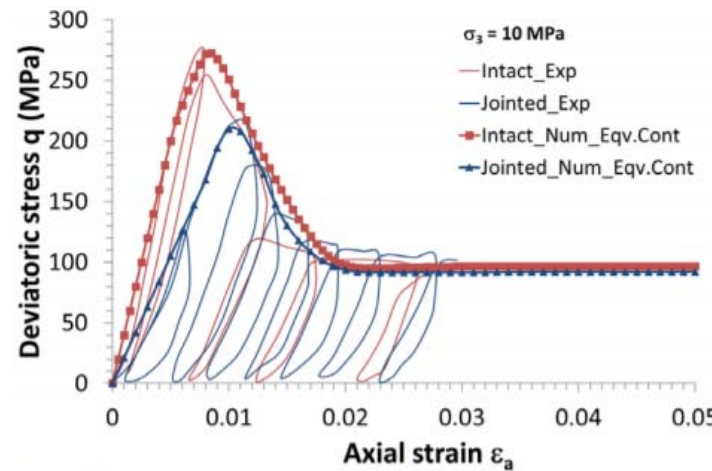


FLAC MODELS ON INTACT ROCK

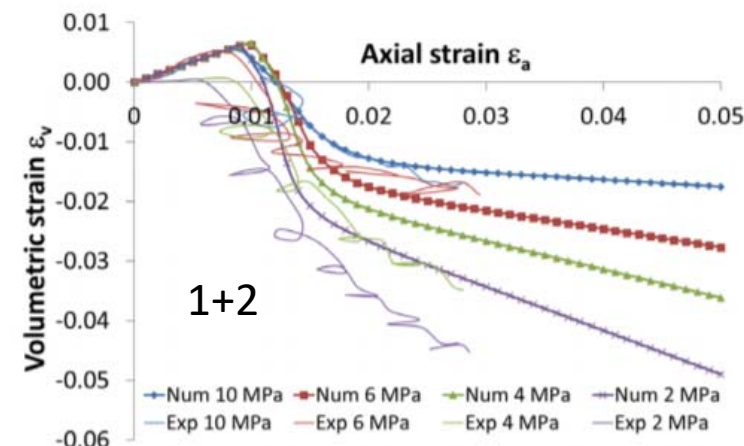
Continuum-based approach. Model formulation composed of two main parts: the continuum (matrix) and the discontinuities, each of them defined by elastic-visco-plastic models which are combined additively in terms of strains.



## 6. MODELLING

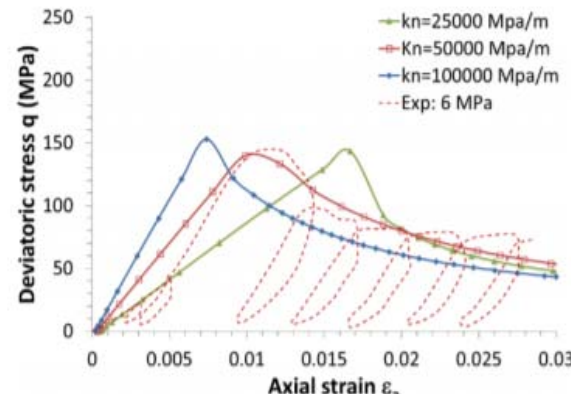


(a) Axial strain - deviatoric stress response

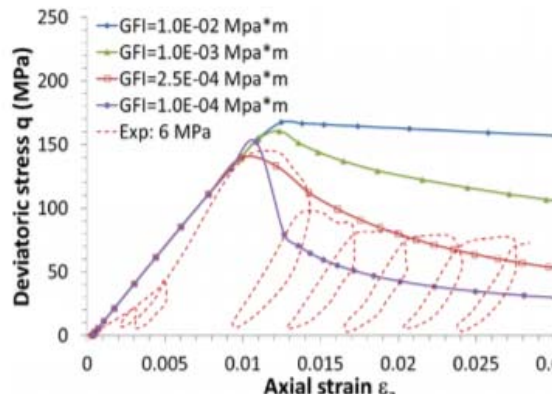


(b) Axial strain – volumetric strain response

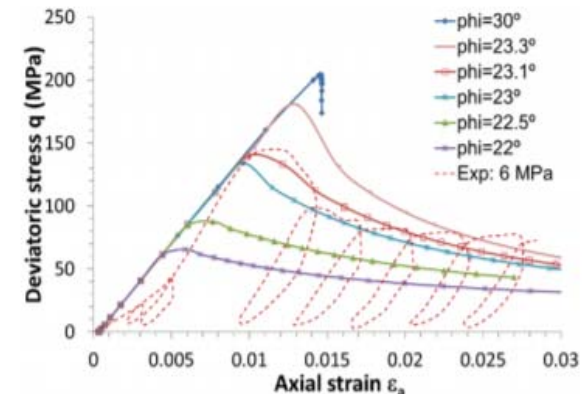
Sensitivity analysis of joint parameters on 1+2 under 6 MPa confining pressure.



(a) Effect of joint stiffness

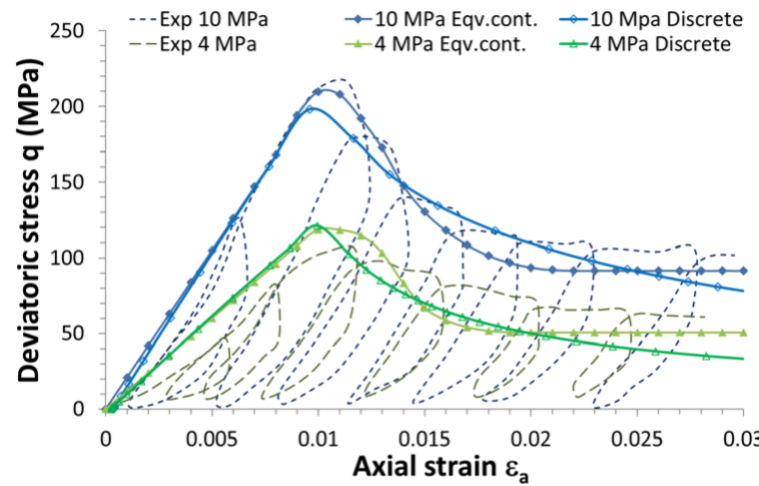


(b) Effect of fracture energy



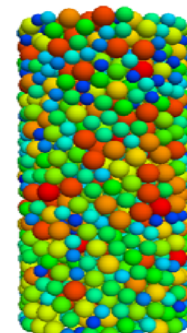
(c) Effect of joint friction angle

Stress-strain plots for 1+2 jointed rock from discrete and equivalent continuum



González-Molano, Alvarellos, Lakshmikanth, Arzúa & Alejano. 2020. Numerical and experimental characterization of mechanical behaviour of an artificially jointed rock. ISRM International Symposium Eurock 2020.

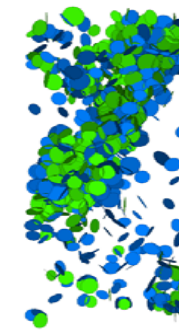
PFC (Particle Flow Code) is a general purpose DEM code framework that models synthetic materials composed of an assembly of variably-sized rigid particles that interact at contacts to represent both granular and solid materials.



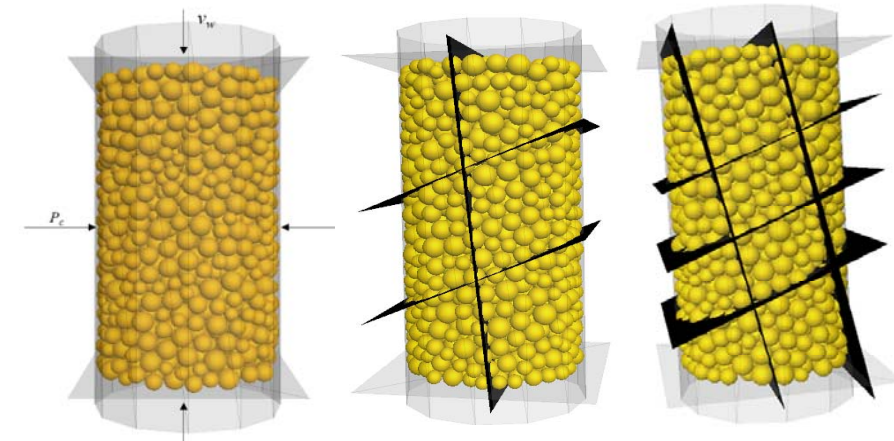
PARTICLES



CONTACTS

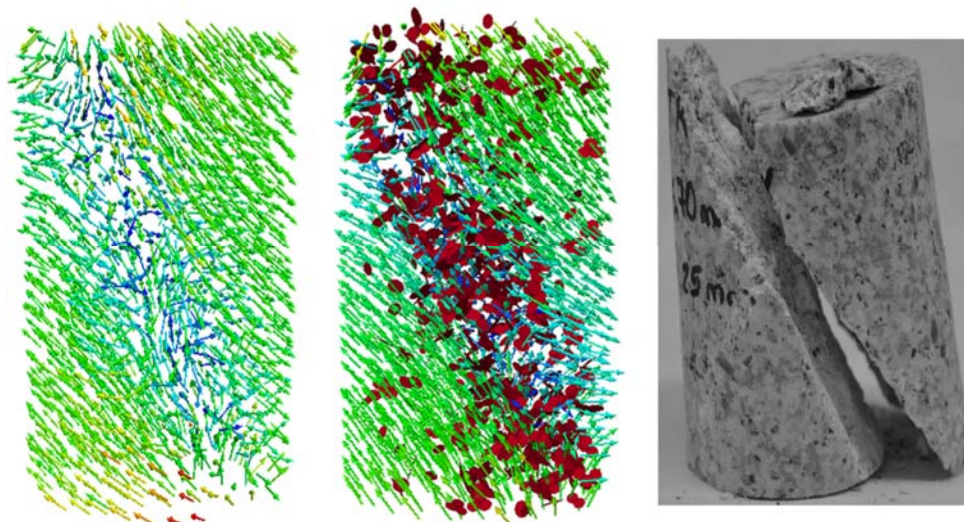
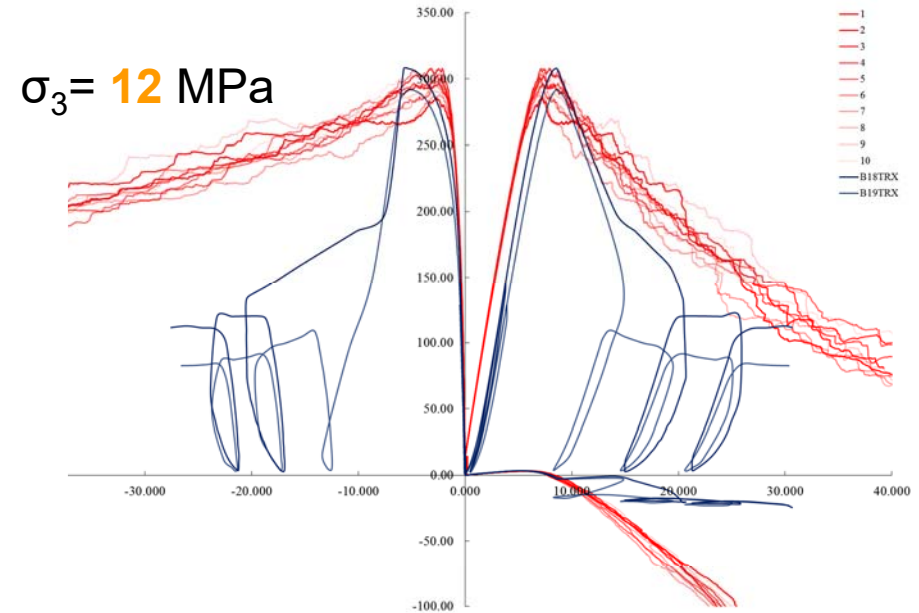
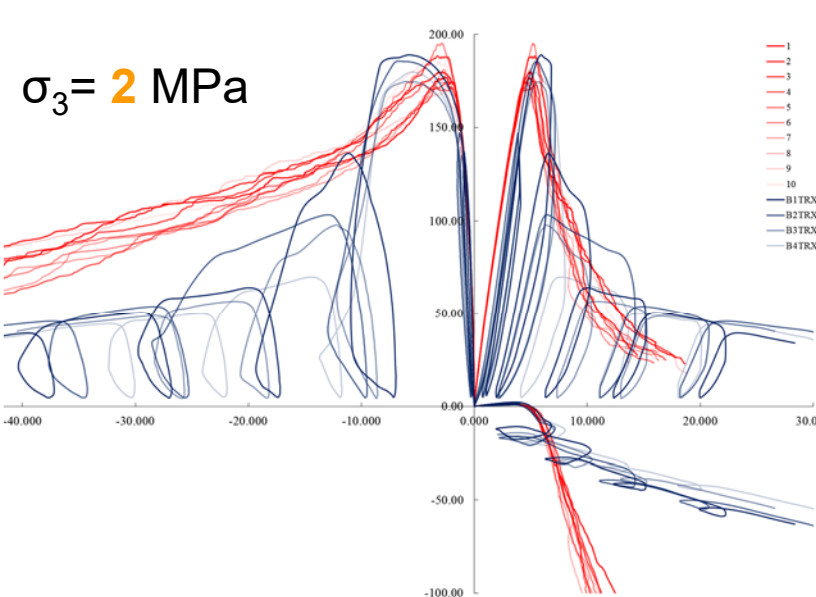


FRACTURES



Castro-Filgueira, U., Alejano, L.R., Ivars, D.M. 2020. Particle flow code simulation of intact and fissured granitic rock samples. Journal of Rock Mechanics and Geotechnical Engineering, 12 (5), pp. 960-974.

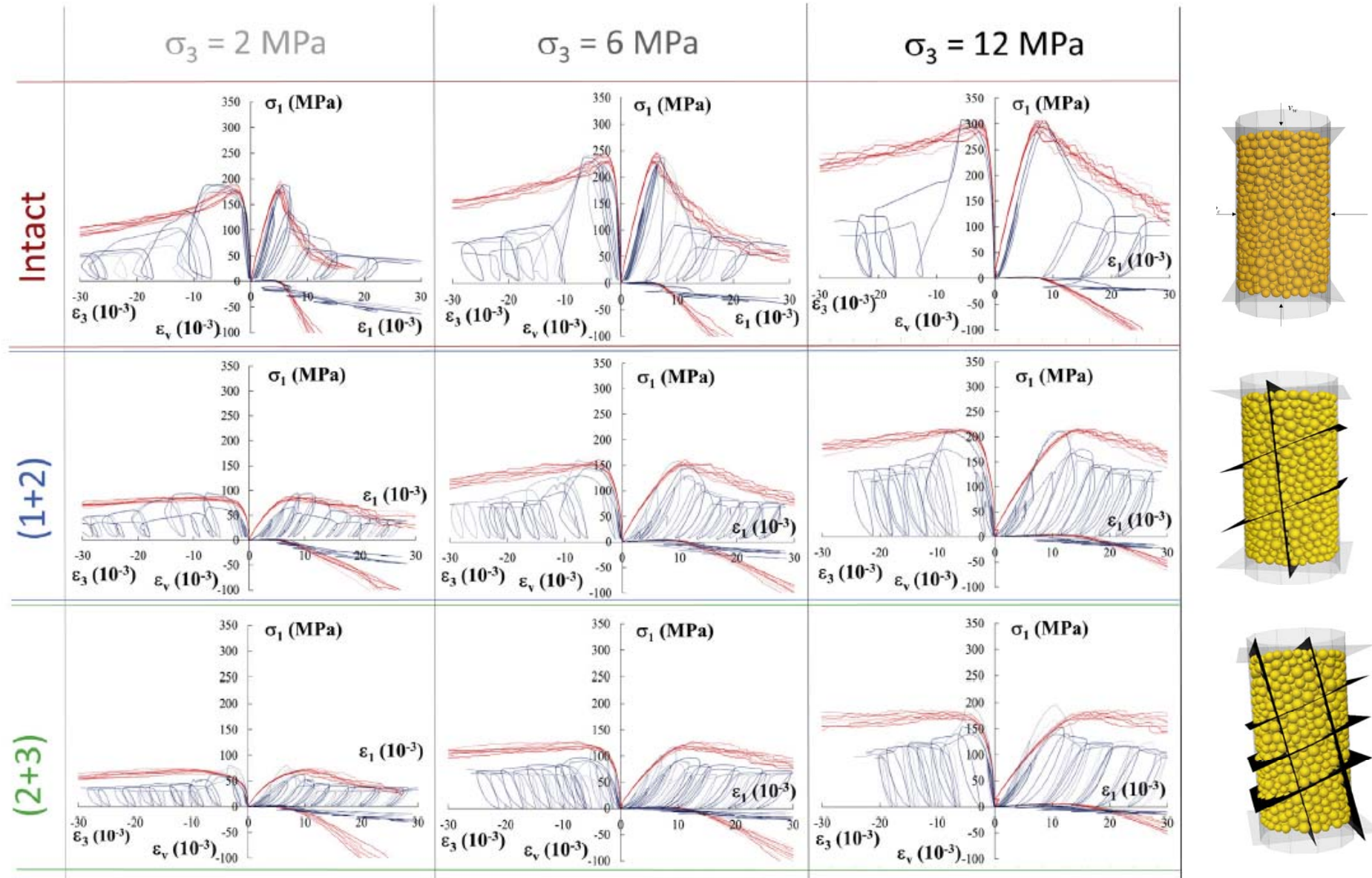
## 6. MODELLING



● Shear cracks

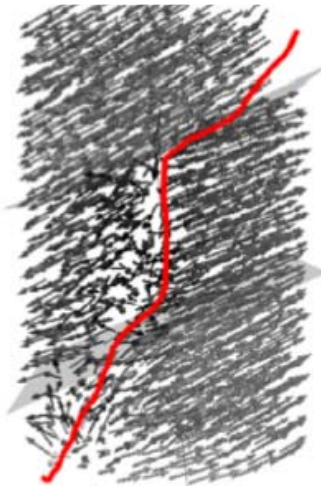
Castro-Filgueira, U., Alejano, L.R., Ivars, D.M. 2020. Particle flow code simulation of intact and fissured granitic rock samples. Journal of Rock Mechanics and Geotechnical Engineering, 12 (5), pp. 960-974.

## 6. MODELLING



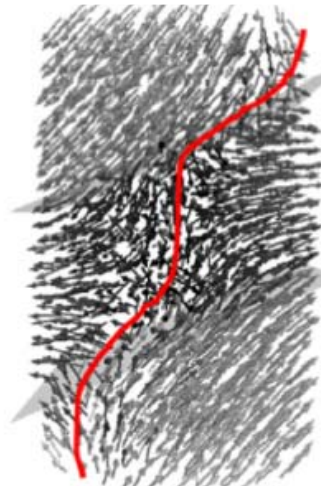
Castro-Filgueira, U., Alejano, L.R., Ivars, D.M. 2020. Particle flow code simulation of intact and fissured granitic rock samples. Journal of Rock Mechanics and Geotechnical Engineering, 12 (5), pp. 960-974.

2 MPa



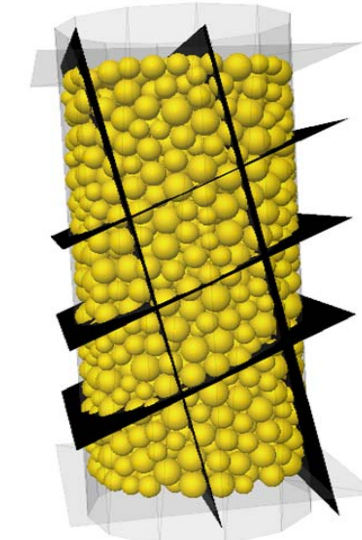
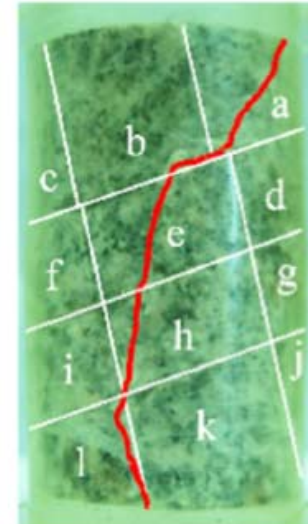
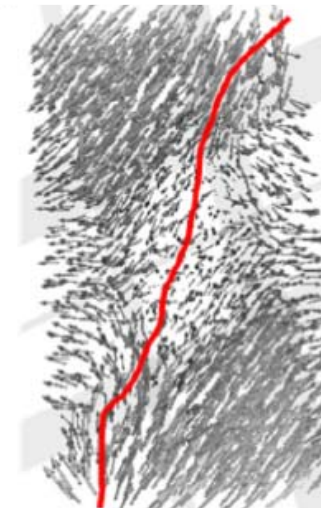
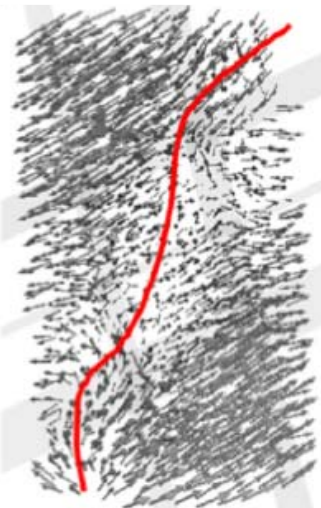
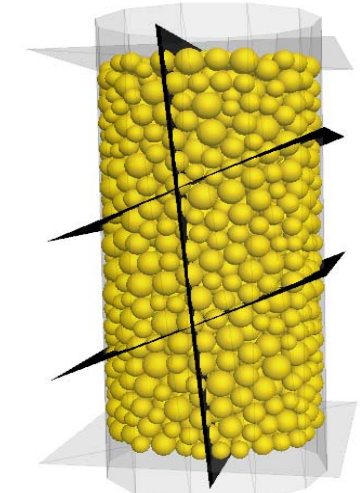
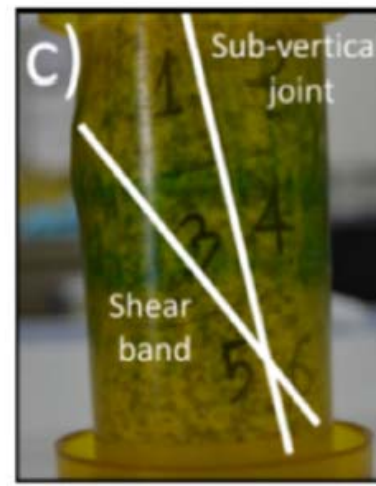
Axial splitting

10 MPa



shear banding

10 MPa



Castro-Filgueira, U., Alejano, L.R., Ivars, D.M. 2020. Particle flow code simulation of intact and fissured granitic rock samples. Journal of Rock Mechanics and Geotechnical Engineering, 12 (5), pp. 960-974.

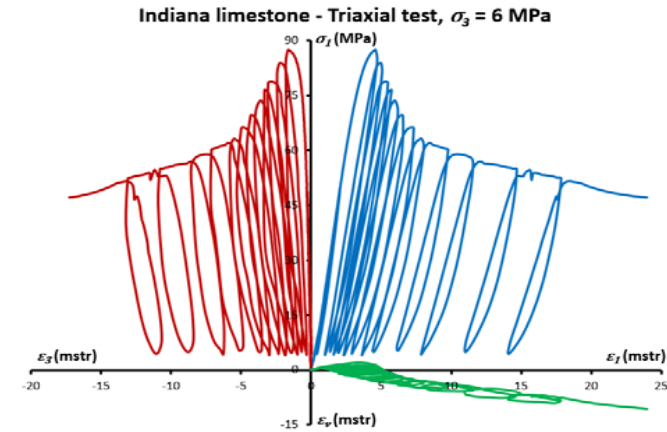
### General conclusions

Results for **laboratory** studies regarding the impact of structure on peak and residual strength, deformability and post-failure behaviour of intact and jointed granite specimens indicate that changes in deformability, peak and residual strength and post-failure behavior in these small-scale rock masses follow similar trends to those observed for decreasing geotechnical quality in rock masses.

Peak **strength** depends on jointing, but it also seems to be somewhat dependent on scale. The level of fracturing (joint intensity) or GSI at a larger scale can therefore be used to assess the evolution of strength. The residual strength does not seem to be affected by the degree of initial jointing.

Peak **dilation** angle decreases with confinement and with the addition of joints to the samples. The result is a lower peak dilation and smaller dilation decay parameter for the jointed samples in relation to that of intact samples.

Ultimately, the results shown represent a potential advancement in the **understanding** of the stress-strain behavior of structured rock masses. By considering the potential for rock masses to be considered as similar in behavior to intact rocks which have undergone prior strain, future studies can exploit the potential practical value of this concept and contribute to advance towards more reliable **numerical approaches**.



Science is rooted in creative interpretation. Numbers suggest, constrain, and refute; they do not, by themselves, specify the content of scientific theories. Theories are built upon the interpretation of numbers...,

...and interpreters are often trapped by their own rhetoric. They believe in their own objectivity, and fail to discern the prejudice that leads them to one interpretation among many consistent with their numbers...

The mismeasure of man  
Stephen J. Gould

# Merci bien!

**Leandro R. Alejano,  
Prof. of Rock Mechanics, University of Vigo, Spain  
ISRM VP for Europe**

[alejano@uvigo.es](mailto:alejano@uvigo.es)

